University of Naples Federico II

Department of Agricultural Science

Ph.D. in Agricultural Science - XXX Cycle

Modelling of rainfall-induced landslides and relationship between flow-like landslides and andic soils

Tutors

Prof. Fabio Terribile

Prof.ssa Simona Vingiani

Ph.D. student

Solange Scognamiglio

Academic year 2016/2017

To daddy.

I'll keep walking in your footsteps.

INDEX

INTRODUCTION AND BACKGROUND INFORMATION

Flow-like landslides (Hungr et al., 2001) are hazardous phenomena that occur all over the world and potentially expose people and infrastructure to a very high danger (Alcantara-Ayala, 2002). In fact, due to their kinematics, they can rapidly travel over long distance and destroy everything they meet during their path. Such landslides always show high internal deformations and spread outside of the failure area by moving downslope over the ground surface and adapting themselves to any morphological slope change as a viscous fluid (Picarelli et al., 2008). Flow-like style is typically considered a consequence of building up of diffuse positive excess pore pressure (Picarelli et al., 2008) which could be developed within a soil when one or more of the following conditions exist (i) the soil is partly or fully water saturated, (ii) the soil is susceptible to liquefaction, (iii) the soil is subjected to unbalanced forces. The cause-effect relationship between the occurrence of intense and/or prolonged rainfall events and the triggering of flow-like landslides is commonly recognized in the scientific literature (*e.g.* Campbell, 1975; Caine, 1980; Guzzetti et al., 2008; Baum and Godt, 2010; Peruccacci et al., 2012).

In Campania (southern Italy), which is an Italian region strongly exposed to hydrogeological risk, flow-like landslides involve pyroclastic materials mantling the limestones of the Campanian Apennines. During last century, flow-like landslides caused several casualties and severe damage to infrastructures and inhabited districts in this region. Among the most widespread flow-like landslides which occurred in this area, there are two events that took place on Salerno and Lattari Mountains, respectively on October 1910 and October 1954, leading to a total of 468 casualties, and another big event which happened on Sarno Mountains on May 1998 and led to 160 victims. After this last last catastrophic debris-flow event, several studies were focused on the comprehension of landslide triggering mechanisms. As a result, there has been a relevant progress in understanding the geomorphological predisposing factors of flow-like landslides (Del Prete et al., 1998; Calcaterra et al., 1999; Guadagno et al., 2005; Di Crescenzo and Santo, 2005; Cascini et al., 2008; De Vita et al., 2013) and the hydrological triggering factors (Cascini et al., 2008; Cascini et al., 2010; De Vita et al., 2013). Furthermore, soil scientists have assessed that another crucial predisposing factor, related to the occurrence of flow-like mass movements on Campanian hillslopes, is the presence of Andosols (IUSS Working Group WRB,

2014). Such soils are typically very fertile (Shoji et al., 1993; Nanzyo, 2002; McDaniel et al., 2005) but, unfortunately, at the same time, they are also very fragile and highly susceptible to land degradation processes, such as erosion (Arnalds et al., 2001; Fontes et al., 2004) and landslides (Basile et al., 2003; Scognamiglio et al., 2016 a,b; Terribile et al., 2000; Terribile et al., 2007; Vingiani et al., 2015; Vingiani and Terribile, 2006). In fact, Andosols have a peculiar set of chemical, physical, hydraulic and mineralogical properties that predispose the soil to the instability. Among the main properties of Andosols related to flow-like landslides there are (i) large porosity (ii) low bulk density, (iii) friable fluffy structure, (iv) high water retention capacity and hydraulic conductivity at quasi-saturated and saturated conditions, (v) short range order clay minerals (allophane, imogolite and ferrihydrite), (vi) high susceptibility to soil liquefaction (Nanzyo, 1993 and 2002; Picarelli et al, 2008).

Such previous studies suggested the existence of a pedological control on flow-like phenomena. Nonetheless, these soil studies were mainly developed by applying a descriptive approach, *i.e.* by studying soil properties. The use of the only descriptive approach is much unfortunate because limits the implementation of soil information towards more practical applications such as the use of dynamic landslide models finalized to future applications to predict these dangerous phenomena.

AIM OF THE WORK

In this framework, the general aims of this work were (i) to implement a dynamic model in order to predict the triggering of flow-like landslides in Swiss and Italian contexts and (ii) to evaluate its potential applications to other Italian study areas where soils showing andic features are settled. We highlight that the implementation of dynamic models is an essential requirement for the understanding, within entire regions where andic soil features (considered as a crucial landslide predisposing factor) are developed, of which could be the most susceptible areas where a flow-like landslide could happen and which could be the most realistic triggering scenarios.

We implemented a physically-based landslide hydromechanical triggering (LHT) model, which is publically available as software STEP-TRAMM (namely, STEP is the developing group and TRAMM is the acronym of Triggering RApid Mass Movements), linking key hydrological processes with threshold-based mechanical interactions (Lehmann and Or, 2012). The main difference respect to other models is that STEP-TRAMM incorporates progression of local failures in a chain reaction culminating into hazardous mass release. In fact, the model is based on the idea that local failures, preceding the triggering of landslides, are intended as real precursors of landslides. Such a model considers the soil cover as an unique and homogeneous layer having assigned mechanical and hydraulic properties. The soil depth is variable within the region of interest and spatially distributed according to a soil depth model which is implemented in the code (Stothoff, 2008).

To pursue the objectives of this thesis, first of all we implemented the previously described landslide model to different contexts for both back-analysis and predicting future rainfall-triggered flow-like landslides. In detail, we carried out the following studies:

1) we selected two Swiss catchments located at the foothill of the northern Alps and very close to each other, where important flow-like landslides were triggered by well-defined rainfall events.
2) Then, we moved our attention to an Italian case study located within the city of Naples (Campania region), *i.e.* Camaldoli hill, where flow-like landslides involve soils showing andic properties.

After these first applications, we made a preliminary study to evaluate the potential application of the same model to more complex areas. More specifically, we analysed soil depth

and soil layering variability for different Italian contexts where complex geometry is found (and where soils involved in past landslides show andic features):

3) The first study area was located on the northern slope of Mt. Camposauro (Telesina Valley - Campania region), where flow-like phenomena often occur in the colluvium, involving Andosols, and spread downslope involving the inhabited districts.
4) In the end, we carried out a national scale study to evaluate morphological, chemical, physical and hydraulic properties of 12 Italian soils located in detachment areas of past flow-like landslides.

1

Rainfall induced shallow landslides at catchment scale – effects of soil properties and initial conditions on landslide patterns

The work included in this chapter was developed at the *ETH* of Zurich in collaboration with Dr. P. Lehmann and Prof. D. Or of the Soil and Terrestrial Environmental Physics (*STEP*), Institute of Biogeochemistry and Pollutant Dynamics. In this study, we selected two Swiss catchments located at the foothill of the northern Alps and very close to each other, where important flow-like landslides were triggered by well-defined rainfall events. For such study areas, we implemented the STEP-TRAMM model in order to understand model behaviour and systematically analyze the role of key soil properties on landslides number and on landslides area and then to compare such results with landslide inventories from Switzerland. By introducing a strength index, which quantifies the role of different soil key parameters, we could integrate the effects of various soil properties on the landslide susceptibility. To explore a larger parameter space at catchment scale, we decreased the spatial resolution (compared to previous studies with a similar model and detailed elevation models) to 10 m. Despite the limited resolution, the model could reproduce fairly well the relationship between landslide area and number reported in the inventory of the different catchments. In addition, several areas within the catchments with high density of landslides were reproduced correctly.

I. INTRODUCTION

Rainfall-induced shallow landslides are dangerous natural hazards that can produce fatalities and severe injuries to people and infrastructures. They usually occur abruptly and without distinct precursory signals. For this reason, the prediction of possible triggering locations for different hydrological scenarios that predispose a slope to unstable conditions is of primary importance for defining landslide mitigation strategies and soil conservation management policy. Such a prediction is typically carried out by means of statistical models or physically based models. The first ones link geomorphological and topographic features to the probability of landslide occurrence by assuming that future landslides will be triggered by the same conditions that triggered past landslides (Guzzetti et al., 1999; Van Western et al., 2008). On the other side, physically based models take into account the hydrological status and infiltration and subsurface water flow pathways in order to link them to the mechanical status of a hillslope. Such models are often based on the calculation of a simple indicator of the mechanical state and landslide susceptibility of a slope. Such indicator is the so-called factor of safety (FOS), defined as the ratio between resisting and driving forces acting on a slope that is often considered to be an infinitive slope (O'Loughlin and Pearce, 1976; Wu et al.,1979; Casadei et al., 2003). Some physically-based models express FOS as a function of seepage flow and rainfall rate (Montgomery and Dietrich, 1994; Fernandes et al., 2004) and include the effect of pore pressure on landslide initiation based on numerical solutions of the Richards equation (Iverson, 2000; Tsai and Yang, 2006). In contrast to the key elements of FOS-based models, *i.e.* the gradual evolution of the FOS value during a rainfall event and the nonlocal definition of the mechanical status of a hillslope (resulting in an assembly of large regions with similar FOS), evidence suggests that rainfall triggered landslides are abrupt and highly localized phenomena (Iverson et al., 2000). In this study, we define as abruptness the release of large soil masses without apparent preceding indicators for imminent mass release. Notwithstanding their apparent abruptness, rainfall-induced shallow landslides can be triggered as a progression of small local failures that coalesce into a continuous failure plane (Petley et al., 2005). Local failures can be ascribed to different processes occurring into the soil, from the buckling of the load bearing, to frictional sliding between grains, to the generation of microcracks within the soil and breakage of capillary bridges or plant roots (Michlmayr et al., 2012). Such local failures can occur during and after a significant or prolonged rainfall event and represent internal damage within the soil cover.

The progressive nature of landslide triggering and the abrupt landslide event is a challenge for physically based models and was reproduced in many studies by means of landslide hydromechanical triggering (LHT) model, linking key hydrological processes with threshold-based mechanical interactions (Lehmann and Or, 2012; von Ruette et al., 2013, Fan et al., 2015). The model is now publically available as software STEP TRAMM (http://www.step.ethz.ch/step-tramm.html). This model approach considers the triggering process of landslide as a chain reaction triggered by weak and damaged soil columns. In the model, the soil mantle overlying a hillslope is discretized into an assembly of hexagonal-shaped soil columns that are mechanically interconnected and interacting with the nearest neighbors by means of frictional, tensile and compressive forces represented by mechanical "bonds". Another mechanical bond connects the base of each soil column to the bedrock surface (which is considered to be a preferential rupture surface). The mechanical "bonds" consist of a bundle of mechanical fiber elements (Peirce, 1926; Daniels, 1945; Cohen et al., 2009), mimicking the mechanical behavior of different soil elements (*e.g.* friction, cementing agents, capillary bridges, plant roots). Each mechanical bond has a prescribed strength, governing the landslide triggering process, that depends on soil type, water content state and root reinforcement (which generates additional cohesion to the soil). Since fibers can break long before the whole soil mass is released, such formalism provides unique and innovative model capabilities to identify and localize the gradual weakening of the wet soil within the whole mass long before it is released. In the model, the process of landslide initiation strictly depends on threshold mechanics. In particular, when the force on a given bond exceeds the strength threshold, the rupture of the bond occurs and the excess load is thus redistributed according to pre-defined load redistribution rules that can be modified to mimic different failure behavior (ductile vs. brittle), as shown in Fan et al. (2016).

Because in this study we will analyze the role of such load redistribution rules and adapt them to different soil types and hydration state, we describe them in some detail in the following. The load redistribution rule defines the criterion to distribute and transfer the amount of excess load into two different directions: downslope by means of "compressive bonds" and upslope (or laterally) by means of "tensile bonds". To determine an appropriate load redistribution rule for each soil type, Fan et al. (2016) defined the *stiffness ratio*, K_2/K_1, a key parameter that quantifies the amount of load redistributed to intact bonds and is defined as the ratio between the load redistributed to downslope compressive bonds, K_2, and the load redistributed to upslope tensile bonds, K_1. Moreover, Fan et al. (2016) also established links between such theoretical stiffness

ratio and measurable soil mechanical properties (*i.e.* Young's modulus *E* and Poisson's ratio *v*, which express the brittleness of a soil): in fact, large values of stiffness ratio characterize soils with large *E* and small *v*, which is typical of brittle materials (*e.g.* sand), whereas, small values of the stiffness ratio represent soils having small *E* and large *v*, typical of ductile materials (*e.g.* clay). In this study we will extend the work of Fan et al. (2016) to define the stiffness ratio not only as function of soil textural class but as function of water content as well.

With the model STEP TRAMM the abrupt release of highly localized landslides can be simulated and has thus the potential to determine susceptible regions for a specific rainfall event. However, due to complex soil architecture and soil heterogeneity, the hydro-mechanical properties of the soil mantle are only known within certain limits and this uncertainty affects the model outcome. To simulate landslide triggering it is thus required to study a certain range of soil properties. For large catchments, modeling of different realizations to determine dominant soil properties is time consuming. So far the model underlying STEP TRAMM was only applied with high spatial resolution (1.0 m in Lehmann and Or, 2012; 2.5 m in von Ruette et al., 2013; and 2.0 m in Fan et al., 2016). For a manifold of simulations and for larger catchments (larger than a few square kilometers), the computational burden for high spatial resolution becomes too high. In addition, highly resolved information on elevation, as used in previous studies, is not available around the globe and less detailed information must be necessarily used. In this study we will use a spatial resolution of 10 m to determine dominant system properties and susceptible regions more effectively. So this is the first time that this new model type is applied with a relatively poor spatial resolution. If the model succeeds to reproduce landslide properties also with this resolution and thus a relatively small computational burden, we can be confident that it can be applied for much larger catchments as well.

The objectives of this study are thus as follows: (i) to test if STEP TRAMM can reproduce landslide number and landslide area reported in inventory using relatively poor spatial resolution, (ii) to test if some local regions of high landslide density within a catchment can be predicted and (iii) to estimate the role of the various soil properties on landslide susceptibility. For the last case we will also study the role of soil and water content dependent rules of load redistribution of progressive failure on landslide triggering.

The study is organized as follows: in section 2 we quantify the relationship between soil mechanical key properties, water content and soil texture and its implementation in the landslide triggering model. A description of landslide inventories and parameterization of soil properties to

quantify the effect of soil properties and load redistribution rules on landslide triggering follows in section 3. In section 4, landslide simulation results are compared to landslide inventories for the two case studies in Switzerland and one case in Italy. In discussion, section 5, the relevance of the findings is generalized for other catchments. The paper is closed in section 6 with summary and conclusions.

II. THEORY - LINKING LOAD REDISTRIBUTION RULES TO SOIL TEXTURAL CLASS AND WETNESS

We differentiate soil failure modes preceding a rainfall-induced landslide by distinguishing between brittle and ductile behavior. The soil key mechanical properties which quantify the brittleness or the ductility of a soil are the Young's modulus *E* and the Poisson's ratio *v*. Since Young's modulus has a far more dominant effect on failure propagation in a hillslope than Poisson's ratio (Fan et al., 2016), we focus here on the Young's modulus. The Young's modulus assumes different values depending on soil type (large *E* values are typically associated to brittle materials, whereas small *E* values to ductile materials), but it can also vary as a function of soil water content. In fact, for all soil types, an increase in water content induces a consequent decrease in the Young's modulus and vice versa (Lu et al., 2014, see Fig 1a below). The soil type that is mostly sensitive to the variation of the Young's modulus with varying water content is the ductile clayey one: in fact, the value of *E* rapidly decreases with increasing water content (Fig.1a). In the recent literature, it is possible to find few studies concerning the dependency of the Young's modulus of a soil to the water content. Such a dependency is well described from a power law relationship (Ng et al. 2009; Sawangsuriya et al., 2009; Schuettpelz et al. 2010; Khosravi and McCartney 2011). Between all the recently proposed power law equations, we refer to the empirical power law model from Lu et al. (2014) which simply explains the aforesaid dependency of the Young's modulus to the water content as follows

$$E = E_d + (E_w - E_d)\left(\frac{\theta-\theta_d}{\theta_w-\theta_d}\right)^m \quad (1)$$

where *E* is the Young's modulus, θ is the volumetric water content, subscripts *d* and *w* indicate, respectively, the dry state and the wet state of a soil and *m* is an empirical fitting parameter. To estimate the Young's modulus as a function of the water content, it is necessary to estimate the

parameter *m*, which is inversely proportional to the soil grains size and is well correlated to the specific surface area of soils (Lu et al., 2014). In Lu et al. (2014) the parameter values are listed for eleven different soil. For this study, we grouped the soils into three different classes representing three main soil textures (*i.e.* sandy, loamy and clayey soils). For each one of the 3 soil textures, we have calculated the average values of E_d, E_w, ϑ_{wet}, ϑ_{dry} and *m*, listed in Table 1 and in Figure 1a we show the Young's modulus as a function of water content.

Table 1: *Average fitted parameter values obtained by solving equation 1 for 11 soils of Lu et al. (2014) and by grouping them in three main textural classes. E is the Young's modulus, ϑ is the volumetric water content, subscripts d and w indicate, respectively, the dry state and the wet state and m is an empirical fitting parameter.*

Soil type	$\mathbf{E_w}$	$\mathbf{E_d}$	$\boldsymbol{\theta_w}$	$\boldsymbol{\theta_d}$	***m***
SANDY soil	2.95	3.18	0.39	0.03	0.1
LOAMY soil	0.71	2.46	0.41	0.05	0.76
CLAYEY soil	1.45	5.16	0.34	0.09	1.07

To link the Young's modulus of the three soil textural classes to the stiffness ratio K_2/K_1 implemented in the landslide hydrological triggering framework, we follow Fan et al. (2016) that found the following power law based on numerical experiments:

$$\frac{K_2}{K_1} = 1.3E^{0.88} \qquad (2)$$

where *E* is the Young's modulus and K_2/K_1 is the stiffness ratio. By inserting eq. (1) into eq. (2) we have transformed the Young's modulus into the corresponding stiffness ratio to obtain the relationships between K_2/K_1 and θ for the three soil types shown in Figure 1b. We implemented the linear relationship describing the stiffness ratio as a function of the water content for each of the three main soil textural classes (clay, sand and loam).

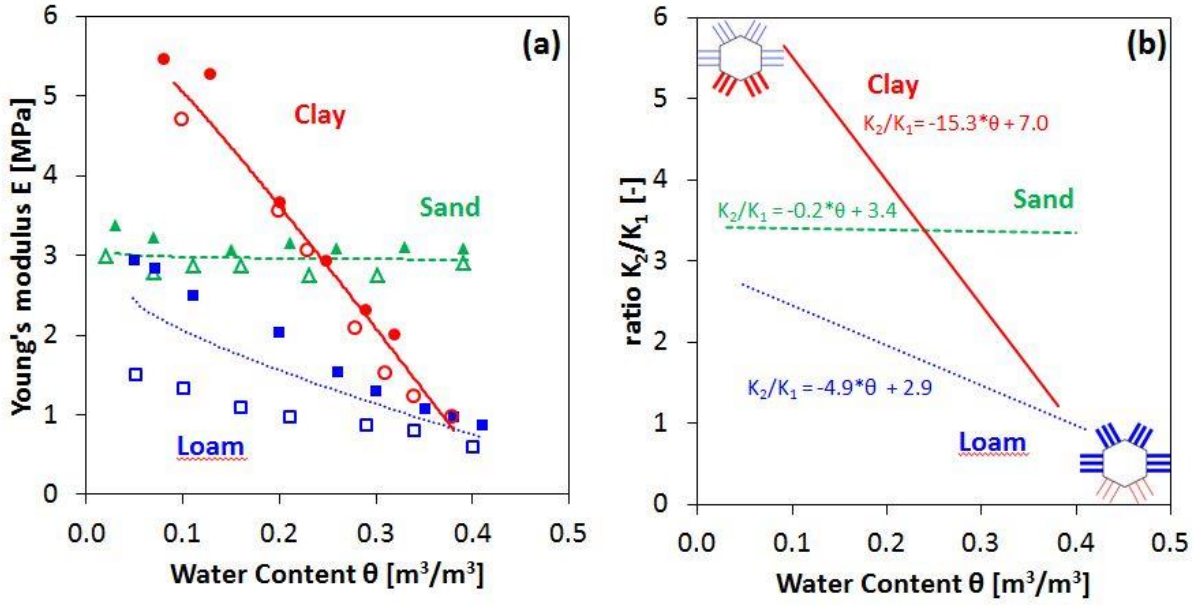

Figure 1: *Variation of mechanical properties as function of soil textural class and water content and its implementation in modeling framework. (a) Young's modulus E vs. volumetric water content* θ *for each of the three main soil textural classes clay, loam, and sand. Data (symbols) of different soils samples from Lu et al., 2014 were fitted (lines) with eq. (1). (b) Stiffness ratio (K_2/K_1) vs. volumetric water content* θ *for each soil textural class. For each soil, the equation describing the relative line is reported. The insets in Fig 1b show a schematic representation of a typical hexagonal-shaped soil column (considered in STEP TRAMM) surrounded by lateral mechanical bonds which constitute the link between the soil column and its nearest neighbors. Colors blue and red are for K_1 (horizontal and upslope stiffness of the tensile bonds) and K_2 (downslope stiffness of the compressive bonds), respectively. The soil column is represented for both moist and wet conditions: thin fibers represent low values of stiffness whereas thick lines are for high stiffness values.*

From figure 1b it becomes clear that the slopes of the linear relationship K_2/K_1 vs. θ, resulting from the described procedure, are different for each one of the three main soil classes. In particular, clay line is characterized from the highest slope. This means that, since the Young's modulus of a clay broadly varies with varying water content (Fig. 1a), the range of stiffness ratios for a clay is large, depending on clay water content. Such a circumstance is not surprising and was expected due to the particular sensitivity of clay soils to the water content, which strongly affect its rheological behavior. On the other side, loamy and sandy soils are characterized from lower slope than clay soils. In particular, since the Young's modulus of a sand exhibits a quasi-constant value with varying water content (Fig. 1a), the stiffness ratio of a sand is almost independently on

its water content. Such a circumstance is explained by considering the very low dependency of the rheological behavior, *i.e.* of the *E* value, of a sand to the variation of water content. As a general consideration valid for every soil type, the stiffness ratio K_2/K_1 decreases with increasing soil water content and, for different water content, it assumes different values, depending on the considered soil type.

III. MATERIALS AND METHODS

III.A Landslide inventories

The model STEP TRAMM was applied to three different catchments (two Swiss and one Italian). In all three cases the reported landslides were triggered by a well-defined rainfall event. At first, we simulated two Swiss landslide events which occurred in two catchments located very close to each other at the foothill of the northern Alps. We named the landslide events as "Napf 2002" and "Napf 2005", corresponding to the geographical region in which they occurred ("Napf") and the year when they happened. The two catchments are only few kilometers apart, have similar dimension (2.4 km^2 for Napf 2002 and 1.4 km^2 for Napf 2005) and are characterized by similar environmental and topographic features, land use, and geological formations (von Ruette et al. 2013). The Napf 2002 event triggered 51 documented shallow landslides (Rickli and Graf, 2009) and is shown in Figure 2a. The triggering rainfall occurred on the 15th–16th July as a local summer storm with a rainfall intensity of 15–25 mm/h and a total rainfall amount of 53 mm. We use this case study as "calibration study" to determine the dominant soil properties of the catchment. Then, these fitted properties will be used to validate the model for the other case study "Napf2005". The rainfall in case of Napf 2005 triggered 36 shallow landslides in the study area but totally involved over 5000 landslides across the northern part of the Swiss Alps (Raetzo and Rickli, 2007). The rainfall event 2005 was longer than the 2002 one and lasted from 18th to 23th August with a total rainfall amount of 229 mm (von Ruette et al., 2013). For Napf 2005, the catchment and inventory landslides are shown in Figure 4a of result section.

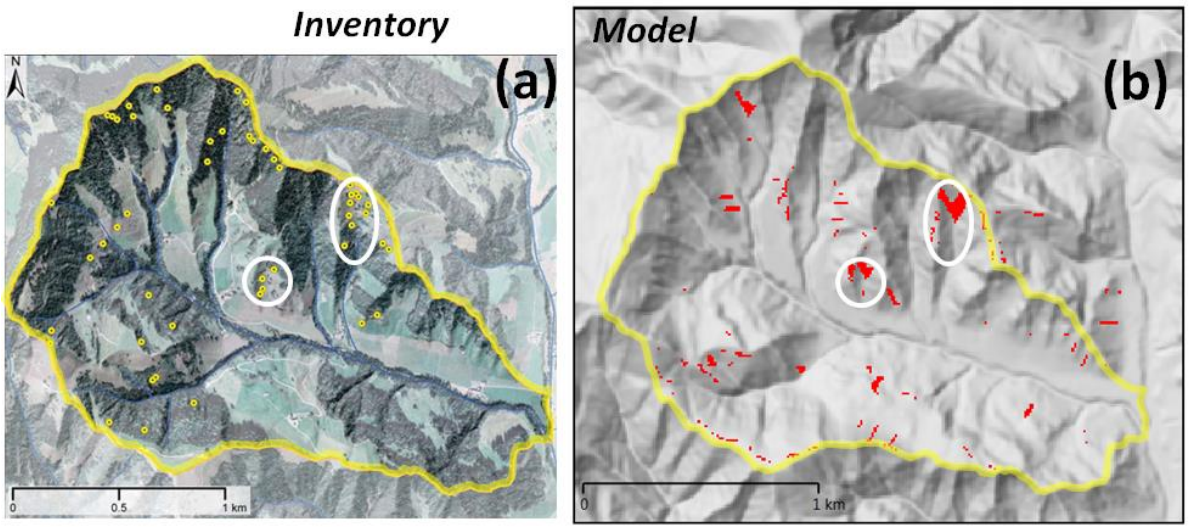

Figure 2: *Comparison of landslide inventory with simulated landslides for the Napf region. Landslides were triggered by a short rainfall event in 2002. (a) Landslide inventory map from von Ruette et al. 2013 with landslides shown as yellow disks. (b) Map of landslides (in red) resulting from simulation with sandy loam and zero stiffness ratio. In (a) and (b) the bold yellow line marks the border of the catchment. The white lines mark regions with high landslide density to show that some susceptible regions were correctly reproduced by the model.*

The selected Italian catchment is named Pogliaschina, which is located in NW Apennines in Liguria region (northern Italy; figure is presented in results section) On 25th October 2011, 588 shallow landslides, covering a total area of 0.44 km^2, where triggered by a very intense rainfall storm which lasted 6 hours with a maximum hourly rainfall intensity of 150 mm h^{-1} and with largest cumulated rainfall varying between northern (250 mm/h) and southern (500 mm/h) parts of the catchment. The event caused injuries and six fatalities (Mondini et al., 2014). The catchment has a dimension of about 25 km^2 and a landslide density around 23 landslides/km^2, which is comparable to the Napf 2002 and 2005 ones (respectively 21 and 25 events/km^2). Note that the size of the catchment is much larger than any other case study that was analyzed so far with this type of model approach.

For the three selected catchments we carried out landslide simulations in order to systematically explore the influence of the various model parameters and to optimize and calibrate the parameter set. To run simulations, a Digital Elevation Map (DEM) is required. For both Napf catchments, it was obtained from a DEM based on Lidar data from Swisstopo (2005) having a resolution of 2m, whereas for Pogliaschina a DEM with a resolution of 26 m was obtained

from the USGS service (https://earthexplorer.usgs.gov/). In both cases the DEM was scaled to a resolution of 10 m that was equal to the numerical resolution of the simulations. The vegetation pattern consists of two classes, *i.e.* grassland and forest. For both Napf catchments vegetation type was determined by subtracting a DEM of terrain without vegetation from a DEM including vegetation (von Ruette et al., 2013), whereas for Pogliaschina catchment forest cover map was taken from the Forest Global Change database (Hansen et al., 2013). For forest regions, lateral root reinforcement will be considered. To compute "loading" of the catchment by rainfall, we used rainfall signals for Napf catchments extracted from rainfall data sets CH02H (SwissMeteo©) based on hourly radar rainfall intensities with a spatial resolution of 2 km (Wüest et al., 2010), whereas for Pogliaschina catchment the rainfall signal was extracted from literature data (Mondini et al. 2014).

With respect to soil properties, we differentiate between soil depth and soil hydraulic properties. Soil depth is modeled using the colluvium-diffusion equation with slope-dependent diffusion flux (Stothoff, 2008; von Ruette et al., 2013). Hydraulic properties are determined based on the soil textural class and the Brooks and Corey (1964) model, that was used to define hydraulic conductivity and capillary pressure as a function of soil water content and was combined with the Lu et al. (2010) formulation for unsaturated soil strength. For the various soil textural classes the hydraulic parameter values were taken from Rawls et al.(1982). For the selected case studies, the predominant soil textural class of the catchments were taken from literature data for both the Napf catchments (von Ruette et al., 2013), whereas for Pogliaschina case study, it was extracted from SoilGrids (Hengl et al., 2014). For all considered catchments the soil textural classes were different types of loamy soils.

III.B Simulated parameter space and definition of strength index

Within one catchment several soil textural classes can be found and the model outcome will change with the chosen class. Similarly, the exact values of other model parameter values, like soil cohesion, root strength and initial water saturation, are unknown although they affect simulation results. To test model sensitivity with respect to such unknown parameter values, we varied systematically "initial water saturation", "soil cohesion" and "root reinforcement". Because for the various catchments not a specific loam type was dominant, we conducted simulations for "sandy loam", "loam" and "silt loam". In addition, we wanted to check if the chosen load redistribution rule will affect model outcome and hence we ran simulations by applying the original stiffness

ratio K_2/K_1=0, for K_2/K_1=1, K_2/K_1=2 and the ratio as a function of water content □ defined for loamy soils by K_2/K_1= -4.9 θ +2.9 (*see* section II and Figure 1).

For the "Napf2002" calibration study, we increased soil cohesion in four steps of 750 Pa, starting from a minimum value of 500 Pa. Root reinforcement was increased in four steps of 1kPa, starting from a minimum value of 1 kPa. Initial water saturation degree was decreased in five steps of 5%, starting from a maximum initial water saturation degree of 70%. For all 150 combinations (five values for soil cohesion and root reinforcement and 6 water saturations) that we ran for each soil textural class and soil redistribution rule, the total landslide number and area were determined.

As we will show in the result section, the strength of the slopes (as manifested by released area) is not controlled by a single factor but is affected by various properties (soil cohesion, root strength, water saturation and soil texture). To classify the parameter space and to combine the various properties we defined a "strength index S" using the most simple linear relationship as follows :

$$S = f_S\left(f_C \cdot C + f_R \cdot R + f_W \cdot W\right) \qquad (3)$$

with weighting factors for effect of soil texture f_S, soil cohesion f_C, root cohesion f_R, and initial water saturation f_W. Because we changed the various parameters in steps, we assigned a strength class index to each parameter value ("C" for soil cohesion, "R" for root reinforcement and "W" for initial water saturation). For example, simulations with root reinforcement values of 1.0, 2.0, 3.0, 4.0 and 5.0 kPa correspond to a class index value "R" of 0, 1, 2, 3 and 4, respectively. Then, we fitted the relationship between strength index "S" and simulated landslide area (also volume and number - data not shown) until we found the highest correlation (*Fig. 3b*).

IV RESULTS

IV.A Model calibration study Napf 2002

For the case study of Napf 2002 we ran 450 simulations (150 for each one of the three soil textural class) for each load redistribution rule, by varying the input parameter set (*i.e.* soil cohesion, root reinforcement and initial soil water saturation). In Figure 3a we show for each simulation the number of triggered landslides and the total landslide area (here shown for original

load redistribution rule of K_2/K_1=0). Note that simulations without landslides or simulations with cumulative landslide areas larger than 15% of total catchment area are not shown (this means that spatial and mechanical interactions between landslide events and locations can no longer be ignored and we stop the model). In Figure 3a it is shown that the relationship between cumulative landslide area and landslide number forms a relatively narrow band. The inventory data fall within this simulated band. For simulations with cumulative area and landslide number close to the inventory data, the landslides occur at least partially at the same locations as the reported inventories, as is shown in Figure 2b. In Figure 3a it is shown that few landslides with small total area were obtained for simulations with large strength index "S" and large areas and many landslides are found for small strength index S. For the original redistribution rule the parameters of eq. (3) were f_C=3.0, f_R=1.0, f_W=4, highlighting that changing the root reinforcement seems to have a relatively small effect on landslide compared to changing soil cohesion or initial water saturation. The parameter values related to soil textural class f_S were 1 for sandy loam, 2 for loam and 3 for silt loam. The resulting strength index of a silt loam is thus three times the strength index of sandy loam. The results for the ratio K_2/K_1 as a function of water content were similar as shown in Figure 3 and did not show a strong dependency of the results on load redistribution rule.

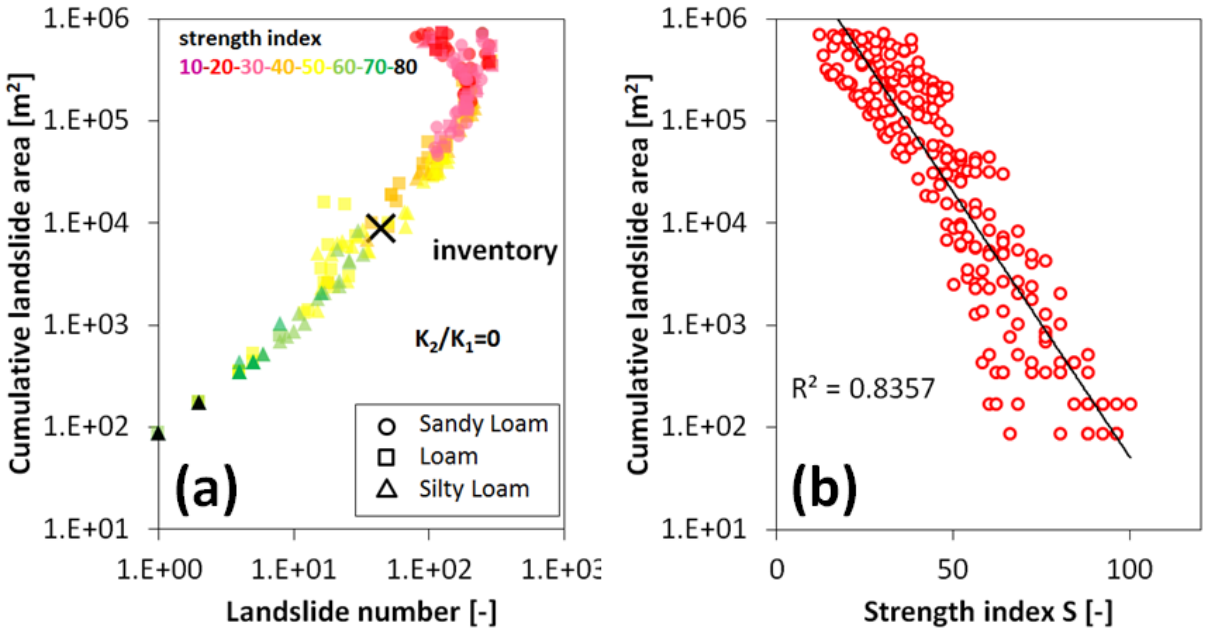

Figure 3: *Relationship between landslide number and cumulative landslide area affected by "strength index". (a) Simulations for calibration study area "Napf 2002". Each symbol stands for one of 450 simulations (with specific soil textural class, soil cohesion, root reinforcement, initial soil water saturation, all for original load redistribution rule K_2/K_1=0). The different shapes of the symbol mark different soil*

textural classes and the colors indicate the strength index (eq. 3). Low values of strength index are associated to simulations with large and many landslides. The black crosses show the inventory data. (b) Relationship between strength index and cumulative landslide area obtained by fitting eq. (3).

IV.B Model validation to estimate landslide numer and area for study Napf 2005

In the calibration study we selected for each textural class the input parameter values resulting in best agreement between measured and simulated cumulative landslide area and landslide number. Then we carried out simulations for "Napf2005" with calibrated root and soil cohesion values and increasing initial soil water saturation by 5% starting from an initial saturation degree of 0.2. To reduce computational costs we split the catchment into two parts (northeast, NE, and southwest, SW) as shown in Figure 4b.

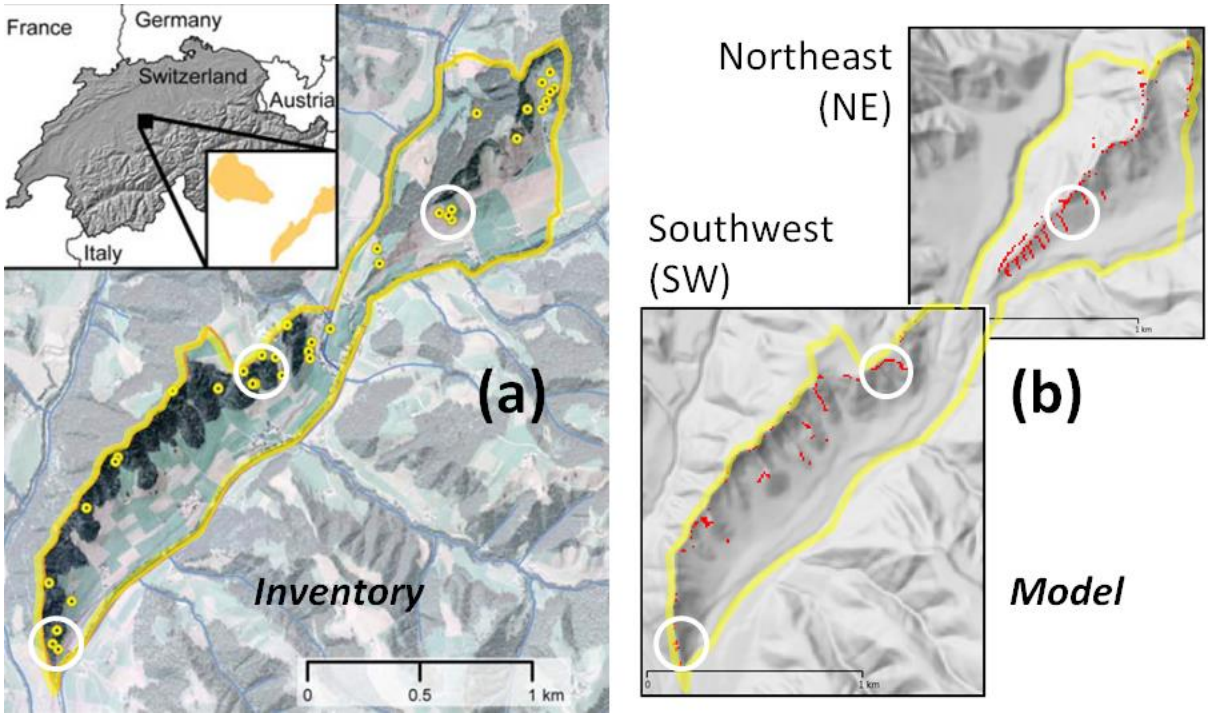

Figure 4: *Comparison of landslide inventory with simulated landslides for the Napf region. Landslides were triggered an extreme rainfall event in 2005. (a) Landslide inventory map from von Ruette et al. 2013 with landslides shown as yellow disks. The inset shows the position of the catchment within Switzerland and the proximity to the event of 2002 (b) Map of landslides (in red) resulting from simulation with silt loam and zero stiffness ratio. In (a) and (b) the bold yellow line marks the boundary of the catchment. The white lines mark region with high landslide density to show that some susceptible regions were correctly reproduced by the model.*

In Figure 4b the results for the silt loam with the original load redistribution rule of K_2/K_1=0.0 are shown. The cumulative landslide area is about 50% of the inventory but the number of landslides is higher. However, the landslides are simulated in similar regions as reported in the inventory. In general, with increasing initial soil water saturation more landslides with larger cumulative area were simulated, as shown in Figure 5. Even for small initial water saturation, the total number and cumulated area of landslides were often larger than the inventories. However, for the initial water saturation of 20% and simulations with silt loam, results are in good agreement with the inventory.

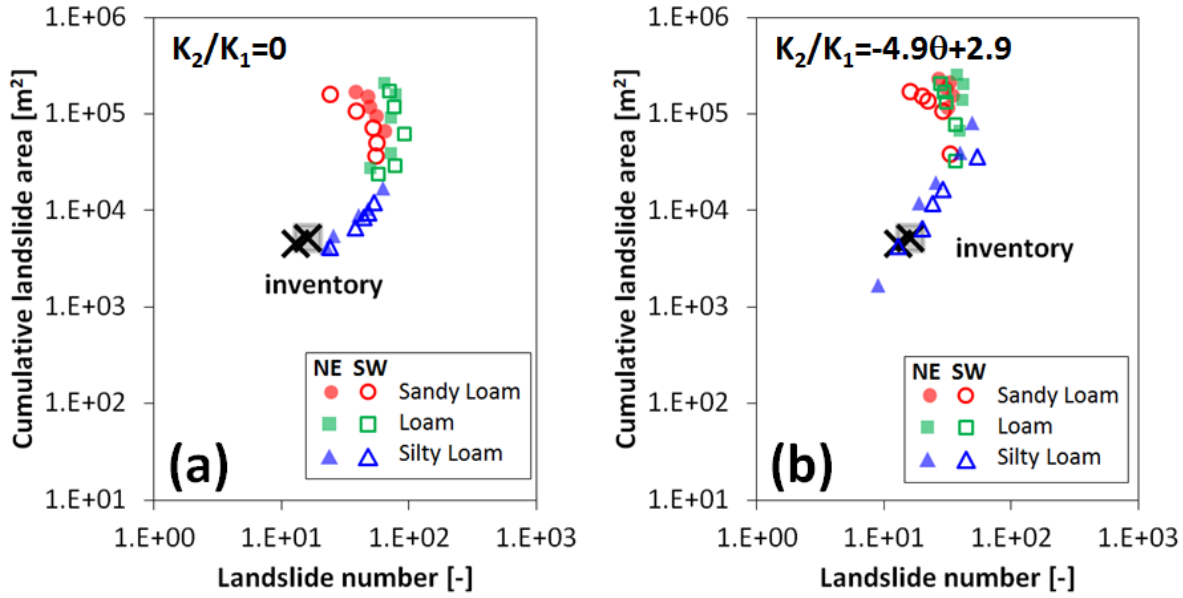

Figure 5: *Relationship between landslide number and cumulative landslide area for the original load redistribution rules (a) and water content dependent load redistribution rules (b) for Napf 2005 validation study. The Napf 2005 catchment was subdivided into a northeast (NE) and a southwest (SW) part. For values of root reinforcement and soil cohesion calibrated for Napf 2002 and for each of the three different loam soil textural classes, five simulations were conducted for five initial water saturation degrees (in the range 0.2 to 0.4). In figure (a) and (b) for each soil and cohesion value there are five symbols of identical shape and color for the five different water saturation degrees. Black crosses mark the inventory data.*

IV.C Modeling large catchment

For the Italian case study, (i.e. Pogliaschina landslide) with tenfold area compared to the Napf catchments, we ran much less simulation (16 per soil textural class) for different soil cohesion and root reinforcement values (1, 2, 3 and 4 kPa) and initial water saturation (0.25 and

0.35). To reduce computational costs we only ran simulations for the eastern part of such a catchment where the most part of landslides occurred (around 70%).

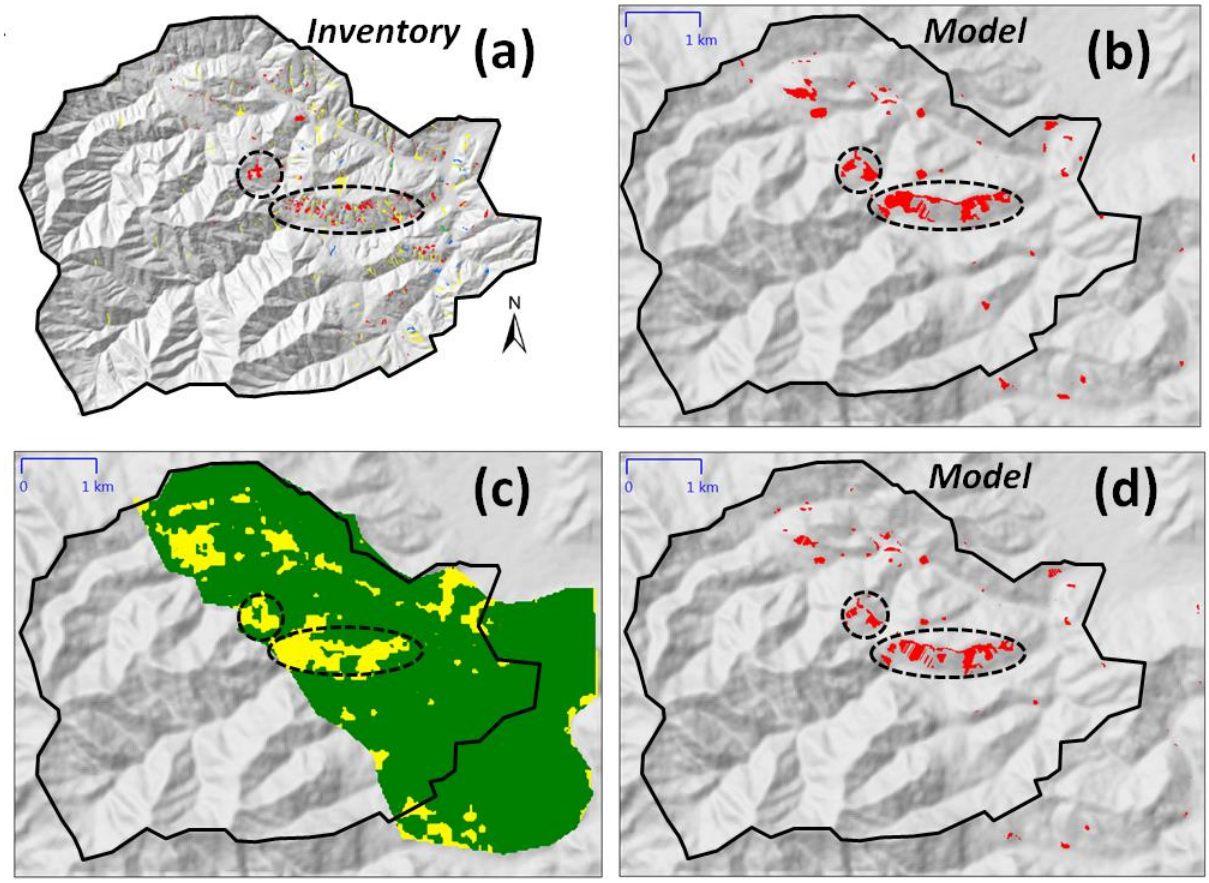

Figure 6: *Comparison of landslide inventory with simulations for Pogliaschina catchment. (a) Inventory map modified from Mondini et al. 2014 with soil slips in red and earth flows in yellow. (b) Landslide (in red) map resulting from simulation with sandy loam and stiffness ratio as a function of water content. (c) The vegetation map with forest in green and meadow in yellow indicates the simulated region. (d) Landslide (in red) map resulting from simulation with sandy loam and original stiffness ratio of zero. The dashed lines mark region with high landslide intensity. The figures show that the susceptible regions are captured by the model and highlight the role of forest cover on landslide triggering.*

In Figure 6 we show the landslides map resulting from simulations carried out for sandy loam for load redistribution rule as a function of water content θ (Fig. 7b; soil and root cohesion of 2 kPa, initial water saturation of 0.35) and original redistribution rule (Fig. 7d; soil cohesion 2 kPa, root cohesion 4 kPa, initial water saturation 0.25). From the comparison of the simulated landslide map with the landslide inventory map from Mondini et al. (2014), it is evident that the simulations reproduce the large density of landslides triggered in deforested areas.

In Figure 7a the number of landslides and cumulative landslide area are shown for the Pogliaschina catchment. In contrast to the similar plots shown in Figures 3a and 5 for “Napf2002” and “Napf2005”, we show here as well the results for other constant values of the stiffness ratios (K_2/K_1=1 or 2). Despite the small numbers of simulations, the figure reveals that the envelope of simulation results contains the inventory data. For this small set of simulations, the original stiffness ratio of zero provide better results in terms of landslide number and cumulated landslide area than the other adopted stiffness rules, but more simulations would be required to make a more definitive statement.

V. DISCUSSION

By changing soil type from sandy to silt loam, root reinforcement and soil cohesion between 1 to 4 kPa and initial water saturation between 0.2 and 0.7, the landslide number and total area changed by several orders of magnitude for the landslide inventories of Napf and Pogliaschina. Interestingly, simulations for the "Napf2002" catchment (see Figure 3a) indicate that only a relative narrow range of cumulative landslide area for a specific landslide number is possible. This means that in the simulations the average landslide size is relatively constant despite the existence of a few large landslides. Here we try to verify the existence of a narrow range of average landslide size with inventory data. In Figure 7b all landslide simulations are plotted together with eleven landslide inventories (WSL landslide database; and data from Rice et al., 1969; Rice and Foggin, 1971; Bellugi et al., 2015). The average landslide area for all simulations is quite similar and about 200 m^2.

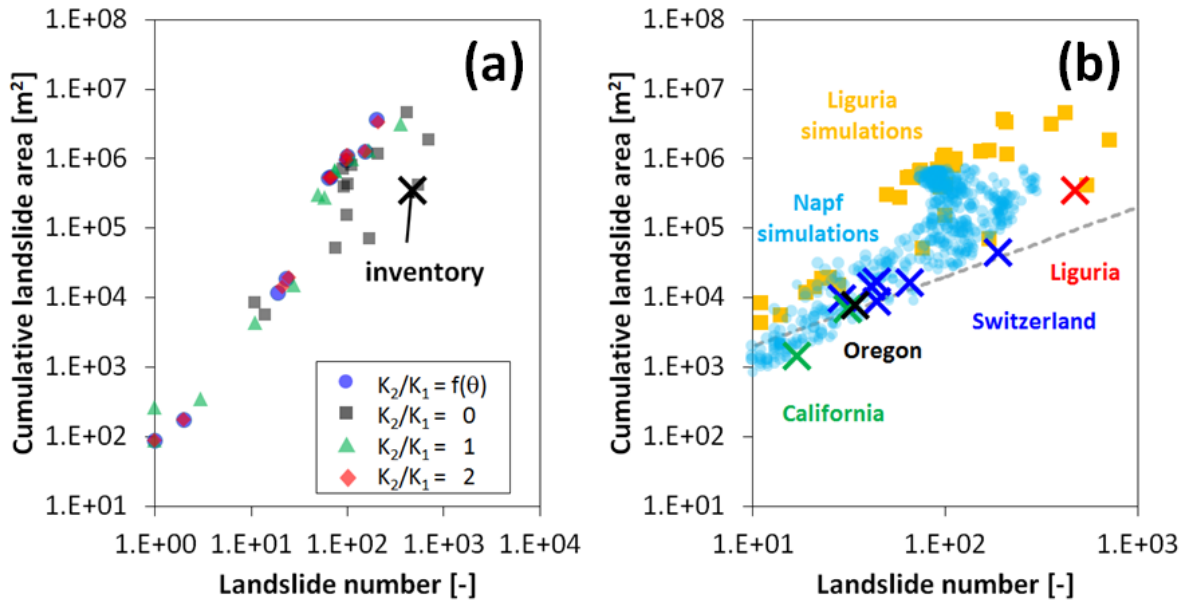

Figure 7: *Relationship between cumulative landslide area and landslide number for Pogliaschina catchment (a) and collection of other inventories (b). Inventories are marked by crosses, all other symbols stand for simulations with different soil properties and load redistribution rules. The dashed line that shows that an average landslide area of 200 m^2 captures most of the inventory data.*

To analyze the size distribution of the inventories in more detail, we show in Figure 8a the entire size distributions (cumulative distribution function, CDF) for the seven Swiss inventories collected by research institute WSL. The CDF shows that most of landslide areas are between 100

and 400 m^2. In Figure 8b the median and average are shown for the Swiss inventories and three other inventories. The median is considerably smaller than the average due to the existence of a few large landslides.

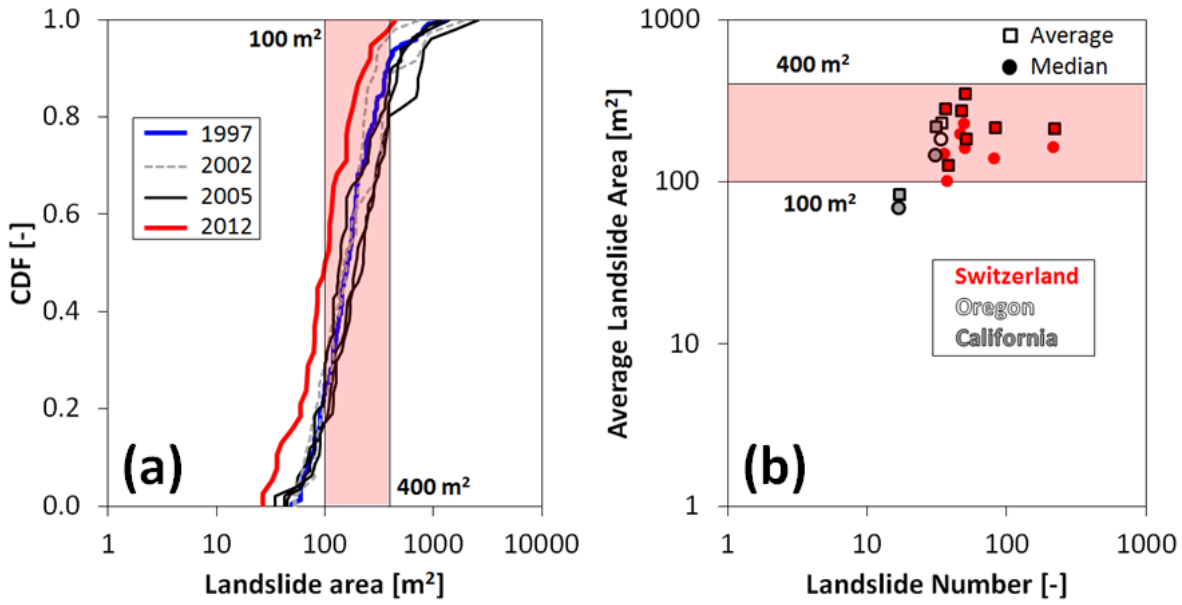

Figure 8: *Size distribution of rainfall induced shallow landslides collected in various landslide inventories. (a) Cumulative distribution function (CDF) for seven rainfall induced event based inventories from Switzerland (WSL landslide data base). The data were collected between 1997 and 2012 after the triggering rainfall event. The majority of landslides has an area between 100 and 400 m^2. (b) Average and median of landslide inventories including Swiss inventories and data from Rice et al., 1969; Rice and Foggin, 1971; and Bellugi et al., 2015.*

VI. SUMMARY AND CONCLUSIONS

We simulated rainfall induced shallow landslides in two small Swiss catchments (Napf 2002 and Napf 2005) and in a larger Italian catchment (Pogliaschina) using the publicly available landslide model STEP TRAMM. For the first time we applied this model concept with a relatively poor spatial resolution of 10 m and tested if inventory data can be reproduced (enabling to run many scenarios also for large catchments) and to test how sensitive the model outcome is with respect to parameterization of soil properties. The findings can be summarized as follows:

- Despite the poor spatial resolution we could reproduce inventory characteristics for Napf and Pogliaschina (landslide number and total landslide area and regions of large landslide density);

- Using soil cohesion and root reinforcement values calibrated for the Napf 2002 case study, the predictions for Napf 2005 were in fair agreement with inventories;
- We introduced a strength index to quantify the role of different soil parameters to condense and synthesize the dependency of simulation outputs on different soil parameter values;
- We implemented a new type of load redistribution rule that depends on soil type and water content to mimic different brittleness of soils but there were only minor effects on model outcome;
- The range of total landslide area assigned to a certain landslide number is relatively narrow for both simulations and inventories and the average landslide area in simulations and landslide inventories is between 200 and 400 m^2.

The findings of this study support the conclusion that the model concept of STEP TRAMM, that is based on threshold mechanics and simulation of progressive failure, can be applied successfully for larger catchments (in the range of up 100 km^2).

REFERENCES

Bellugi, D. G. Milledge, W. E. Dietrich, J. T. Perron, and J. McKean (2015), Predicting shallow landslide size and location across a natural landscape: Application of a spectral clustering search algorithm, J. Geophys. Res. Earth Surf., 120, 2552–2585, doi:10.1002/ 2015JF003520.

Brooks, R. J., and A. T. Corey (1964), Hydraulic properties of porous media, Hydrology Paper 3, Colorado State University, Fort Collins.

Casadei, M., W. E. Dietrich, and N. L. Miller (2003), Testing a model for predicting the timing and location of shallow landslide initiation in soil-mantled landscapes, Earth Surf. Processes Landforms, 28(9), 925–950, doi:10.1002/esp.470.

Cohen, D., P. Lehmann, and D. Or (2009), Fiber bundle model for multi-scale modeling of hydromechanical triggering of shallow landslides, Water Resour. Res., 45, W10436, doi:10.1029/2009WR007889.

Daniels, H. E. (1945), The statistical theory of the strength of bundles of threads: I, Proc. R. Soc. London Ser. A, 183, 405–435.

Dietrich, W. E., R. Reiss, M.-L. Hsu, and D. R. Montgomery (1995), A process-based model for colluvial soil depth and shallow landsliding using digital elevation data, Hydrol. Processes, 9(3-4), 383–400, doi:10.1002/hyp.3360090311.

Fan, L., Lehmann, P., & Or, D. (2016). Load redistribution rules for progressive failure in shallow landslides: Threshold mechanical models. *Geophysical Research Letters*, *44*(1), 228-235.

Fernandes, N. F., R. F. Guimaraes, R. A. T. Gomes, B. C. Vieira, D. R. Montgomery, and H. Greenberg (2004), Topographic controls of landslides in Rio de Janeiro: Field evidence and modeling, Catena, 55, 163–181.

Guzzetti, F., A. Carrara, M. Cardinali, and P. Reichenbach (1999), Landslide hazard evaluation: A review of current techniques and their application in a multi-scale study, central Italy, Geomorphology, 31, 181–216.

Iverson, R. M. (2000), Landslide triggering by rain infiltration, Water Resour. Res., 36(7), 1897–1910.

Iverson, R. M., M. E. Reid, N. R. Iverson, R. G. LaHusen, M. Logan, J. E. Mann, and D. L. Brien (2000), Acute sensitivity of landslide rates to initial soil porosity, Science, 290, 513–516.

Hengl T, de Jesus JM, MacMillan RA, Batjes NH, Heuvelink GBM, et al. (2014) SoilGrids1km — Global Soil Information Based on Automated Mapping. PLoS ONE 9(8): e105992. doi:10.1371/journal.pone.0105992 ISRIC – World Soil Information, 2013.

Khosravi, A., and McCartney, J. S. (2011). " Resonant column test for unsaturated soils with suction-saturation control. " J. ASTM Geotech Test., 36(6), 730 – 739.

Lehmann, P., and D. Or (2012), Hydromechanical triggering of landslides: From progressive local failures to mass release, Water Resources Research, 48(3).

Lu, N., J. Godt, and D. T. Wu (2010), A closed form equation for effective stress in unsaturated soil, Water Resour. Res., 46, W05515, doi:10.1029/2009WR008646.

Lu, N., & Kaya, M. (2014). Power law for elastic moduli of unsaturated soil. *Journal of Geotechnical and Geoenvironmental Engineering*, *140* (1), 46-56.

Michlmayr, G., D. Cohen, and D. Or (2012), Sources and characteristics of acoustic emissions from mechanically stressed geologic granular media — A review, Earth Sci. Rev., 112(3), 97 – 114.

Mondini, A. C., Viero, A., Cavalli, M., Marchi, L., Herrera, G., & Guzzetti, F. (2014). Comparison of event landslide inventories: the Pogliaschina catchment test case, Italy. *Natural Hazards and Earth System Sciences*, *14* (7), 1749.

Montgomery, D. R., and W. E. Dietrich (1994), A physically based model for the topographic control on shallow landslides, Water Resour. Res., 30(4), 1153–1171.

Ng, C. W. W., Xu, J., and Yung, S. Y. (2009). " Effects of imbibition-drainage and stress ratio on anisotropic stiffness of an unsaturated soil at very small strains. " Can. Geotech. J., 46(9), 1062 – 1076.

O'Loughlin, C. L., and A. J. Pearce (1976), Influence of Cenozoic geology on mass movement and sediment yield response to forest removal, North Westland, New Zealand, Bull. Eng. Geol. Environ., 13, 41–46.

Peirce, F. T. (1926), Tensile tests for cotton yarns, V: The weakest link, J. Textile Inst., Trans., 17, 355–368.

Petley, D. N., T. Higuchi, D. J. Petley, M. H. Bulmer, and J. Carey (2005), Development of progressive landslide failure in cohesive materials, Geology, 33, 201–204.

Raetzo, H., and C. Rickli (2007), Rutschungen, in Ereignisanalyse Hochwasser 2005: Teil 1—Prozesse, Schäden und erste Einordnung [in German] (Analysis of the 2005 Flooding Event. Part 1—Processes, Damages and First Assessments), edited by G. Bezzola and C. Hegg, pp.

195–209, Bundesamt für Umwelt BAFU, Birmensdorf, Eidgenössische Forschungsanstalt WSL, Bern.

Rawls, W. J., D. L. Brakensiek, and K. E. Saxton (1982), Estimation of soil water properties, Trans. Am. Soc. Agric. Eng., 25(5), 1316–1320.

Rice, R.M., E.S. Corbett, R.G. Bailey (1969), Soil slips related to vegetation, topography, and soil in Southern California, WRR, 5, 647-659.

Rice, R.M., and G.T. Foggin (1971), Effect of high intensity storms on soil slippage on mountainous watersheds in southern California, WRR, 7, 1485-1496.

Rickli, C., and F. Graf (2009), Effects of forests on shallow landslides—Case studies in Switzerland, For. Snow Landsc. Res., 82(1), 33–34.

Sawangsuriya, A., Edil, T. B., and Bosscher, P. J. (2009). " Modulus-suction-moisture relationship for compacted soils in postcompaction state. " J. Geotech. Geoenviron. Eng., 135(10), 1390 – 1403.

Schuettpelz, C. C., Fratta, D., and Edil, T. B. (2010). " Mechanistic corrections for determining the resilient modulus of base course materials based on elastic wave measurements. " J. Geotech. Geoenviron. Eng., 136(8), 1086 – 1094.

Stothoff, S. (2008), Infiltration tabulator for Yucca mountain: Bases and confirmation. Prepared for U.S. Nuclear Regulatory Commission, [Available at: http://pbadupws.nrc.gov/docs/ML0823/ML082350701.html.].

Tsai, T.-L., and J. C. Yang (2006), Modeling of rainfall-triggered shallow landslide, Environ. Geol., 50, 525–534.

Van Westen, C., A. E. Castellanos, and S. Kuriakose (2008), Spatial data for landslide susceptibility, hazard and vulnerability assessment: An overview, Eng. Geol., 102, 112-131.

Von Ruette, J., Lehmann, P., & Or, D. (2013). Rainfall-triggered shallow landslides at catchment scale: Threshold mechanics-based modeling for abruptness and localization. *Water Resources Research*, *49*(10), 6266-6285.

Wang, L., and Z. H. Shi. "Size selectivity of eroded sediment associated with soil texture on steep slopes." Soil Science Society of America Journal 79.3 (2015): 917-929.

Wu, T. H., W. P. McKinnel, and D. N. Swanston (1979), Strength of tree roots and landslides on Prince of Wales Island, Alaska, Can. Geotech. J., 16, 19–33.

2

Modelling rainfall-triggered landslides on Camaldoli Hill in the city of Naples: application of the STEP-TRAMM model

The work included in the second chapter was developed in collaboration with Dr. P. Lehmann (Soil and Terrestrial Environmental Physics - *STEP*, Institute of Biogeochemistry and Pollutant Dynamics, *ETH* – Zurich), Prof. Calcaterra and Dr. D. Di Martire (Department of Earth, Environment and Resources Sciences - *DISTAR* of the University of Naples Federico II) and with Prof. S. Vingiani and Prof. F. Terribile (Department of Agricultural Sciences - *DIA*, University of Naples Federico II). In this study, we implemented the model *STEP-TRAMM* to the Camaldoli hill, located within the urban district of the city of Naples (southern Italy) in order to detect main susceptible landslide areas and obtain useful information about the slope condition that triggered a typical past landslide event for Camaldoli hill. Due to its geological, geomorphological and pedological features (presence of andic soils), Camaldoli hill is a national priority in terms of landslide risk. We simulated 26 different possible scenarios, by changing initial water content, soil and root cohesion, soil texture, internal friction angle and the stiffness rule governing the load redistribution of failing soil elements. We evaluated the location and the cumulated areas of predicted landslides in comparison with position and areas of landslides from inventory and with the official landslide susceptibility map, available for Camaldoli hill. Our results revealed that, depending on the input parameter set, the model predicted (i) landslide positions with a maximum error of 30 m and (ii) cumulated landslide area of the same order of magnitude of cumulated area from inventory. . We also found a good agreement with total cumulated area for simulated landslides resulting from scenarios considering sandy loam soil texture, soil cohesion values of about 3 kPa and high values of the stiffness rule.

1. INTRODUCTION

Landslides are dangerous hazards that usually occur in natural environments. Nevertheless, during last century, the expansion of human activity and metropolitan areas has often taken place in regions located in steep mountainous regions or in lowlands between or under steep slopes. All over the world such a circumstance highly increased the exposure to this natural hazardous phenomena. *Sidle and Ochiai* (2006) estimated the direct costs associated to rebuilding or replacing infrastructures destroyed by landslides to several billion dollars per year all over the world. Among other Italian regions, the territory of the Campania region (southern Italy) is strongly exposed to hydrogeological risk, having the 92% of the municipalities enclosed (subjected, exposed) in a risky area (Palmieri, 2011). In Campania region, both (i) the highly urbanized foothill regions along the carbonate mountains bordering the Campanian plain and (ii) the Phlegrean Fields borders (slopes) are among the most landslide-prone areas of Italy. In the framework of landslides occurring in Campania, we consider flow-like mass movements affecting Camaldoli hill, which is located within the western part of the city of Naples (in Campania region - southern Italy). Among different landslide types and different material that can be involved in landslides, in this paper we focus on flow-like mass movements (Hungr et al., 2001) involving the soil cover originated from pyroclastic deposits and induced by intense and/or prolonged rainfall events. These landslide phenomena are typical of Campania region, where unconsolidated ash-fall deposits derived from both Somma-Vesuvius and Phlegrean field volcanic eruptions overlap a Mesozoic carbonate series (De Vita et al., 2006). Flow-like mass movements are characterized by high destructive power because they can rapidly travel across large distances with very high energy and, consequently, they can cause significant damage and injuries, especially when they occur in urban and very densely populated areas. Recent works from soil scientists have emphasized that flow-like mass movements in certain geographic domains are related to the occurrence of andic soils (Basile et al. 2003; Terribile et al, 2007, Scognamiglio et al., in preparation, Scognamiglio et al., 2016 a,b, Vingiani et al., 2015). In particular, in Campania region, they usually involve soils with andic properties developed from the pedogenesis of the previously mentioned loose ash and pumice fallout deposit. Because of an unique combination of properties, andic soils are highly fertile (Leamy, 1984) and, for this reason, they naturally have the potentiality to support some of the most densely populated areas of the world (Shoji et al., 1993; McDaniel et al., 2005). On the other side, andic soil properties affect the vulnerability to land degradation processes and the occurrence of flow-like movements (Arnalds et al., 2001; Fontes et al., 2004;

Basile et al., 2003; Scognamiglio et al., 2016 a,b; Scognamiglio et al., in preparation; Terribile et al., 2000; Terribile et al., 2007; Vingiani et al., 2015). Among their key properties, there are (i) large porosity (ii) low bulk density, (iii) friable structure, (iv) high water retention capacity and hydraulic conductivity near saturation, (v) short range order clay minerals (allophane, imogolite and ferrihydrite), (vi) high organic matter content, (vii) large reserves of easily weatherable minerals (Nanzyo, 2002; Vingiani and Terribile, 2006; Terribile et al., 2007). Even if Phlegrean soils exhibit andic features of variable degrees (degree) and sometimes not very pronounced (marked), on Camaldoli hill, in the uppermost humified layers, allophane is the dominant mineral associated with subordinate smectite and halloysite (Calcaterra et al., 2007). The formation of these secondary minerals is a process acting on the glass matrix available in the primary deposit. The high water conductivity typical of Camaldoli soils favours leaching and crystallization of hydrous aluminosilicates (formed during secondary mineralization processes). On the other side, the very high water retention plays a paramount role in affecting the soil stability because it is responsible of great weighting on deepest layers. Hence, both the high hydraulic conductivity and the high water retention capacity of Camaldoli soils have to be considered among the main predisposing factors of landslides because they crucially increase the vulnerability to land degradation phenomena: the hydraulic conductivity causes chemical alteration and/or physical erosion (Arnalds et al., 2001; Fontes et al., 2004) and the high water storage capacity dramatically increases the weight of the soil that can be consequently involved in a landslide phenomena (Terribile et al., 2000; Basile et al., 2003; Terribile et al., 2007).

1.1 Objectives and structure of the paper

In this study, we carry out a back analysis of the landslide event that occurred on January 10th -11th January 1997 on Camaldoli hill, located within the western sector of the territory of Naples. To pursue this objective, we implement for the first time ever for the western area of the city of Naples, the model STEP-TRAMM (Lehmann and Or, 2012), recently developed to simulate the triggering of shallow rainfall-triggered landslides. It is a non-traditional physically based landslide hydromechanical triggering model (LHT), linking key hydrological processes with threshold-based mechanical interactions (Lehmann and Or, 2012). We carried out landslide simulations to (i) obtain useful information about the hydraulic and physical conditions that existed at the time of the failure of the slope and (ii) detect most critical areas of Camaldoli slopes

where could possibly occur rainfall-triggered landslides. The idea to perform a back-analysis is strictly related to the circumstance that field observations on Camaldoli hillslopes showed that the same landslide detachment areas are often reactivated several times after the first occurrence. Hence, the information about the condition of the slope at the time of a past landslide event is required to (i) understand the dynamics and the extension of future failure mechanisms which could happen on Camaldoli hill and (ii) be used as a basis for setting up flow-like risk mitigation strategies aimed at defending both people living downhill (at the foothill of Camaldoli) and infrastructures, but also as a basis for soil conservation management policy aimed at protecting and preserving the very fertile (andic) soils settled on Camaldoli hill, having great agricultural potential and ecological importance for the city of Naples.

The current study is organized as follows: in section 2 we describe the geological and geomorphological settings of Camaldoli hill and we give a brief overview of landslide types and landslide records in the studied area; in section 3 some basic elements about how the LHT model works and what main theoretical differences it shows in comparison to other available models are given; in addition, in section 3, we also quantify the parameter space of soil key properties, required for the implementation of the LHT model. In section 4 landslide simulation results are compared to the landslide susceptibility map of Camaldoli hill and we discuss the relevance of the findings of the current study. The paper is closed in section 5 with summary and conclusions.

2. GEOLOGICAL AND GEOMORPHOLOGICAL SETTINGS OF CAMALDOLI HILL AND SLOPE MOVEMENTS

Camaldoli hill is settled within the western part of the metropolitan area of Naples, having a population density of more than 9000 inhabitants/km^2. It has a height of 458 m a.s.l. and is characterized by two main slopes having different aspect and very close to two highly populated districts: Pianura at the western footslope and Soccavo at the southern one.

Geologically (the geology of), Camaldoli hill mainly consists of volcanic products originated by Plio-Quaternary volcanism of the past 39 ky that markedly influenced the morphostructural setting of the Neapolitan-Phlegrean district. Such an intense volcanic activity was essentially due to the extensional tectonics that deformed the western margin of the Appenine and formed the graben structure of Campanian Plain (Calcaterra et al., 2007; Ippolito et al.,1973; D'Argenio et al., 1973; Finetti and Morelli, 1974; Bartole, 1984) (Figure 1). The stratigraphic sequence of Camaldoli hill is

very thick and mainly composed of different primary volcanic deposits and old-landslide, slope, plain and valley-bottom deposits related to water laid transport and slope movements. At the top of the sequence, volcanic products younger than 15 ky (having an average thickness of about 10 m) are settled. In particular, the upper part of these materials is composed by poorly consolidated and highly weathered soils, having a maximum thickness of 10m and homogenously mantling Camaldoli hill (Calcaterra et al., 2007).

From a geomorphological point of view, the general subsidence of Phlegrean Field caldera and the uplift of the central part of Neapolitan Yellow Tuff caldera played a crucial role in building up the complex morphology of this area. In detail, Camaldoli hill represents the north-eastern rim of the Phlegrean Field caldera, a morphological structure originated from two collapses related to the Campanian Ignimbrite (39 ka De Vivo et al., 2001) and the Neapolitan Yellow Tuff (15 ka Deino et al., 2004) volcanic eruptions (Calcaterra et al., 2007). The transverse profile of the hillslopes of Camaldoli hill can be ideally subdivided into four different parts: summit plateau, main slope, footslope, and basal plain. Because of its high to very high slope angle, the main slope is the only sector (i) not to be inhabited and (ii) where landslides usually originate. The structural setting of Camaldoli hill is characterised by two main fault systems, trending N–S and N80E, and by another subordinate N40W system. The N-S system includes vertical faults, active at least between 39 and 15 ka, which downthrown to west the geological units exposed on the western slope of the Camaldoli hill. The scarps exposed at the foot of the slope, bordering the Pianura plain to the east, result from the morphological evolution of fault planes (Calcaterra, 2007).

In recent years, several episode of slope movements, occurred in Naples and in other Campanian sites (January 1997, May 1998, September 2001, April 2002, December 2004 and March 2005), caused damage and injuries and pushed earth scientists, land planners and decision makers to develop studies aimed at evaluating landslide hazard and mitigating the related risks (Calcaterra et al., 2007; Di Martire et al., 2012). Concerning this question, the Italian government has declared the city of Naples, with a special emphasis on the Camaldoli hill, a national priority in terms of landslide risk mitigation (Calcaterra et al., 2007).

Depending on geomorphological conditions and the material involved, different type of landslides can occur on Camaldoli hill. In some cases, falls and topples take place on vertical or near vertical rock cliffs. Nonetheless, slides evolving to flows are the most common type of landslide and affect soil cover in the loosest surficial portion, in a thickness range between 0.5-1m, which is poorly consolidated and is mostly exposed to weathering. The triggering factor of such

shallow landslides is the occurrence of prolonged and/or intense rainfall phenomena. Furthermore, there are additional noteworthy predisposing factors to take into account for Camaldoli hill: (i) the negative effect of the anthropic activities on the slope, *i.e.* the presence of mountain pathways that interrupt the hydraulic and physical continuity of the soil cover (Basile et al., 2003) and modify the surface drainage network, (ii) the very high slope angle between 25° and 90° (in correspondence of vertical or subvertical cliff) and (iii) the andic features of the soil that, as previously discussed, contribute to increase the susceptibility of the soil to be involved in landslides. About the dynamics of landslides on Camaldoli hill, the involved material initially slides downslope and, during its displacement, it can evolve in flow when it is channelized in the pre-existent hydrographic network. Sometimes, the flowing material can only travel for short distances and then it stops along the slope. Consequently, such a circumstance cause the partial or the total temporary obstruction of the drainage pattern and a sudden deviation of the path of water. Even if the evolution of slides into flows is not particular frequent, the high slide-flow risk on the Camaldoli hill depends on the occurrence of such phenomena very close to the inhabited districts, located immediately downslope the hill. A different evolution of these landslides can result when the debris, which is stored within the deep and narrow valleys, is mobilized due to extraordinary rainfall events so that landslides evolve into hyperconcentrated streamflow. In these cases, large quantity of material, together with trees and solid wastes can flow till the mouth of the valley, as it happened during two events on 15th September 2001 and 5th April 2002 (Calcaterra et al., 2007)

During the time span 1886-1996 the slope movements which occurred in Naples seemed to progressively affect areas where urban expansion developed in the last ten years (Calcaterra et al., 2007). In the years 1996-1997, during the winter, many episodes of shallow slides, sometimes evolving to flows, happened on the Neapolitan hillslopes. The most important one occurred on January 10-11 January 1997 on Camaldoli hill (Calcaterra and Guarino, 1999 a,b) when about 300 rainfall-triggered shallow landslides involved the soil of Camaldoli hill and caused severe damage to man-made structures (Calcaterra et al., 2007).

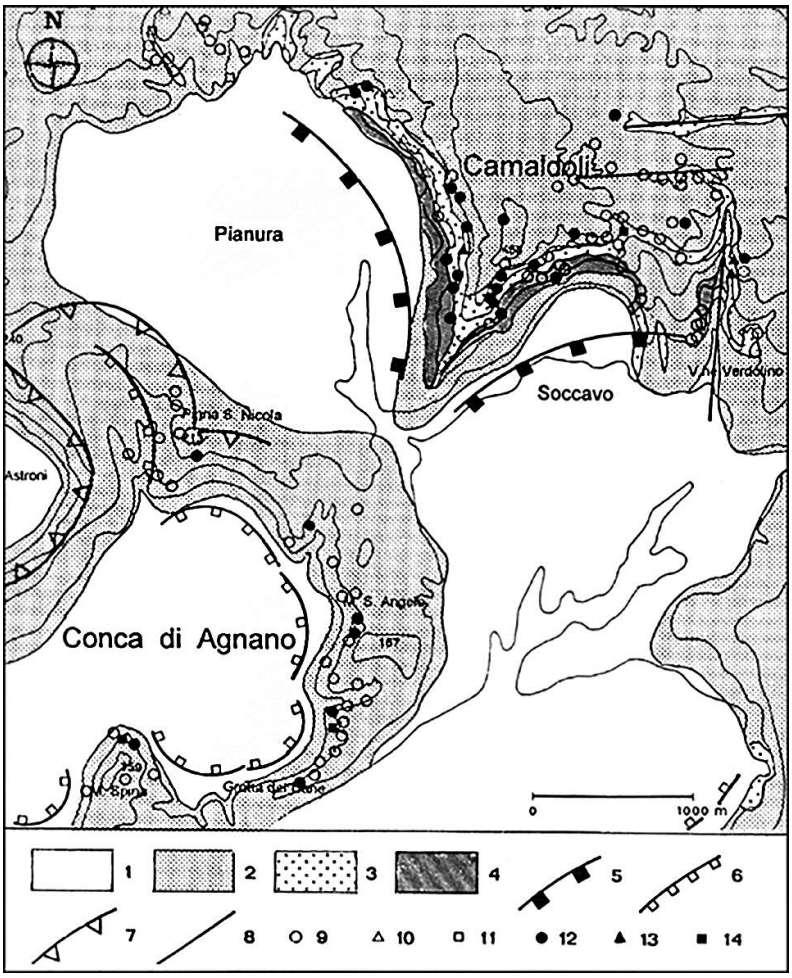

Figure 1: *Geological sketch and landslide inventory of the western urban area of Naples (after Calcaterra and Guarino, 1999a). Explanation: (1) reworked pyroclastics, alluvial deposits, fills; (2) loose pyroclastics younger than 15,000 years BP; (3) Neapolitan Yellow Tuff (about 15,000 years BP); (4) pyroclastics of the pre-NYT volcanic activity (Stratified Whitish Tuffs, Breccia Museo, Piperno, Torre Franco Tuffs); (5) rim of volcano-tectonic collapse (Phlegraean Caldera); (6) minor rim of volcano-tectonic collapse; (7) crater rim; (8) main fracture; (9) translational slide; (10) flow; (11) fall; (12) translational slide – flow; (13) fall – flow; (14) translational slide – fall. Contour interval 50m. (from Calcaterra, 2007. Modified)*

3. MATERIALS & METHODS

In this section we (i) illustrate the essential operating principles of the STEP-TRAMM model that we implemented to conduct the current study, (ii) list the input parameter set required to implement the model and (iii) present the input parameter space that we used for the selected case study.

3.2 Modelling Rainfall Triggered Landslides: the LHT (Landslide Hydromechanical Triggering) Model

The prediction of the triggering locations and the hydrological scenarios that predispose a slope to unstable conditions is typically carried out by means of statistical model or physically based models. The first ones link geomorphological and topographic features to the probability of landslide occurrence (Guzzetti et al., 1999; Van Western et al., 2008), whereas physically based models take into account the hydrological status and infiltration and subsurface water flow pathways in order to link them with the mechanical status of a hillslope. These models are conventionally based on the calculus of an indicator representing the mechanical status and the landslide susceptibility of a slope, the so-called factor of safety (FoS), defined as the ratio between resisting and driving forces acting on a slope. The FoS usually has a nonlocal definition within a hillslope (described as an assembly of large regions with similar FoS) but, contrariwise, evidence suggests that rainfall triggered landslides are abrupt and highly localized phenomena, whereby a large mass of soil is suddenly mobilized without apparent warning signals (Iverson et al., 2000). Hence, to carry out our study we applied a physically based landslide hydromechanical triggering (LHT) model which is publically available as software STEP-TRAMM (namely, STEP is the developing group and TRAMM is the acronym of Triggering RApid Mass Movements-http://www.step.ethz.ch/step-tramm.html), linking key hydrological processes with threshold-based mechanical interactions (Lehmann and Or, 2012). Respect to other models, it incorporates progression of local failures in a chain reaction culminating into hazardous mass release. Such a model is based on the idea that the local failures, preceding the triggering of landslides, are intended as real precursors of landslides themselves. In fact, local failures can be formed after a significant rainfall event and essentially represent internal damage within the soil cover. Since these “benign” internal local failures (i) can occur long before the whole soil mass is released and

(ii) provoke a weakening of the soil, they can literally be intended as actual precursors of the landslide process. In LHT model, the soil mantle overlying a hillslope is discretized into an assembly of hexagonal-shaped soil columns that are mechanically interconnected and interacting with the nearest neighbours by means of frictional and tensile mechanical bonds, represented by a bundle of mechanical fiber elements (Peirce, 1926; Daniels, 1945; Lehmann and Or, 2012), mimicking the mechanical behaviour of different soil elements (e.g. friction, cementing agents, capillary bridges, plant roots). Moreover, a further mechanical bond joins the base of each soil column to the bedrock surface (which is considered to be a preferential rupture surface). Each mechanical bond has a prescribed strength threshold mechanics, governing the landslide triggering process, that depends on soil type, water content state and root reinforcement (which generates additional cohesion to the soil). In the model, the process of landslide initiation strictly depends on threshold mechanics (Lehmann and Or, 2012). When the force on a given bond exceeds the basal friction threshold, the rupture occurs. After the rupture of a mechanical bond, the excess load is redistributed according to the load redistribution rule, governing the propagation of the rupture to the nearest neighbour soil columns by means of lateral bonds. In particular, the load redistribution rule defines the criterion to distribute and transfer the amount of excess load into two different directions: downslope by means of "compressive bonds" and upslope (or laterally) by means of "tensile bonds". To determine an appropriate load redistribution rule for each soil type, Fan et al. (2016) defined the stiffness ratio, K_2/K_1, a key parameter that quantifies the amount of load redistributed to intact bonds and is defined as the ratio between the load redistributed to downslope compressive bonds, K_2, and the load redistributed to upslope tensile bonds, K_1. Moreover, they also established links between such a theoretical stiffness ratio and measurable soil mechanical properties (Young's modulus *E* and Poisson's ratio *v*, which express the brittleness of a soil): in fact, large values of the stiffness ratio characterize soils with large E and small ν, which is typical of brittle materials (sand), whereas, small values of the stiffness ratio represent soils having small E and large ν, typical of ductile materials (clay) (Fan et al., 2016).

3.3 Landslide inventory data and input model parameter set

The previously described LHT model was applied to an area of interest enclosing both the two main slopes of Camaldoli hill (southward and westward), having a total dimension of of 8.47 km^2. We simulated one of the main rainfall-induced landslide events occurred on Camaldoli hill in

order to detect the most susceptible area which could be involved in rainfall-triggered landslides. The landslide event took place on 9^{th}-10^{th} January 1997 and developed on both western and southern slopes of Camaldoli hill. For such an event, we compared simulation results susceptibility map (Hydrographic District of southern Apennines, 2015).

3.3.1 Event Description and Rainfall Information

The triggering rainfall event lasted 40 hours and was characterized by a cumulated rainfall of 110 mm, a hourly peak intensity of 10 mm and a mean intensity of 2.7 mm. This rainfall event was preceded by a total cumulated precipitation of about 1000 mm in 4 months, which is a higher value than the mean annual rainfall (Calcaterra et al., 2007). Such a rainfall event triggered more than 300 landslides, mostly soil slide-debris flows, which essentially involved the loose soil of pyroclastic origin (Calcaterra et al., 2007).

We ran landslide simulations by applying an input rainfall signal having a hourly time-resolution and lasting the 40 hours preceding the event because (i) the triggering rainfall event was not characterized by a very high and narrow rainfall peak over a shorter period of time and, consequently, (ii) we hypothesize that landslides were triggered by the entire rainfall sequence covering the 40 hours preceding the event (Figure 2). The input rainfall signal was extracted from rainfall records by the Hydrological Annals (Idrographic Service of Naples, 1997).

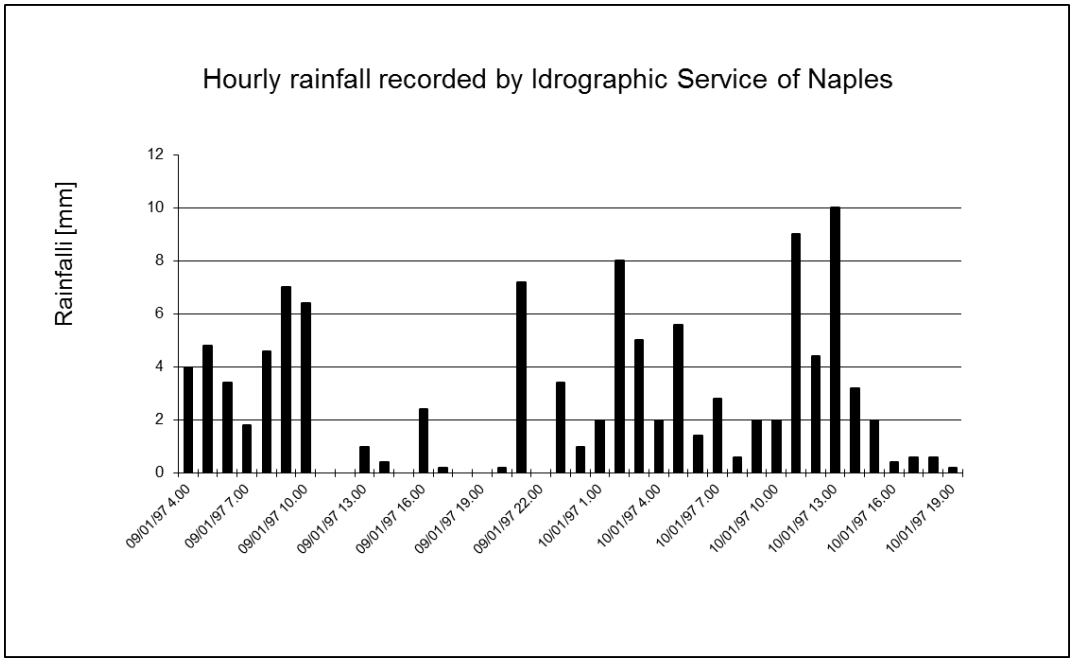

***Figure 2**: Rainfall sequence triggering the January 1997 landslide event. Such a rainfall amount was used as input rainfall signal for landslide simulations.*

3.4 Input Model Parameters

In addition to the rainfall input signal, the LHT STEP-TRAMM model (Lehmann and Or, 2012) required other information to be implemented for running landslide simulations. In the following, we list such information and we specify typical rage of values for key parameters of Camaldoli soils:

- Digital Terrain Model (DTM) to compute water flow and surface runoff: we used a DTM with 5x5m resolution cells obtained from Technical Regional Map (2004) (scale 1:5000).
- Vegetation pattern for the assessment of lateral root reinforcement: it simply consists of two classes, i.e. grassland and forest. We produced such a map by modifying the original land use map (Comune di Napoli, 1999) and by assigning it binary values representing vegetated and non-vegetated areas.
- Hydraulic functions to compute water flow. For sake of simplicity, we link Brooks and Corey (1964) soil hydrologic parameterization with the Lu et al. (2010) formulation for unsaturated soil strength so that the characterization of soil specific hydromechanical properties is based on one single parameter λ, obtained from the Brooks and Corey model (1964) describing soil water characteristic curve (Lehmann and Or, 2012). Each soil textural class is characterized by a typical value of the parameter λ (Rawls et al., 1982), which is also known as “pore size distribution index”. For the selected case study, object of this paper, the predominant soil textural classes of the catchments were obtained from granulometric curves available in literature (De Riso et al., 2002). In Figure 3 we show that the prevalent soil textures are loamy sand and sandy loam.
- Initial soil water saturation degree: we varied the value of this parameter in the range 20%-40%, extracted from literature data (De Riso et al., 2002) and representing typical water saturation values for Camaldoli soils during the winter season.
- Soil key mechanical properties are internal friction angle, mechanical soil cohesion, and root reinforcement. Camaldoli soils are characterized from the following values that we extracted from literature data (De Riso et al., 2002) and that we used to perform landslide simulations:
- friction angle varied in the range 30°-40° depending on soil texture: in particular, finer soil (*i.e.* sandy loam) were characterized by low internal friction angle (30°-35°), whereas coarser soil (*i.e.* loamy sand) showed typical highest friction angle values (35°-40°);
- soil cohesion varied in the range 2-4 kPa. Such values were obtained from field measurements covering a time span of two years;

- additional root cohesion 500-3500 kPa. Such values were hypothesize by considering the different species of vegetation characterizing Camaldoli hill.

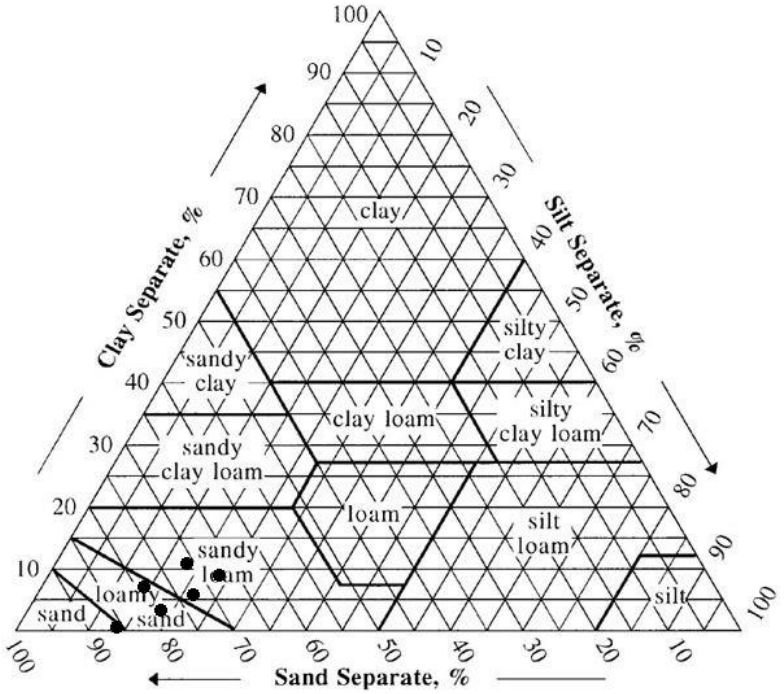

Figure 3: *Soil textural classes according to USDA (2006) for Camaldoli field samples (data from De Riso et al., 2002)*

4. RESULTS AND DISCUSSION

In this section, we show results of 26 simulations that we ran in order to (i) explore the sensitivity of key input parameters on landslide triggering, (ii) identify one or more input parameter set mostly representative of slope conditions at the time of the simulated landslide event (January 1997) and (iii) identify most critical zone of Camaldoli hill to be involved in landslides of the same type of the ones occurred on January 1997 (*i.e.* flow-like landslides). Among the 26 simulated scenarios, having different parameter sets in accordance with literature data (Table 1), 18 resulted in simulated landslides (having a variable pattern depending on the input parameter set), 1 did not simulate any landslide and 7 made the entire system unstable from the beginning of the rainfall event so that simulations stopped because more than 15% of the total study area failed (which is a non-realistic scenario). The computation time for scenarios that we tested was between 4 and 5 hours, depending on the number of load redistribution and chain reactions occurring during the rainfall event. For all simulations, we used an input rainfall signal with a hourly resolution having a total duration of 40 hours (*cfr.* Section 3.3.1 and Figure 2). In

figure 4 we report a typical landslide dynamics for one of the simulation carried out in this study to show that simulated landslides were triggered at the end of the rainfall event lasting 40 hours and that the trend of the triggered landslide volume was consistent with the amount of rainfall (the same for simulated landslide areas – data not shown). Since we were interested in exploring a certain range of soil properties and since the study area was relatively wide (8.47 km^2), we set the numerical resolution (*i.e.* the space resolution of the numerical grid) to 10 m not to increase (even) more the computation costs. In figure 5, we show an illustrative example of one simulation for Camaldoli hill with soil textural class sandy loam, soil cohesion 2 kPa, root strength 500 Pa, initial water saturation degree 20%, internal friction angle 35°. Depending on the input parameter set that we chose on the basis of reference values from literature (*cfr.* Section 3.4 and Table 1), simulated landslide areas had a greater or smaller extension than the ones reported in Figure 5. In Table 2 we report the cumulated landslide area for each simulated scenario. The 18 scenarios which resulted in landslides provided a total extension of the landslide area in a range between 10^{-2} km^2 and 10^0 km^2, depending on the input parameter set (Table 2). For the January 1997 landslide event, only the order of magnitude of cumulated landslide area, which is 10^{-1} km^2, was available because not all the detachment areas were surveyed in the field immediately after the event and often the rapid vegetation growth obliterated the real limit of the detachment areas, making impossible an exact evaluation of the total detachment area. Among the 18 simulated scenarios, 10 scenarios predicted a cumulated landslide area in good accordance the aforesaid order of magnitude from inventory, 4 simulations gave a cumulated area one order of magnitude smaller than value from inventory and the lasting 4 simulations predicted a landslide area one order of magnitude greater than value from inventory (Table 2). Notwithstanding the limited numerical resolution, the model reproduced a landslide pattern in good accordance with the real landslide pattern from inventory, by detecting most critical and weakest zones of Camaldoli hill (Figure 5) where flow-like landslides could be triggered if a rainfall event occurred with rainfall intensity/duration similar to the simulated one. Furthermore, the model generated localized patterns of mass release in the exact position or in the strict vicinity of real landslides (in a range of distance between 0 m and 40 m from real landslides) (Figure 5). We also underline that, due to the georeferentiation process, it is probable that the landslide positions of the inventory have an associated error of about 10 m.

By considering that simulated mass releases represent the weakest zones of the hill and hence the most susceptible areas where landslides could occur, we compared simulated landslide

extension with the landslide susceptibility map available for Camaldoli hill (Hydrographic District of southern Apennines, 2015) (Figure 6). In particular, such a susceptibility map is classified in 4 different classes: I_0 (no susceptible areas), I_1 (low susceptibility areas), I_2 (medium susceptibility areas), I_3 (high susceptibility areas). The susceptibility map resulted from the implementation of a semi-probabilistic approach (Amanti et al., 1996) which clusters the original area into 4 different classes (*i.e.* I_0, I_1, I_2 and I_3) by applying the natural break method (Jenks, 1967). Such a method is essentially based on the slope angle as main landslide predisposing factor.

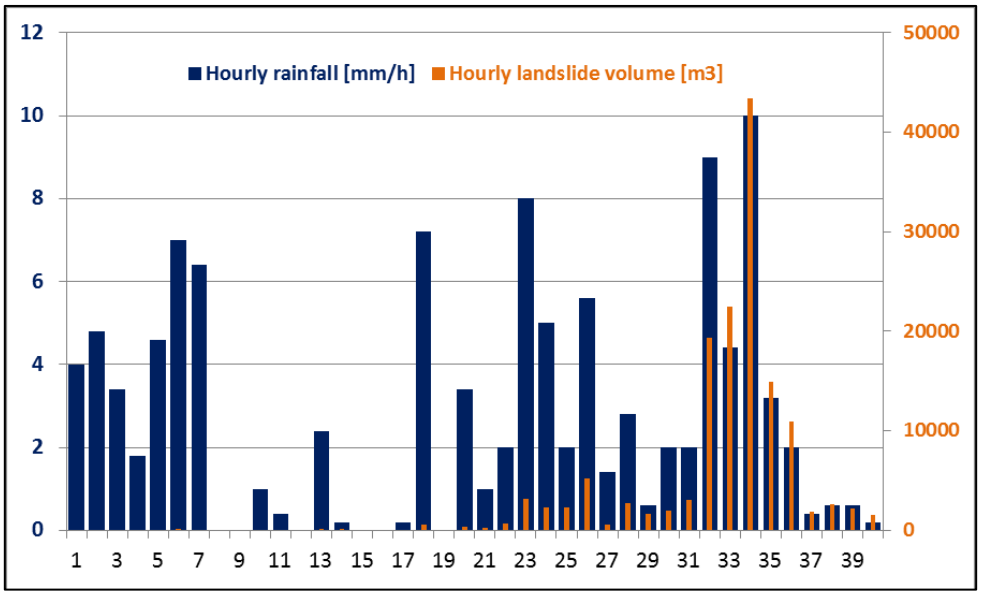

Figure 4: *Relationship between rainfall intensities (blue histogram) and failure dynamics (orange histogram) for one of the simulations carried out in this study. Numbers on x axis refer to the hourly time steps of the input rainfall signal. The rainfall event represented by the blue histogram coincides with the rainfall event reported in figure 2 that triggered the January 1997 landslides.*

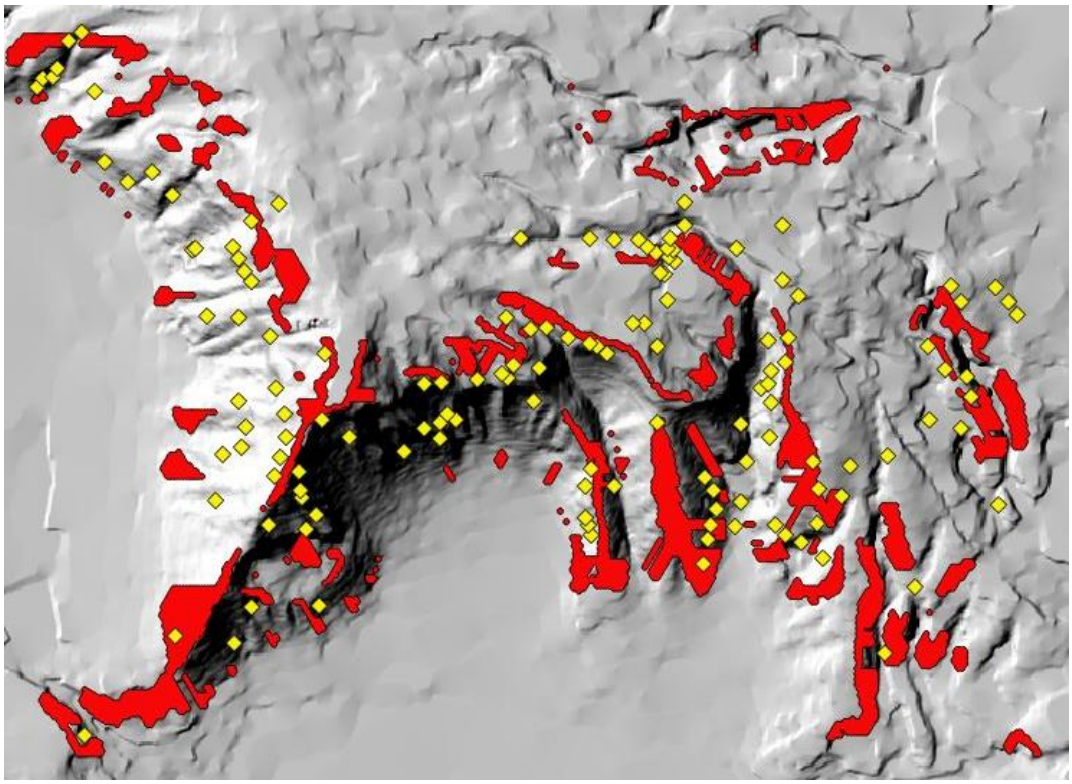

Figure 5: *Landslide map of the study area for simulation with soil textural class sandy loam, soil cohesion 2kPa, root strength 500Pa, intial water saturation degree 20%, internal friction angle 35°. The input rainfall signal had a hourly resolution with a total duration of 40 hours. Total study area is 8.47 km^2. In yellow, locations of landslides from inventory, whereas, red areas are simulated landslides.*

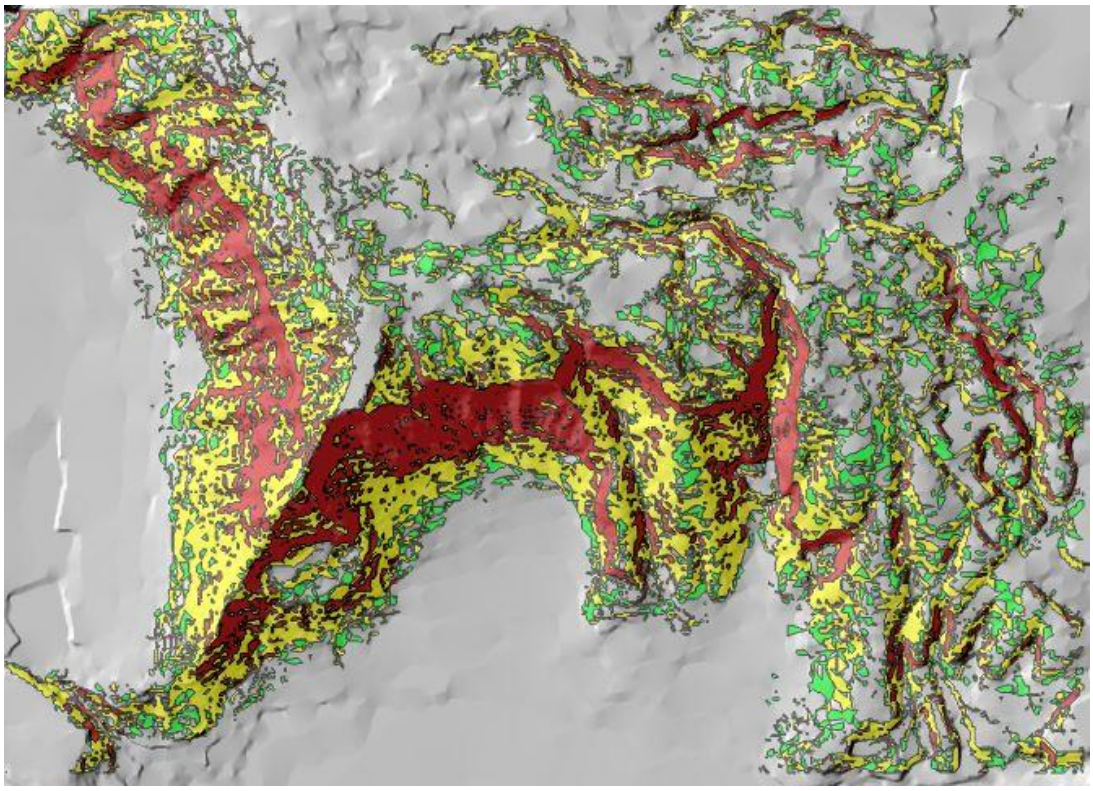

Total study area [km^2]	I_0 %	I_1 %	I_2 %	I_3 %
8.47	56.41	10.12	22.02	11.45

Figure 6: *Distribution of the entire area of interest in the classes I_0 (grey areas), I_1 (green areas), I_2 (yellow areas) and I_3 (red areas) of the susceptibility map for Camaldoli hill (Hydrographic District of southern Apennines, 2015). In the study area of Camaldoli hill, having a total dimension of 8.47 km^2, about the 56% of the total area falls in class I_0, the 10% in class I_1, the 22% in class I_2 and the 11% in class I_3.*

Among the 26 simulation results, we discarded the 8 non-realistic scenarios listed in Table 2 (*i.e.* 7 scenarios resulting in more than 15% of total study area being involved in landslides and 1 scenario that did not result in any landslide). The findings of remaining 18 landslide simulations are summarized in the following:

- in comparison to the order of magnitude of the total landslide area of the event, which is 10^{-1} km^2, simulations carried out by adopting the soil textural class sandy loam, were much more realistic, in terms of total simulated landslide area, resulting in cumulated landslide areas of the same order of magnitude of cumulated landslide area of the January 1997 event.
- Loamy sand texture revealed less realistic scenarios than sandy loam: in fact, all of the 7 simulations resulting in more than 15% of total study area being involved in landslides were carried out by using this soil texture.
- Model results were very sensitive to soil textural class (as previously discussed), soil cohesion and initial water saturation. In particular, for sandy loam soil texture, an increase of the initial soil cohesion of 2 kPa caused a decrease of the cumulated landslide area of one or two orders of magnitude. Moreover, by considering the total simulated area for sandy loam, possible soil cohesion values that predispose the hillslope to the instability were around 3 kPa. In fact, the soil cohesion value of 4 kPa that we tested for sandy loam gave too small simulated area for simulation number *15* and *5* and did not produce any landslide for simulation number *22*; on the other side, soil cohesion values of 2 kPa resulted in too high simulated area up to one order of magnitude bigger than cumulated landslide area from inventory (simulation numbers *1, 11, 20, 21*).
- root reinforcement and internal friction angle were less important than soil textural class, soil cohesion and initial water saturation in affecting simulation results.
- Overall, simulations carried out by applying lowest values of the stiffness ratio (*i.e.* $K_2/K_1=0$ and $K_2/K_1=1$) resulted in predicted area more extended than the ones obtained by applying $K_2/K_1=2$, both for sandy loam and loamy sand texture (Table 2), but more simulations would be required in order to confirm this first indication, suggesting that the soil involved in landslides on Camaldoli hill at the time of 1997 landslide was characterized by a low ductile behaviour. In fact, we remind that lowest values of the stiffness ratio are usually associated to ductile materials, whereas highest values represent brittle behaviour (*cfr.* Section 3.2).

Furthermore, the analysis of the distribution of simulated landslides resulting from the 18 *realistic* scenarios within the 4 susceptibility classes of the susceptibility map revealed that simulated areas were clustered not only in I_3 class of the map but within all of the different susceptibility classes. On average, for all of the 18 simulations, around the following values: 15% of simulated landslide areas falls in class I_3, the 50% in class I_2, the 20% in class I_1 and the 15% in class I_0 (Table 2). We highlight that the ostensible underestimation of landslide area in class I_3 and the ostensible overestimation in class I_1 and I_2 could be possibly due to: (i) a methodological gap between the semi-probabilistic approach used (Jenks, 1967; Amanti et al., 1996) to calculate the clustering into the different 4 susceptibility classes and to produce the susceptibility map (Hydrographic District of southern Apennines, 2015) and the physically-based LHT model implemented to predict landslides, considering not only the slope as landslide predisposing factor but also hydrological, physical and mechanical properties of the soil; (ii) the circumstance that the susceptibility map is not referred to the specific landslide event of 1997 that we simulated.

Nb.	Soil textural class	Soil Cohesion [Pa]	Root Cohesion [Pa]	Int. Frict angle [°]	Initial W.Sat. Degree [%]	stiffness ratio K_2/K_1
1	sandy loam	2000	1000	35	30	0
2	sandy loam	2000	3000	30	40	0
3	sandy loam	3000	1000	35	30	0
4	sandy loam	3000	5000	30	20	0
5	sandy loam	4000	1000	35	30	0
6*	Loamy sand	2000	1000	35	30	0
7*	Loamy sand	3000	1000	35	30	0
8*	Loamy sand	3000	1000	40	30	0
9	loamy sand	3000	5000	30	10	0
10	Loamy sand	4000	1000	35	30	0
11	sandy loam	2000	500	35	20	1
12	sandy loam	2000	1000	35	30	1
13	sandy loam	2000	3000	30	25	1
14	sandy loam	2500	3500	30	25	1
15	sandy loam	4000	1000	35	30	1
16*	loamy sand	2000	1000	35	30	1
17*	loamy sand	3000	1000	35	30	1
18*	loamy sand	3000	1000	40	30	1
19	loamy sand	4000	1000	35	30	1
20	sandy loam	2000	1000	35	30	2
21	sandy loam	2000	3000	30	25	2
22**	sandy loam	4000	1000	35	30	2
23	loamy sand	2000	1000	35	30	2
24	loamy sand	3000	1000	35	30	2
25	loamy sand	3500	500	35	22.5	2
26	loamy sand	4000	1000	35	30	2

Table 1: *Input parameter set of the 26 simulations carried out with the STEP-TRAMM model. The three block are for the three different stiffness ratio that we used (i.e. 0, 1, 2).*

** Scenario producing more than 15% of landslide areas. ** Scenario that did not produce landslides.*

Nb.	Tot. simulated landslide area [km^2]	% area in I_0	% area in I_1	% area in I_2	% area in I_3
15	0.005	11.28	15.18	60.43	13.10
26	0.013	20.07	16.54	43.19	20.20
2	0.031	21.16	20.38	47.59	10.87
5	0.061	16.32	17.14	49.63	16.91
4	0.160	17.56	18.00	51.04	13.40
13	0.308	19.37	18.89	50.34	11.40
14	0.308	19.32	18.89	50.34	11.45
19	0.432	13.35	15.65	54.71	16.28
3	0.497	18.00	16.41	48.46	17.13
21	0.503	20.56	20.18	48.83	10.43
25	0.543	17.52	17.06	50.39	15.04
10	0.664	14.68	14.48	54.92	15.92
20	0.695	19.27	18.98	49.59	12.16
11	0.735	20.26	17.11	49.38	13.26
12	1.072	16.00	15.86	52.08	16.06
1	1.147	16.18	15.47	52.10	16.25
9	1.189	14.67	14.17	48.88	22.28
24	1.317	17.49	16.29	48.14	18.08
22	no simulated landslides				
6	more than 15%				
7	more than 15%				
8	more than 15%				
16	more than 15%				
17	more than 15%				
18	more than 15%				
23	more than 15%				

Table 2: *Overview of the distribution of simulated landslide areas (based on parameter set from Table 1) within the classes I_0, I_1, I_2 and I_3 of the susceptibility map (Hydrographic District of southern Apennines, 2015). Numbers in the first column refer to simulation numbers of Table 1. Simulation results are sorted by increasing total simulated landslide area.*

5. SUMMARY AND CONCLUSIONS

Camaldoli hill (Southern Italy) is strongly exposed to rainfall-triggered landslide risk because of its geological and geomorphological setting, the pedological features of shallow soils mantling its hillslopes and its position within the municipality of the highly populated city of Naples. In this framework, we carried out landslide simulations by implementing a recently developed physical based LHT model, *i.e.* STEP-TRAMM. Our aim was to (i) evaluate the hydraulic and physical conditions that existed at the time of one of the main event occurred on Camaldoli hill and (ii) detect most susceptible area of Camaldoli slopes that could possibly be involved in rainfall-triggered landslides.

To simulate landslide triggering, it is required to study a certain range of soil properties. For large catchments, modelling different scenarios to determine most representative soil properties immediately before the rupture is time consuming. Due to the high computation time, we carried out 26 simulations with a limited numerical resolution (set to 10m). Nonetheless, the model was able to reproduce the main characteristics of landslide pattern and to predict landslides in the exact position or in the strict vicinity of landslide from inventory. Furthermore, cumulated landslide areas, predicted by the model, were in good accordance with inventoried cumulated area. Since mass releases occur in the most susceptible areas of the hillslopes, we compared simulated landslide areas with the official susceptibility map available for Camaldoli hill (Hydrographic District of southern Apennines, 2015) and we found that, for the input parameter sets that we chose, the simulated areas were in fairly good agreement with the susceptibility map. On average for the simulations that resulted in landslides, the 15% of total cumulated landslide area was located in the highest susceptibility class, the 50% in the medium and the 20% in the low susceptibility class. The distribution of simulated landslide areas within susceptibility classes I2 and I1 (and not only in the highest susceptibility class I3), was probably due to a discrepancy in the methodologic approach of the model applied to produce the susceptibility map and the LHT model that we applied to predict landslides.

We found more realistic scenarios by using (i) a sandy loam texture and (ii) soil cohesion values around 3 kPa. Root reinforcement and internal friction angle were less important than soil textural class, soil cohesion and initial water saturation in affecting simulation results.

Predicted cumulated areas were of the same order of magnitude or cumulated area from inventory for simulations carried out by applying $K_2/K_1=2$, which could be a clue of a not very ductile rheological behaviour of the soils involved in landslides on Camaldoli hill.

This results represent an indication of which could be weakest regions and which could be possible triggering scenarios on Camaldoli hillslopes, if a rainfall event, similar to the one that triggered the landslides of January 1997, occurred. However, more simulation of other possible triggering scenarios would be required and strongly encouraged in order to systematically explore the sensitivity of the input parameters on predicted landslides and to shrink the range of possible scenarios existing immediately before the triggering of the landslide event. Nonetheless, these results were unexpected because this is the first implementation ever of a landslide model for Camaldoli hill and also because we utilized a "*non-traditional"* and innovative LHT model, linking key hydrological processes with threshold-based mechanical interactions.

We highlight that the prediction of the occurrence of hazardous landslide phenomena in the vicinity of urban and highly populated districts, which are currently still in expansion (Di Martire et al., 2012), makes the evaluation of landslide hazard assessment of Camaldoli hill a crucial task to help decision makers and land planners to manage landslide risk in the metropolitan area of Naples and to protect the very fertile soils of Camaldoli hill, which represent a great agricultural potential for the city of Naples.

REFERENCES

Amanti M., Casagli N., Catani F., D'Orefice M., Motteran G. (1996) - Guida al censimento dei fenomeni franosi ed alla loro archiviazione. Miscellanea del Servizio Geologico Nazionale, VII, SGN, Roma, 109 pp. (in Italian)

Arnalds, O., Thorarinsdottir, E.F., Metusalemsson, S., Jonsson, A., Gretarsson, E. & Arnason, A. 2001. Soil Erosion in Iceland. Soil Conservation Service and Agricultural Research Institute, Reykjavik, Iceland.

Bartole, R., 1984. Tectonic structures of the Latian – Campanian shelf (Tyrrhenian sea). Boll. Oceanol. Teor. Appl. 2, 197 – 230.

Basile, A., Mele, G., Terribile, F. (2003) - Soil hydraulic behavior of a selected benchmark soil involved in the landslide of Sarno 1998. Geoderma, 117, 331–346.

Brooks, R., & Corey, T. (1964). HYDRAU uc Properties Of Porous Media. Hydrology Papers, Colorado State University.

Calcaterra, D., Coppin, D., De Vita, S., Di Vito, M.A., Orsi, G., Palma, B. and Parise, M., 2007. Slope processes in weathered volcaniclastic deposits within the city of Naples: The Camaldoli Hill case. Geomorphology, 87(3), pp.132-157.

Calcaterra, D., Guarino, P.M., 1999a. Dinamica morfologica e fenomeni franosi recenti nell'area collinare napoletana (settore occidentale). Geol. Tec. Ambientale 2/99, 11 – 17 (in Italian).

Calcaterra, D., Guarino, P.M., 1999b. Fenomeni franosi recenti nell'area urbana napoletana: il settore centro-orientale. Proc. Congr. C.N.R.-Regione Emilia Romagna " Geologia delle grandi Aree Urbane " , Bologna, 4 – 5 November 1997, pp. 257 – 261 (in Italian).

Daniels, H. E. (1945), The statistical theory of the strength of bundles of threads: I, Proc. R. Soc. London Ser. A, 183, 405–435.

D'Argenio, B., Pescatore, T.S., Scandone, P., 1973. Schema geologico dell'Appennino Meridionale. Quad. Acc. Naz. Lincei 183, 49 – 72 (in Italian).

Deino, A.L., Orsi, G., Piochi, M., de Vita, S., 2004. The age of the Neapolitan Yellow Tuff caldera forming eruption (Campi Flegrei caldera — Italy) assessed by 40Ar/39Ar dating method. J. Volcanol. Geotherm. Res. 133, 157 – 170.

De Riso, R., Evangelista, A., Pellegrino, A., & Mazzoleni, S. (2002). Stabilità delle coltri piroclastiche nelle aree collinari della città di Napoli. Atti XXI Conv. Naz. di Geotecnica, L'Aquila, 143-155. (in Italian).

De Vita P., P. Celico, P. Siniscalchi and R. Panza (2006b) - Distribution, hydrogeological features and landslide hazard of pyroclastic soils on carbonate slopes in the area surrounding Mount Somma-Vesuvius (Italy). Italian Journal of Engineering Geology and Environment, 1, pp. 75-98.

De Vivo, B., Rolandi, G., Gans, P.B., Calvert, A., Bohrson, W.A., Spera, F.J., Belkin, A.E., 2001. New constraints on the pyroclastic eruption history of the Campanian volcanic plain (Italy). Mineral. Petrol. 73, 47 – 65.

Di Martire, D., De Rosa, M., Pesce, V., Santangelo, M.A. and Calcaterra, D., 2012. Landslide hazard and land management in high-density urban areas of Campania region, Italy. Natural Hazards and Earth System Sciences, 12(4), p.905.

Fan, L., Lehmann, P., & Or, D. (2016). Load redistribution rules for progressive failure in shallow landslides: Threshold mechanical models. Geophysical Research Letters, 44(1), 228-235.

Finetti, I., Morelli, C., 1974. Esplorazione sismica a riflessione dei Golfi di Napoli e Pozzuoli. Boll. Geofis. Teor. Appl. 16 (62/63), 175 – 222 (in Italian).

Fontes, J.C., Pereira, L.S. & Smith, R.E. 2004. Runoff and erosion in volcanic soils of Azores: simulation with OPUS. Catena, 56, 199–212.

Guzzetti, F., A. Carrara, M. Cardinali, and P. Reichenbach (1999), Landslide hazard evaluation: A review of current techniques and their application in a multi-scale study, central Italy, Geomorphology, 31, 181–216.

Hungr O., S.G. Evans, M.J. Bovis and J.N. Hutchinson (2001) - A review of the classification of landslides of flow type. Environmental and Engineering Geoscience, 7, pp. 221-238.

Ippolito, F., Ortolani, F., Russo, M., 1973. Struttura marginale tirrenica dell'Appennino Campano: reinterpretazione di dati di antiche ricerche di idrocarburi. Mem. Soc. Geol. Ital. 12, 227 – 250 (in Italian).

Iverson, R. M. (2000), Landslide triggering by rain infiltration, Water Resour. Res., 36(7), 1897–1910.

Iverson, R. M., M. E. Reid, N. R. Iverson, R. G. LaHusen, M. Logan, J. E. Mann, and D. L. Brien (2000), Acute sensitivity of landslide rates to initial soil porosity, Science, 290, 513–516.

Jenks G.F. (1967) – The data model concept in statistical mapping. International Yearbook of Cartography, 7, 186- 190.

Leamy, M.L. 1984. Andisols of the world. p. 369-387. In Comm. Congr. Int. Suelos Volcan. Secretariado de Publicaciones Serie Informes 13, Universidad de la Laguna, La Laguna, Spain.

Lehmann, P., and D. Or (2012), Hydromechanical triggering of landslides: From progressive local failures to mass release, Water Resources Research, 48 (3).

Lu, N., J. Godt, and D. T. Wu (2010), A closed form equation for effective stress in unsaturated soil, Water Resour. Res., 46, W05515, doi:10.1029/2009WR008646.

McDaniel, P.A., Wilson, M.A., Burt, R., Lammers, D., Thorson, T.D., Mcgrath, C.L. et al. 2005. Andic soils of the inland Pacific Northwest, USA: properties and ecological significance. Soil Science, 170, 300–311.

Nanzyo M. (2002) - Unique properties of volcanic ash soils. Global environmental research, 6 (2), 99-112.

Palmieri W. (2011) - Per una storia del dissesto e delle catastrofi idrogeologiche in Italia dall'Unità ad oggi (in Italian), National Research Council of Italy, Quaderno ISSM n. 164.

Peirce, F. T. (1926), Tensile tests for cotton yarns, V: The weakest link, J. Textile Inst., Trans., 17, 355–368.

Rawls, Walter J., D. L. Brakensiek, and K. E. Saxtonn. "Estimation of soil water properties." Transactions of the ASAE 25, no. 5 (1982): 1316-1320.

Scognamiglio, S., Calcaterra, D., Iamarino, M., Langella, G., Orefice, N., Vingiani, S., & Terribile, F. (2016a). Andic soil features and debris flows in Italy. New perspective towards prediction. In *EGU General Assembly Conference Abstracts* (Vol. 18, p. 10543).

Scognamiglio, S., Terribile, F., Iamarino, M., Orefice, N., & Vingiani, S. (2016b). Soil properties and debris flows in Italy: potential relationships. *RENDICONTI ONLINE SOCIETA GEOLOGICA ITALIANA*, *41*, 199-202.

Shoji, S., M. Nanzyo, and R.A. Dahigren. 1993. Volcanic ash soils: Genesis, properties and utilization. Elsevier, Amsterdam, Netherlands.

Shoji, S., M. Nanzyo, and R.A. Dahigren. 1993. Volcanic ash soils: Genesis, properties and utilization. Elsevier, Amsterdam, Netherlands.

Sidle, R. C., and H. Ochiai (2006), Landslides: Processes, Prediction and Land Use, American Geophysical Union, Washington, DC.

Terribile F., Basile, A., De Mascellis R., Di Gennaro A., Mele G., Vingiani S. (2000) – I suoli delle aree di crisi di Quindici e Sarno: proprietà e comportamenti in relazione ai fenomeni franosi. Quaderni di Geologia Applicata, 7 (1), 59-79.

Terribile, F., Basile, A., De Mascellis, R., Iamarino, M., Magliulo, P., Pepe, S., Vingiani S. (2007) – Landslide processes and Andosols: the case study of the Campania region, Italy. In: O.

Arnalds, F.Bartoli, P.Buurman, H. O´ Skarsson, G. Stoops, & E. Garcıa-Rodeja (eds.), Soils of Volcanic Regions in Europe (eds O. Arnalds, F Bartoli, P Buurman, H O´ skarsson, G Stoops, & E Garcı´a-Rodeja), pp. 545–563. Springer Verlag, Berlin and Heidelberg, 545–563.

USDA 2006 Keys to Soil Taxonomy, 10th edn. United States Depart- ment of Agriculture NRCS, Washington, DC. USDA-NRCS

Van Western, C., A. E. Castellanos, and S. Kuriakose (2008), Spatial data for landslide susceptibility, hazard and vulnerability assessment: An overview, Eng. Geol., 102, 112-131.

Vingiani, S., Mele, G., De Mascellis, R., Terribile, F., Basile, A. (2015). Volcanic soils and landslides: A case study of the island of Ischia (southern Italy) and its relationship with other Campania events. Solid Earth, 6 (2), pp. 783-797. DOI: 10.5194/se-6-783-2015

Vingiani, S. and Terribile, F., 2006. Properties, geography, classification and management of volcanic ash soils: an overview. Acta Volcanologica, 18(1/2), p.113.

3

Relationship between soil depth and plan curvature of flow-like detachment areas at Mt. Camposauro (southern Italy)

The work included in the third chapter was developed in collaboration with Dr. M. Iamarino, Dr. P. Moretti, Prof. F. Terribile, Dr. G. Turco and Prof. S. Vingiani of the Department of Agricultural Sciences (*DIA*) - University of Naples Federico II. In this study, within the general framework of evaluating the potential applicability of STEP-TRAMM to other Campanian environments, we made a preliminary estimation of the soil depth variability in detachment areas of landslides occurred on the northern slope of Mt. Camposauro (southern Apennines), where landslides involve Andosols. The estimation of soil depth variability in this region of interest is an essential requirement to implement dynamic landslide models. At the local scale, we measured soil depth in 10 representative detachment areas of flow-like landslides, selected from the IFFI archive. Then, we evaluated the relationship between soil depth and plan curvature (a geomorphological index which affects the erosion-deposition processes of the soil-forming materials) of the considered slope. Such a relationship showed that soil depth increases (i.e. from 0.40 to 0.54 m of soil depth) from the watershed (class 1) to linear slope (class 5) and then decreases (i.e. from 0.54 to 0.23 m) from the linear slopes (class 5) to the ridges (class 9). The described relationship would be useful to estimate indirectly soil depth on the entire slope. we spatialized such information by means of quantitative morphological indices. In general terms, our study revealed that the distribution of the soil was very complex and that the soil depth varies as a function of the different geomorphological contexts on the hillslope. Such important variability, presently is not considered by the model; thus STEP-TRAMM cannot be efficiently applied to this study area.

Introduction

The territory of Campania region (southern Italy) is highly exposed to hydrogeological risk (Palmieri 2011, 2011). In particular, flow-like landslides (Hungr et al., 2011) represent one of the most severe and dangerous geohazard of Campania region. Besides the geomorphological, hydrological and physical landslide predisposing factors commonly recognized (Del Prete et al., 1998; Calcaterra et al., 1999; Guadagno et al., 2005; Di Crescenzo and Santo, 2005; Cascini et al., 2008; De Vita et al., 2013; Cascini et al., 2008; Cascini et al., 2010; De Vita et al., 2013), in recent studies soil scientists suggested that the occurrence of flow-like landslides is also related to the presence of andic soils (i.e. soils affected by andosolization process). Indeed, in different environmental Italian contexts, in particular for Campania region, flow-like landslides are related to the presence of Andosols (IUSS Working Group WRB, 2015), suggesting a pedological control on flow-like phenomena (Basile et al., 2003; Scognamiglio et al., 2016 a,b; Scognamiglio et al., in preparation; Terribile et al., 2000; Terribile et al., 2007; Vingiani et al., 2015). In fact, Andosols are characterized by a peculiar set of chemical, physical, hydrological and mineralogical properties that predispose the soil to instability. Among the main properties of Andosols related to flow-like landslides, there are (i) large porosity, (ii) low bulk density, (iii) friable consistence and fluffy structure, (iv) high water retention capacity and hydraulic conductivity at quasi-saturated and saturated conditions, (v) short range order clay minerals (such as allophane, imogolite and ferrihydrite), (vi) high susceptibility to soil liquefaction (Nanzyo, 1993 and 2002; Picarelli et al, 2008). Therefore andic soils are very fragile and highly susceptible to land degradation processes, such as erosion (Arnalds et al., 2001; Fontes et al., 2004) and landslides (Basile et al., 2003; Scognamiglio et al., 2016 a,b; Terribile et al., 2000; Terribile et al., 2007; Vingiani et al., 2015).

In this work, we focus our attention on flow-like landslides involving the mountain forest environment of the northern slope of Mt. Camposauro (southern Apennines), in the Telesina Valley (Campania region). This area is of primary interest for flow-like landslides that often occur in the *colluvium* and threaten the inhabited districts located immediately downslope. The mountain environments of the northern slope of Mt. Camposauro could be predisposed to flow-like hazard because of the four following reasons: (i) the soil map of Telesina Valley (Regione Campania, 2002) reveals the presence of Andosols on this slope, (ii) the north aspect of the slope could be an indirect landslide predisposing factor because frequently soils settled on north facing slopes are considerably deeper than those on south facing slopes (Terribile et al., 2007). The high thickness of

the soil could provide a significant potential of water storage, responsible of great weight and high pressure (both considered main landslide predisposing factors) on deepest layers (Scognamiglio et al., in preparation; Terribile et al., 2007; Vingiani et al., 2015); (iii) the northern hillslope of Mt. Camposauro is characterized by high and very high slope angles (20-45°); (iv) the frequent road cuts of the pedo-continuity act as a risk factor because they can cause hydraulic anisotropy (Basile et al., 2003).

In this framework, the estimation of the soil depth is an essential factor to take into account for the evaluation of the landslide susceptibility in this environment. Furthermore, information on soil thickness are also necessary towards practical applications, such as the implementation of landslide dynamic models, taking into account the role of the soil depth in affecting the landslide susceptibility. Geographic Information Systems (GIS) allow the management of study areas information to carry out a geo-morphometric analysis of the sites with determination of the main morphometric parameters. The importance of this information is due to the fundamental role of the topography in conditioning the processes of the hydrological and erosive cycle of the mountain basins. From the basic parameters, more articulate indices (such as profile curvature, plan curvature and topographic wetness index) have been developed. Particular interpretative meaning has the plan curvature of the slopes, which shows the variation of the slope shape in the space.

Hence, since soil depth is considered to be an important landslide predisposing factor, the aim of this work is to estimate soil depth on the north-facing slope of Mt. Camposauro, in areas both involved and potentially involved by landslide phenomena. In order to properly implement such information in dynamic landslide models, we measured soil depth in 106 points distributed within 10 landslide areas representative of different sectors of the slope.

Environmental setting

By the geological point of view, the Telese Valley is an intra-apennine graben approximately East-West oriented. Two main sectors (East and West) divided by a N-S oriented fault were identified. The valley is bordered by an important fault, almost entirely buried, along which the carbonatic massif of M.te Camposauro is built. Such tectonic complexity results in a strong asymmetry of the valley. In the northern sector there are apennine (NW-SE) and anti-appennine (NE-SW) faults.The foothill deposits of the M.te Camposauro are very gravel, in alluvial fan facies

(consisting of limestone and calcareous-dolomitic clasts in a matrix of volcanic origin). The oldest fan deposits rest on cemented breccia.

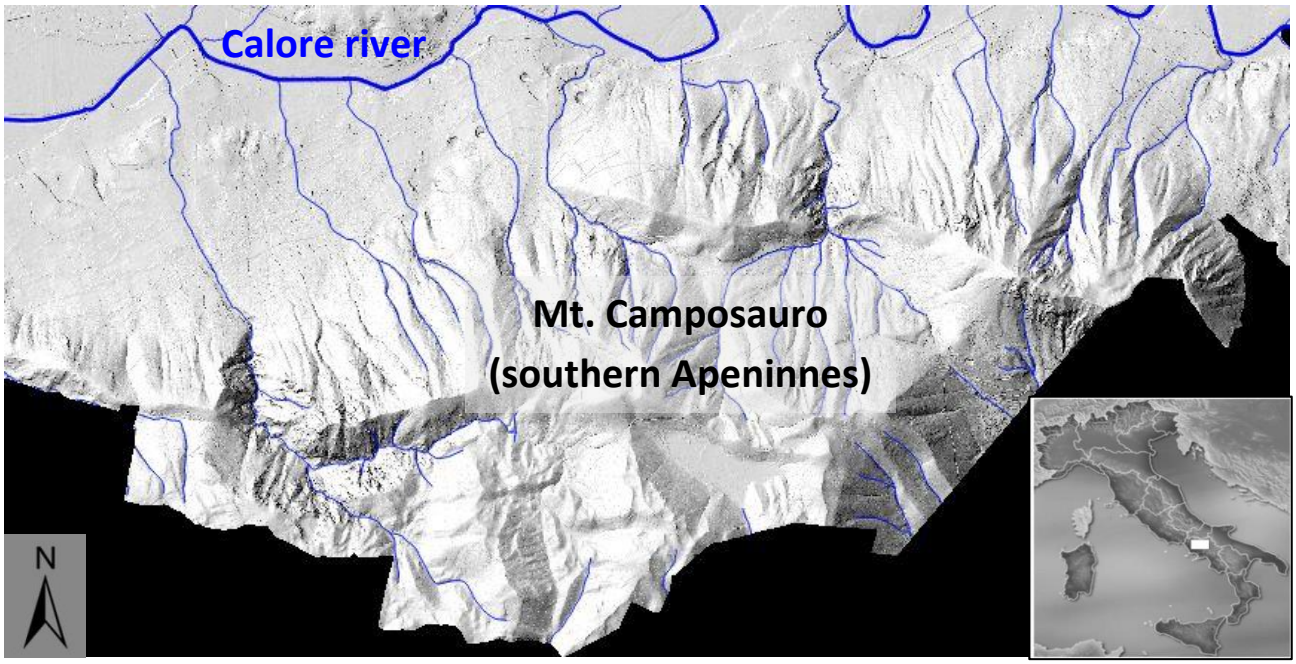

Figure 1: *North facing slope of Mt. Camposauro. The inset shows the location of the study area in Italy.*

On the basis of the soil map (Regione Campania, 2002), both the Intermountain Plain System (mainly represented by foothill detritic-colluvial areas) and the Apennine Mountain System (made by limestone relief) are involved by the flow-like landslide phenomena.

The transition area between the Mt. Camposauro and the alluvial plain of the Calore River includes the alluvial fans and detritic deposits originated from the dismantling of the mountain relief. Here pyroclastic deposits (primary or reworked deposits) alternated with coarse calcareous sediments (i.e. breccia). Altitudes are between 60 and 400 m asl. The environment of the mountain relief is characterized by high-to-very high energy, where the slopes are straight to very steep, often with gorges. Altitudes are typically between 150 and 1390 m asl.

The forestry cover of the Telese Valley has an extension of 6082 ha, 3038 of which are located on the orographic left of the Calore River and cover the M.te Camposauro. The forests of orno-ostriets occupy 1850 ha of the wooded area and represent the forestry type mainly present in the study area. They include species with a high degree of rusticity and ecological flexibility, such as the black horn and the ornate. This category includes both mesophilic and mesoxerofile orno-ostriets. Formations are mainly cedar, but they are also found in neo-formed secondary

forests. These formations have a high ecological spectrum and are spread in different altimetric ranges (between 95 and 1235 m asl), different soils and geomorphological conditions. Subordinately, beechwood (755 ha, altitude between 1025-1180 m. asl), planks (188 ha, altitude between 540-825 m asl), chestnuts, mesophiles and fruit (196 ha altitude between 545 and 1015 m asl), and oaks (roverella) (50 ha) are also found.

Materials and methods

The identification and selection of the studied landslides was done from the IFFI database (APAT, 2006) and the risk map of Riserva Liri-Garigliano and Volturno basins (Autorità di Bacino dei Fiumi Liri-Garigliano e Volturno, 2003). Using as basis the DTM Lidar, with a resolution of 10 m, we crossed different layers in order to identify the environmental context of these landslide. In details, we used the: i) geo-lithological map, ii) soil map (Regione Campania, 2002), iii) forestry cover map (Cona et al., 2013). GIS system (QGis 2.18.12 version) was used to overlap the different layers.

The field survey has been carried out on 10 landslide areas, representative of the different geomorphological sectors of the slope. In particular, we have i) directly measured soil depth in 106 georeferred points (102 points in detachment areas and 4 in accumulation deposits) and ii) described and sampled (following FAO, 2006) 3 soil profiles, in 2 detachment areas (Figure 2).
Each measurement of soil depth has been performed in triplicate by means of a pointed iron spar (having a length of 150 cm and a diameter of 1 cm), which was vertically inserted in the soil with a beating mass, avoiding soil anomalies (such as animal nest, holes, fractures), thick plant roots and highly gravel rich zones.

Soil analyses were performed on 3 soil profiles (12 soil horizons, in total) in order to evaluate the presence of andic soils within landslide detachment areas. The choices of detachment areas to be sampled along with each specific sampling site were done considering both easy access and good soil conservation status. Bulk samples after air (25°C) drying for 2 weeks were sieved to less than 2 mm and used for further analyses (USDA-NRCS, 2004): pH was potentiometrically measured on 1:2.5 soil/water ratio suspensions; soil organic matter was determined following Walkley & Black procedure (Walkley, 1947); a selectively extraction has been performed by ammonium oxalate (Feo, Alo, Sio,) treatment at pH = 3 (Schwertmann, 1964; Blakemore et al., 1987) in order to calculate the Alo+0.5Feo (%) index, since it represents a base parameter for the andic soil

identification. Feo, Alo, Sio content levels were determined by inductively coupled plasma atomic emission spectroscopy (ICP-AES) Varian Liberty model 150.

Geomorphological indices analyses

Geographic Information Systems (GIS) allow the management of study areas information to carry out a geo-morphometric analysis of the sites. The first GIS analyses concerned the determination of the main morphometric parameters such as slope, exposure, etc. The importance of these information is due to the fundamental role of the topography in conditioning the processes of the hydrological and erosive cycle of the mountain basins. From these simple indices, more articulate indices (such as profile curvature, plan curvature and topographic wetness index) have been developed. Among these three indices, it was decided to use the plan curvature for spatialization of the soil thicknesses. In fact, it was considered that the shape of the slope (identified by the plane curvature calculated orthogonally to the maximum slope line) is among the geomorphological factors mostly affecting the erosion-deposition processes of the soil-forming materials.

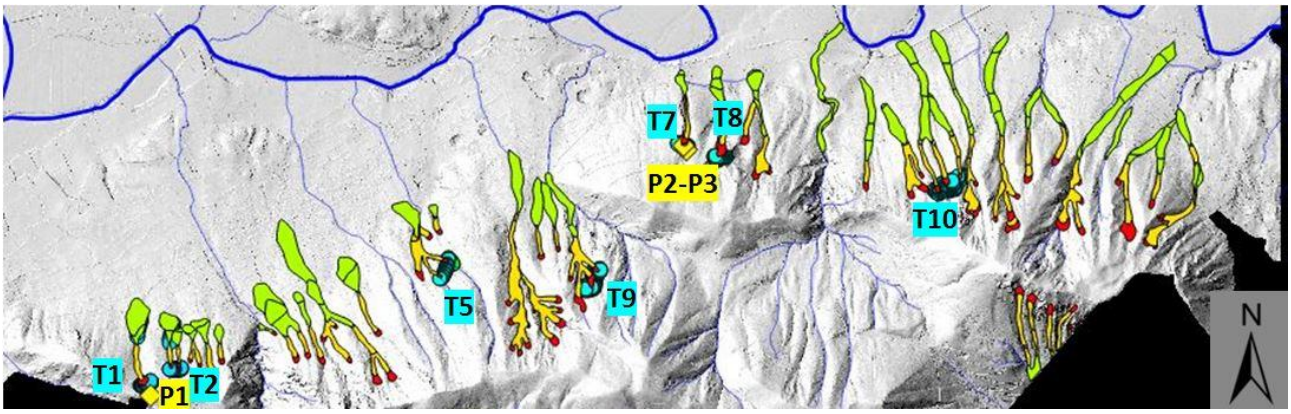

Figure 2: *Landslide location on northern slope of Mt. Camposauro (from IFFI archive, 2007; modified). Legend: detachment areas in red, channels in yellow and accumulation areas in green. Light blue points represent the positions of the survey points. Yellow diamonds represent the position of the 3 soil profiles. Highlighted text represents the name of soil profile (in yellow, P1, P2, P3) and of soil surveys (in light blue, T1, T2, T5, T7, T8, T9, T10).*

The curve calculated orthogonally to the slope line provides an important measure of convergence and divergence of the outflow and is often used in literature as an index for the classification of ridges and channels. Areas with a concave surface can be associated with a convergent flow type, while convex shapes can be related to a divergent stream.

Results and discussion

On the basis of the risk map of Riserva Liri-Garigliano and Volturno basins (Autorità di Bacino dei Fiumi Liri-Garigliano e Volturno, 2003), we estimated total area affected by landslides in the entire Telesina Valley amounts to 1885 hectares, which represents less than 10% of the total area (corresponding to 21,000 hectares). The different types of landslide which occur in the Valley are the following: rotational slides, soil creeps, deep gravitational slope deformations and flow-like movements (generally debris flows). Within these different landslide types, debris flows represent 16.3% (307 ha) of total valley, of which the 97% (298 ha) lies on the northern slope of Mount Camposauro.

From the comparison of the geo-lithological map and the landslide hazard map of Liri-Garigliano and Volturno basins (Autorità di Bacino dei Fiumi Liri-Garigliano e Volturno, 2003), flow-like phenomena affecting the northern slope of Taburno-Camposauro massif, having a regular and straight profile, happen where the substrate of the detachment areas is represented by: 1) compact limestones (green regions in Figure 3) and 2) breccia or *colluvium* (brown regions in Figure 3). Accumulation areas are generally settled in the geo-lithological unit of "fan deposits" (light blue areas in Figure 3).

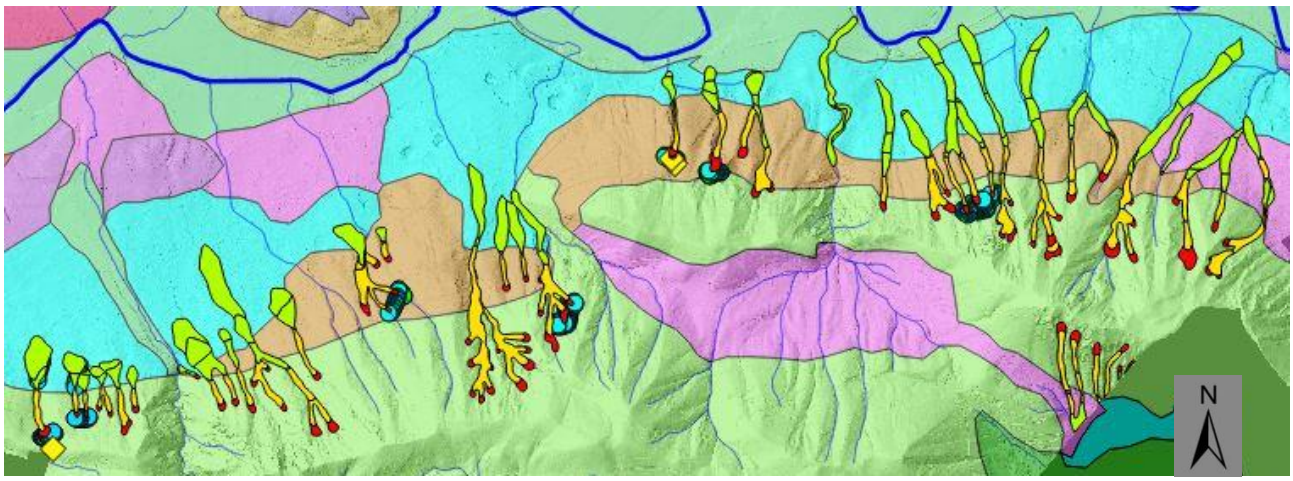

Figure 3: *Distribution of the landslide areas in the lithological map. We represented detachment areas in red, channels in yellow and accumulation areas in green. Green regions represent limestone, brown areas are breccia or colluvium, pink regions are not cemented gravel and light blue are fan deposits. Light blue points represent the location of the soil depth surveys. Yellow diamonds represent the position of the 3 soil profiles.*

With respect to the slope gradient map (Figure 4), the detachment areas and sliding channels are located in region of the slope having a gradient ranging from 36% to over 60%, whereas the accumulation areas lie at slopes ranging from 12 to 36%. Furthermore, the highest elevation of landslide detachment areas is 1060 m asl, whereas the accumulation areas extent between 300 and 70 m asl.

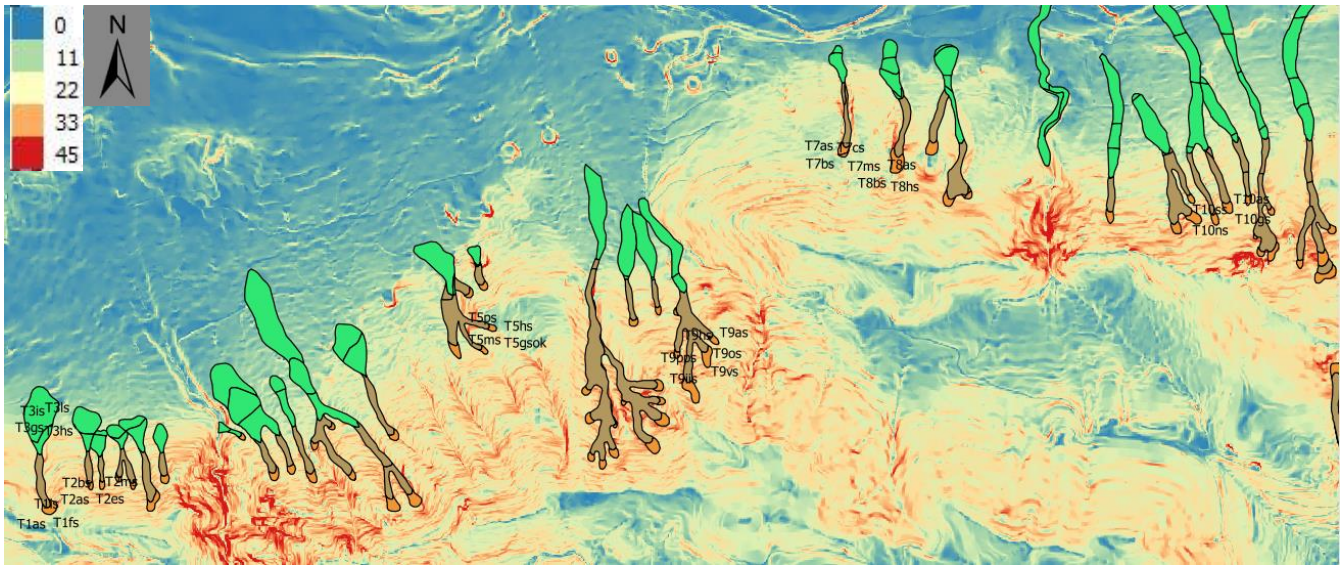

Figure 4: *Landslide areas in the slope gradient map. We represented detachment areas in orange, channels in brown and accumulation areas in green. Codes are the names of the surveyed points. Numbers in the legend refer to slope angle (degrees).*

The evaluation of the position of landslides in the forestry cover map (Figure 5) reveals that flow-like phenomena are concentrated in the mixed forest (pink regions in Figure 5) for a total of 296 ha; beech cover (violet regions in Figure 5) are affected only for a total area of 1.86 ha.

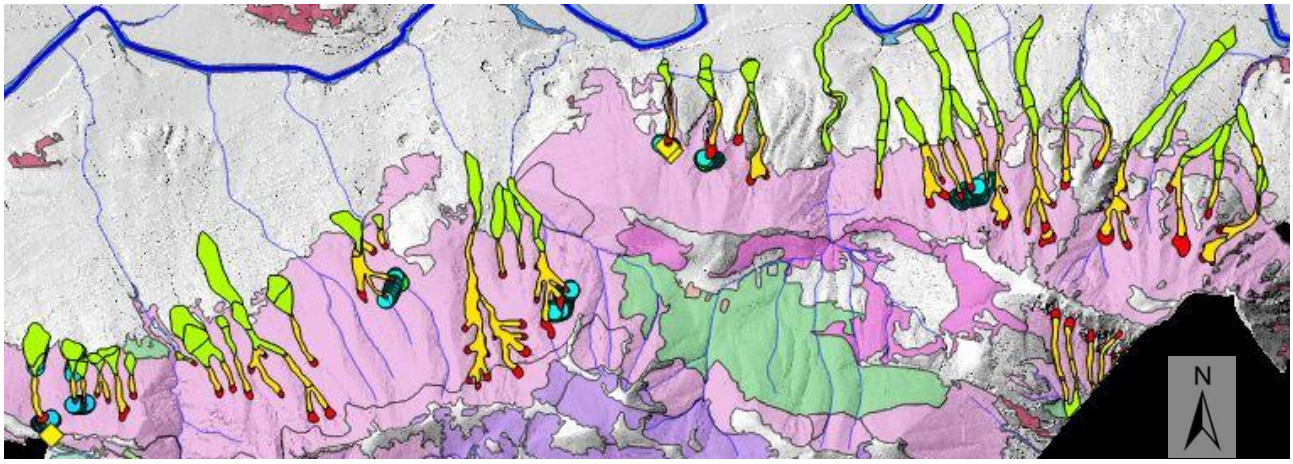

Figure 5: *Distribution of the landslide areas in the forestry cover map. We represented detachment areas in red, channels in yellow and accumulation areas in green. Pink regions represent mixed forest, green regions are chestnut forest, violet regions are beech and dark pink areas represent oak forest. Light blue points represent the location of the soil depth surveys. Yellow diamonds represent the position of the 3 soil profiles.*

Soil properties

From the morphological and chemical analyses conducted on the three soil profiles P1, P2 and P3 resulted that the organic matter content is very high in the upper horizon and decreases rapidly with depth, as expected for forestry soils. Furthermore, soil reaction is generally slightly alkaline on the surface, but increases with depth until moderately alkaline. Variable is the coarse fragments (generally carbonatic) content in the soil, from common (9-10%%) to many (22%) on the soil surface. However, the soil matrix is non-calcareous. The Alo+0.5Feo index results generally higher than 2%, except for the P3, and is very high for the P1 (from 2.4 to 3.3%). As known, the Alo+0.5Feo index is a key parameter for andic properties identification. Therefore, data of chemical analyses confirm the similarity of the analyzed soils with the Andosols reported by the soil map (Regione Campania, 2002) (Table 2).

Profile	horizon	depth (cm)	color (moist)	$Al_o+0.5Fe_o$ (%)	Organic Matter (g kg^{-1})	pH H_2O	coarse fragments (%)
P1	A1	0-20	7.5 YR 2.5/2	2.50	143.17	7.59	22
	A2	20-55	7.5 YR 3/2	3.27	41.24	7.84	5
	AB	55-70	7.5 YR 3/3	3.20	24.16	8.09	6
	Bw1	70-90	7.5 YR 3/4	3.19	22.79	8.18	5
	Bwb1	90-120	7.5 YR 4/3	2.43	9.36	8.38	9.5
	Bwb2	120-140+	7.5 YR 4/3	2.49	8.66	8.31	2.5
P2	A	0-20	7.5 YR 2.5/2	1.72	72.48	7.72	9.6
	AB	20-40	7.5 YR 3/3	2.70	48.85	8.06	39
	Bw	40-60+	5YR 4/4	2.41	29.01	8.01	13.5
P3	A	0-20	7.5 YR 2.5/2	1.32	93.6	7.4	8.5
	AB1	20-60	7.5 YR 2.5/3	1.29	45	7.44	2.8
	AB2	60-80+	7.5 YR 3/2	1.46	41.9	7.44	5

Table 1: *Results of morphological and chemical analysis on the horizons of the three soil profiles P1, P2, P3.*

Relationship between soil depth and plan curvature

Soil surveys reveal that the soils of the detachment areas have an approximate depth of 50 cm (Table 2). These generally shallow soils are very likely the result of landslides and erosional processes associated to the very high slope.

The plan curvature map was calculated for the entire northern facing slope of the Mt. Camposauro, with the same DTM resolution (10 m). Then, from such map we extracted the value of the plan curvature in correspondence of the surveyed points (Table 2). On the basis of a geomorphological evaluation, we grouped plan curvature values in 9 main classes. The classes correspond to different shapes of the slope, from the very concave form (watershed) to the convex, to the ridge (Table 2). At each class is corresponding an average soil depth value calculated from the soil depth measurements in that class (Table 2).

Table 2 : *Soil depth (mean and standard deviation) and plan curvature data, grouped for classes of plan curvature.*

Observation	Altitude (m a.s.l.)	Soil depth (m)	Slope (%)	Plan curvature value (-)	Plan curvature class	Average soil thickness (m)	Standard deviation soil depth (m)	Description of the plane curvature class
T5ls	497	0.15	53.40	-86.38				
T2bs	553	0.45	69.22	-83.63				
T9ds	734	0.25	56.42	-80.44				
T9es	736	0.50	56.42	-80.44	1	0.40	0.23	watershed
T8as	432	0.10	64.84	-80.26				
T10ls	628	0.50	73.41	-79.02				
T1es	586	0.45	51.43	-77.25				
T7es	397	0.80	59.47	-76.28				
T8hs	425	0.24	41.18	-70.95				
T10es	610	0.38	72.95	-70.78				
T8ds	434	0.35	54.45	-70.30				
T5hs	506	0.30	75.52	-67.34				
T5gsok	513	0.22	75.52	-67.34				
T2ms	547	0.80	73.73	-66.08				
T9ffs	833	0.50	93.50	-65.27				
T9bs	734	0.50	59.73	-64.25				
T10ms	628	0.63	83.73	-63.29				
T10ps	620	0.86	83.73	-63.29				
T2ds	544	0.65	78.94	-62.36				area having accentuated concavity right on the top of the watershed
T8fs	431	0.25	40.44	-62.11	2	0.47	0.30	
T8gs	425	0.70	40.44	-62.11				
T7fs	388	0.47	67.06	-61.06				
T10is	633	0.61	73.07	-59.97				
T10qs	618	0.33	92.86	-58.64				
T10rs	616	0.05	92.86	-58.64				
T1fs	594	1.35	44.32	-55.24				
T5ns	496	0.19	63.09	-54.96				
T10fs	622	0.43	87.82	-50.49				
T2hs	550	0.85	60.38	-50.14				
T2is	553	0.41	60.38	-50.14				
T10ds	602	0.20	69.33	-49.60				
T8bs	435	0.10	56.25	-48.99				
T9bbs	822	0.64	76.68	-40.58				
T9mms	821	0.70	74.17	-38.58				
T9hhs	828	0.44	111.13	-37.49				
T9dds	826	0.10	86.98	-33.25				
T7hs	395	0.15	95.78	-33.23				
Tl1s	589	0.55	45.17	-33.20				
T9oos	810	0.44	81.55	-31.45	3	0.44	0.21	low accentuated concavity
T9pps	805	0.44	84.79	-29.98				
T9rs	776	0.61	69.55	-29.77				
T9ls	744	0.20	60.69	-27.55				
T10ns	633	0.32	82.00	-25.66				
T1as	588	0.75	54.74	-21.08				
T7gs	399	0.22	67.33	-20.33				
T9lls	824	0.60	75.54	-18.33				

Table 2 *(continued): Soil depth (mean and standard deviation) and plan curvature data, grouped for classes of plan curvature.*

Observation	Altitude (m a.s.l.)	Soil depth (m)	Slope (%)	Plan curvature value (-)	Plan curvature class	Average soil thickness (m)		Description of the plane curvature class
T1bs	578	0.70	57.06	-15.27				
T8cs	440	0.30	57.26	-15.12				
T2cs	549	0.26	79.35	-15.12				
T9aas	812	0.60	77.65	-13.89				
T1ms	593	0.44	57.33	-11.65				very low concavity, towards the linear slope
T9fs	735	0.53	63.48	-11.58	4	0.58	0.21	
T9gs	738	0.62	63.48	-11.58				
T1cs	572	0.70	54.40	-9.54				
T8es	431	0.50	56.06	-9.17				
T9vs	797	0.75	67.87	-7.56				
T1is	591	1.00	47.90	-6.35				
T9isthic	735	0.75	63.64	-2.71				
T9as	732	0.35	58.96	-2.39				
T10gs	625	0.32	68.65	-2.15				
T9zs	803	0.60	70.44	-1.73	5	0.54	0.20	linear slope
T1ds	568	0.40	55.20	0.13				
T1gs	595	0.55	42.31	0.97				
T1hs	578	0.82	42.31	0.97				
T9ees	830	0.40	91.14	4.03				
T9ns	758	0.70	66.27	9.30				
T3ls	261	0.30	26.40	14.19				
T9ps	767	0.96	65.34	14.84				
T3is	267	0.27	31.98	15.61	6	0.52	0.28	linear-convex slope
T9ss	785	0.83	67.52	17.47				
T2fs	540	0.20	62.87	19.20				
T2gs	549	0.66	62.87	19.20				
T9cs	735	0.32	72.72	20.08				
T9iis	826	0.65	76.43	20.69				
T7ms	406	0.15	43.76	21.00				
T9us	793	0.52	69.72	21.20				
T7ls	404	0.10	45.17	22.84				
T9qs	774	0.84	66.46	24.62				
T10ss	614	0.35	77.43	25.66				
T9os	760	0.45	64.56	25.96	7	0.45	0.20	low convex slope
T10cs	600	0.67	73.67	31.96				
T9ts	789	0.47	71.11	33.05				
T3hs	271	0.30	25.22	35.83				
T9hs	728	0.40	60.21	36.60				
T2ls	553	0.55	76.28	45.25				
T10hs	630	0.50	82.44	48.49				
T9ms	744	0.34	66.56	49.85				

***Table 2** (continued): Soil depth (mean and standard deviation) and plan curvature data, grouped for classes of plan curvature.*

Observation	Altitude (m a.s.l.)	Soil depth (m)	Slope (%)	Plan curvature value (-)	Plan curvature class	Average soil thickness (m)		Description of the plane curvature class
T9ggs	828	0.32	106.78	52.74				
T2as	551	0.32	88.35	54.26				
T7is	401	0.23	40.81	56.44				
T5is	506	0.25	72.27	56.52				
T10as	575	0.30	69.00	59.12	8	0.32	0.10	very convex
T3gs	278	0.50	29.75	63.76				
T9nns	814	0.48	77.03	66.21				
T10bs	582	0.35	64.21	66.24				
T5ms	505	0.21	95.78	67.48				
T10os	632	0.27	73.29	71.26				
T9ccs	828	0.21	86.01	73.70				
T5ps	491	0.18	60.32	73.83				
T7as	397	0.20	34.00	74.77				
T7ds	391	0.22	47.85	75.15	9	0.23	0.04	ridge
T2es	542	0.26	72.91	75.39				
T5os	514	0.22	87.34	75.63				
T7bs	400	0.23	54.95	75.68				
T7cs	397	0.30	88.72	84.63				

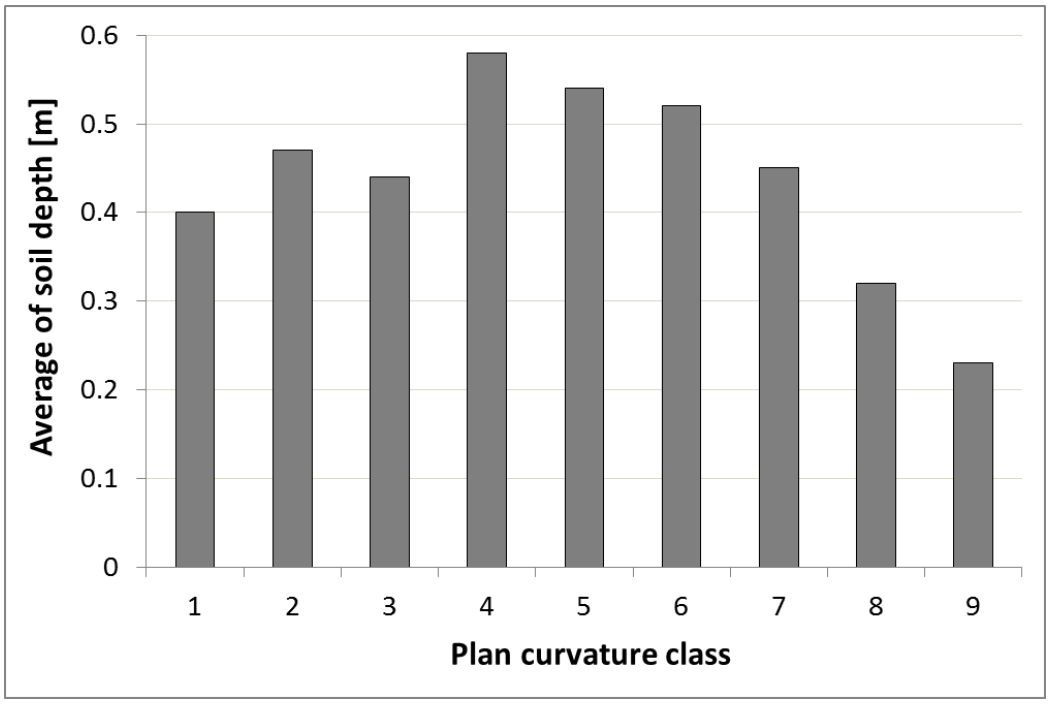

***Figure 6**: Average soil depth for each plan curvature class*

The mean soil depth is lower (0.23 m) on the ridge (class 9) than in the areas of watershed (class 1, mean depth = 0.40 m) and very convex (class 8, mean depth = 0.32 m) (Figure 6). As a whole, soil depth increases (i.e. from 0.40 to 0.54 m of soil depth) from the watershed (class 1) to linear slope (class 5) and then decreases (i.e. from 0.54 to 0.23 m) from the linear slopes (class 5) to the ridges (class 9). The distribution of the soil thickness seems coherent with natural slope processes affecting mountain environments. However, within each plan curvature class, values of standard deviation (relative to the measured soil depth) suggest a high variability of soil depth. Indeed, notwithstanding the similar shape of the slope within each class, soil depth can assume a wider range than expected as a consequence of additional variables governing the deposition/erosion processes (such as position on the slope, overlapping of different landslide phenomena, etc.). In order to spatialize and estimate soil depth, we extended the plan curvature classification (9 classes) to the entire region of interest (*i.e.* northern slope of Mt. Camposauro) (Figure 7). In such a way, from the plan curvature values it would be possible to retrieve soil depth values by means of the previously found relationship soil depth/plan curvature in regions of interest.

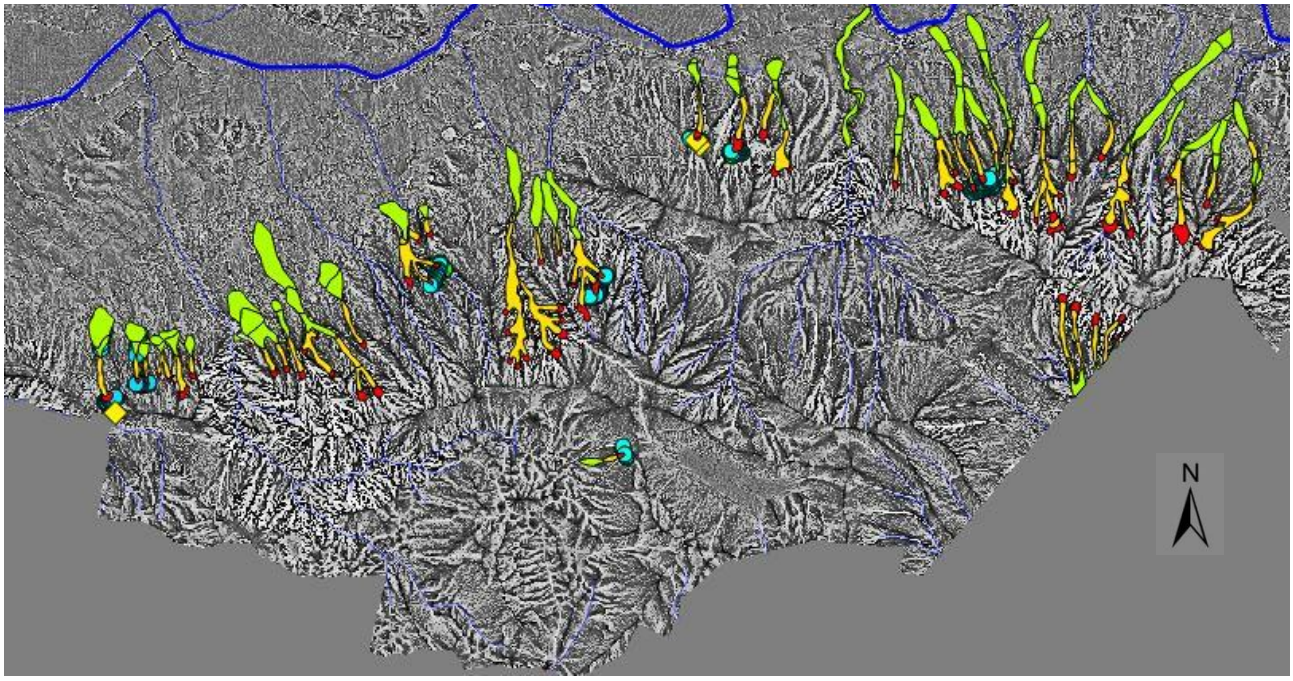

Figure 7*: Plan curvature map of the northern slope of Mt. Camposauro. Dark pixels represent low plan curvature values, whereas light pixels are for high values of the plan curvature. Light blue points represent the location of the soil depth surveys. Yellow diamonds represent the position of the 3 soil profiles.*

Conclusions

In this paper, we aimed at (i) evaluating the presence of andic soils within detachment areas of flow-like landslides and (ii) preliminarly estimating soil depth on the northern slope of Mt. Camposauro which is highly exposed to flow-like susceptibility. In fact, such a hillslope is characterized by (i) the presence of andic soils which are strongly exposed to landslides because of their peculiar set of physical and hydraulic properties; (ii) high and very high slope angles; (iii) frequent road cuts interrupting the hydraulic and pedo-continuity.

Our approach was to (i) evaluate the andic properties of soils sampled in flow-like detachment areas and (ii) measure soil depth in different sectors of such a hillslope in detachment areas of flow-like landslides selected from the IFFI archive (APAT, 2006) and (iii) evaluate the relationship between soil depth and plan curvature (a geomorphological index which is related to the erosion-deposition processes of the soil-forming materials). We highlight that the estimation of soil depth variability in a region of interest is essential to implement dynamic landslide models, taking into account such a variability and hence ameliorating the evaluation of landslide susceptibility. Moreover, soil depth is a well-known landslide predisposing factor. In fact, thick soils are responsible of great weight and pressure on deepest layers, especially when saturated or quasi-saturated. In this framework, the presence of andic soils could be an additional predisposing factor, since they are very susceptible to slope processes, such as erosion and landslide phenomena. The morphological and chemical analyses conducted on the horizons of the three sampled soil profiles, confirmed the presence of andic properties in the detachment areas of the surveyed landslides and are in agreement with the soil map (Regione Campania, 2002). The relationship between soil depth and plan curvature showed that soil depth increases (i.e. from 0.40 to 0.54 m of soil depth) from the watershed (class 1) to linear slope (class 5) and then decreases (i.e. from 0.54 to 0.23 m) from the linear slopes (class 5) to the ridges (class 9). Notwithstanding the similar shape of the slope within each class, soil depth can assume a wider range than expected as a consequence of additional variables governing the deposition/erosion processes (such as position on the slope, overlapping landslide phenomena, etc.).The subdivision in 9 classes of plan curvature was extended to the entire northern slope of Mt. Camposauro in order to spatialize and estimate soil depth. By means of the previously found relationship soil depth/plan curvature, it would be possible to estimate soil depth from the plan curvature value in regions of interest.

Since not only geomorphological factors affect the soil depth, which is the result of combined factors, we highlight that the proposed approach, aimed at evaluating soil depth on large areas where landslide susceptibility is diffused, could be integrated by introducing some more factors which, together with the plan curvature, contribute to affect soil depth (*e.g.* position on the slope, the elevation asl, overlapping of different landslide phenomena and other environmental conditions). Such an improvement would ameliorate the estimation of the soil depth, which, at the moment, is limited to one single parameter, *i.e.* the plan curvature.

References

APAT, 2006. Progetto IFFI. Inventario dei fenomeni Franosi in Italia. Relazione Tecnica – Regione Campania.

Arnalds, O., Thorarinsdottir, E.F., Metusalemsson, S., Jonsson, A., Gretarsson, E. & Arnason, A. 2001. Soil Erosion in Iceland. Soil Conservation Service and Agricultural Research Institute, Reykjavik, Iceland.

Basile, A., Mele, G., Terribile, F. 2003. Soil hydraulic behaviour of a selected benchmark soil involved in the landslide of Sarno 1998. Geoderma, 117, 331–346.

Autorità di Bacino dei Fiumi Liri-Garigliano e Volturno, 2003. Piano Stralcio per l'assetto idrogeologico - rischio frane bacini Liri-Garigliano e Volturno. Gazzetta Ufficiale n°88 del 15/04/2003.

Basile, A., Mele, G., Terribile, F. 2003. Soil hydraulic behaviour of a selected benchmark soil involved in the landslide of Sarno 1998. Geoderma, 117, 331–346.

Blakemore, L.C., Searle, P.L., Daly, B.K. (1987). Methods for Chemical Analysis of Soils. New Zealand, Soil Bureau, Scientific Report 80.

Calcaterra D., M. Parise, B. Palma and L. Pelella (1999) - The May 5 th 1998, landsliding event in Campania (southern Italy): inventory of slope movements in the Quindici area. In Proc. Intern. Symp. on "Slope Stability Engineering", IS – Shikoku 1999, Matsuyama, Japan, pp. 1361-1366.

Campbell R.H. (1975) - Soil slips, debris flows, and rainstorms in the Santa Monica Mountains and vicinity, southern California. In: US Geological Survey Professional Paper 851. Washington DC: U.S. Government Printing Office, 51 pp.

Cascini L., S. Cuomo and D. Guida (2008) - Typical source areas of May 1998 flow-like mass movements in the Campania region, Southern Italy. Engineering geology, 96, pp. 107-125.

Cascini L. S Cuomo, M. Pastor and G. Sorbino (2010) - Modeling of rainfall-induced shallow landslides of the Flow type. Journal of Geotechnical and Geoenvironmental Engineering, pp.85-98.

Cona, F., Vella, M., Saulino, L., Quattrocchi, M., Migliozzi, A., 2013. Carta delle tipologie forestali - Progetto Life SoilConsWeb.

Del Prete M., F.M. Guadagno and A.B. Hawkins (1998) - Preliminary report on the landslides of 5 May 1998, Campania, southern Italy. Bull Eng Geol Environ, 57, pp. 41-50.

De Vita P., E. Napolitano, J.W. Godt and R. Baum (2013) - Deterministic estimation of hydrological thresholds for shallow landslide initiation and slope stability models: case study from the Somma-Vesuvius area of southern Italy. Landslides, 10, pp. 713-728.

Di Crescenzo G. and A. Santo (2005) - Debris Slides-Rapid Earth Flow In The Carbonate Massifs Of The Campania Region (Southern Italy): Morphological And Morphometric Data For Evaluating Triggering Susceptibility. Geomorphology, 66, pp. 255-276.

FAO (Food and Agriculture Organization) (2006) - Guidelines for Soil Profile Description (Revised), 4th ed. (Rome).

Fontes, J.C., Pereira, L.S. & Smith, R.E. 2004. Runoff and erosion in volcanic soils of Azores: simulation with OPUS. Catena, 56, 199–212.

Guadagno F.M, R. Forte, P. Revellino, F. Fiorillo and M. Focareta (2005) - Some aspects of the initiation of debris avalanches in the Campania Region: The role of morphological slope discontinuities and the development of failure. Geomorphology, 66, pp. 237-254.

Hungr O., S.G. Evans, M.J. Bovis and J.N. Hutchinson (2001) - A review of the classification of landslides of flow type. Environmental and Engineering Geoscience, 7, pp. 221-238.

IUSS Working Group WRB, 2014. World Reference Base for Soil Resources 2014. International soil classification system for naming soil and creating legends for soil maps. Food and Agriculture Organization of the United Nations. Rome: 182 ss.

Nanzyo, M., Shoji, S. and Sudjadi, M., 1993. Properties and classification of Andisols from West Java, Indonesia.

Palmieri W. (2011) - Per una storia del dissesto e delle catastrofi idrogeologiche in Italia dall'Unità ad oggi (in Italian), National Research Council of Italy, Quaderno ISSM n. 164.

Picarelli L., L. Olivares, L. Comegna and E. Damiano (2008) - Mechanical aspects of flow-like movements in granular and fine-grained soils. Rock Mech. Rock Eng., 41(1), pp. 179-197.

Regione Campania, 2002. Carta dei suoli della Valle Telesina 1:50 000. Assessorato all'Agricoltura Settore SIRCA. System Cart S.r.l. Roma

Schwertmann, U. (1964) – Differenzierung der Eisenoxide des Bodensdurch Extraction mit Ammoniumoxalat-Losung. Zeitschrift Pflanzenernhar. Dungung Bodenkunde, 105, 194-202.

Scognamiglio, S., Calcaterra, D., Iamarino, M., Langella, G., Orefice, N., Vingiani, S., & Terribile, F. (2016a). Andic soil features and debris flows in Italy. New perspective towards prediction. In *EGU General Assembly Conference Abstracts* (Vol. 18, p. 10543).

Scognamiglio, S., Terribile, F., Iamarino, M., Orefice, N., & Vingiani, S. (2016b). Soil properties and debris flows in Italy: potential relationships. *RENDICONTI ONLINE SOCIETA GEOLOGICA ITALIANA*, *41*, 199-202.

Shoji, S., M. Nanzyo, and R.A. Dahigren. 1993. Volcanic ash soils: Genesis, properties and utilization. Elsevier, Amsterdam, Netherlands.

Terribile, F., Basile, A., de Mascellis, R., di Gennaro, A., Mele, G., Vingiani, S., 2000. I suoli delle aree crisi di Quindici e Sarno: proprietà comportamenti in relazione ai fenomeni franosi del 1998. Quad. Geol. Appl. 7-1, 59–77.

Terribile, F., Basile, A., De Mascellis, R., Iamarino, M., Magliulo, P., Pepe, S. et al. 2007. Landslide processes and Andosols: the case study of the Campania region, Italy. In Soils of Volcanic Regions in Europe (eds O. Arnalds, F Bartoli, P Buurman, H O´ skarsson, G Stoops, & E Garcı´a-Rodeja), pp. 545–563. Springer Verlag, Berlin and Heidelberg.

USDA-NRCS (2004). Soil Survey laboratory methods manual. Soil Survey Investigation Report. 42**,** Version 4, pp 700

Vingiani, S., Mele, G., De Mascellis, R., Terribile, F., Basile, A. (2015). Volcanic soils and landslides: A case study of the island of Ischia (southern Italy) and its relationship with other Campania events. Solid Earth, 6 (2), pp. 783-797. DOI: 10.5194/se-6-783-2015

Walkley, A. (1947). A critical examination of a rapid method for determining organic carbon in soils - effect of variations in digestion conditions and of inorganic soil constituents. *Soil Sci*. 63: 251-265.

4

Andic soils and flow-like mass movements: cause-effect evidence from Italy

The work included in the fourth chapter, was developed in collaboration with Dr. A. Basile (National Research Council - Institute of Agricultural and Forest Systems in the Mediterranean - *CNR-ISAFoM*) and Dr. M. Iamarino, Prof. S. Vingiani and Prof F. Terribile (Department of Agricultural Sciences - *DIA* - University of Naples Federico II). In this study, within the general framework of evaluating the potential applicability of *STEP-TRAMM* to other Italian environments, we aimed at evaluating chemical, physical and hydraulic properties of different Italian soils involved in past flow-like Italian landslides. We also evaluated the potential relationship between andic soil features and flow-like landslides in the selected Italian environmental and geological contexts. For such soils, we found out that despite the lithological heterogeneity of the bedrock and other environmental diversities between the selected sites, the analysed soils show remarkably similar properties. More specifically, we observed the existence of andic properties. Such a circumstance suggests that the pedological control on flow-like landslides hazard is not limited only at Campania region soils (as proved by previous researches demonstrating that catastrophic Campanian flow-like were triggered on Andosols) but it is much more widespread than previously thought. Furthermore, the analysed andic soils show another common property, *i.e.* high water retention capacity, especially at saturated condition, which is typical of andic soils and dramatically increases the weight and, consequently, the stability of these soils. Our findings shed new light on the similarity of the materials involved by flow-like landslides (in Italy), suggesting a pedological control on the flow-like hazard. Despite these important results, we highlight that the diversity that we found regardless soil properties within the same soil profiles was not implementable in the STEP-TRAMM model even if it could be one of the main predisposing factors of flow-like phenomena. In fact, the contrast of hydraulic and physical properties that we found between adjacent horizons could create the conditions to develop a building up of diffuse positive excess pore pressure, responsible of the rupture.

1. INTRODUCTION

Landslides are severe hazards for people and infrastructures all over the world (Alcantara-Ayala, 2002). In particular, in the framework of catastrophic landslides, rainfall triggered flow-like mass movements (Hungr et al., 2001) play a crucial role since they occur in different contexts all over the world and, among all the natural hazard, they are one of the most dangerous because they can cause significant damage of properties and loss of life. Furthermore, they can disturb the natural ecosystem where they occur, by modifying the pre-existent hydrographic network and obliterating soil and vegetation. In fact, flow-like landslides can potentially involve huge amounts of soils typically having high water content and moving downslope with a velocity ranging from very rapid to extremely rapid (i.e. 0.05-5 m/s according to Cruden & Varnes, 1996). Hence, their rheological behaviour is assimilated to a real flow that, especially when channelled in the pre-existent hydrographic network, can quickly and dangerously travel across large distances. In fact these landslides seem to be provoked by soil liquefaction sometimes followed by a complete fluidization (Picarelli et al, 2008, Iverson, 1997; Musso and Olivares, 2004).

It has been established that in Campania region flow-like mass movements are related to the occurrence of Andosols (Basile et al. 2007; Terribile et al, 2007), typically developed over unconsolidated volcanic ash-fall deposits (Somma-Vesuvius and Phlegrean field) and overlapping Mesozoic carbonate series (Revellino et al. 2004; De Vita et al., 2006). These soils have a rather unique set of morphological, chemical, physical and hydraulic properties including (i) large porosity (ii) low bulk density, (iii) friable structure, (iv) high water retention capacity and hydraulic conductivity near saturation, (v) short range order clay minerals (allophane, imogolite and ferrihydrite), (vi) high organic matter content, (vii) soil solution typically rich in cations such as Si, Al, Fe, Ca, Mg, K and Na, (viii) large reserves of easily weatherable minerals, (ix) high susceptibility to soil liquefaction (Picarelli et al, 2008, Nanzyo, 2002) (x) vertical and lateral morphological discontinuities (pumice layers) (Vingiani and Terribile, 2006). Such unique combination of properties make these soils highly fertile (Leamy, 1984, Shoji et al., 1993; McDaniel et al., 2005) but also highly susceptible to land degradation processes such as erosion (Arnalds et al., 2001; Fontes et al., 2004) and landslide (Basile et al., 2003; Scognamiglio et al., 2016 a,b; Terribile et al., 2000; Terribile et al., 2007; Vingiani et al., 2015; Vingiani and Terribile, 2006).

In recent years, soil scientists have assessed the presence of both Andosols and soils exhibiting andic features in many non-volcanic mountain ecosystems (NVME) of the world under different types of parent material and developed under different temperature and water regimes

including areas such as Nepal (Baumler and Zech, 1994; Baumler et al., 2005), India (Caner et al., 2000), Austria (Delvaux et al., 2004), North Appalachians (Canada, USA), Kyushu (Japan), the Alps (Kimble et al., 2000). More recently these soils have also been found in many NVME of Italy (Iamarino & Terribile, 2008) and their formation is not restricted to the volcanic ash parent material but mainly to a large range of fine loess sediments (Mileti et al., 2013).

Thus, considering both the large amount of flow-like movements occurred in Italian NVME and the finding of andic soils in many Italian NVME, here we aim to investigate and to understand, at the Italian country scale, whether there is a potential cause-effect relationship between the occurrence of some large catastrophic flow-like landslides events in Italian NVME and andic soils. More specifically, we have studied soils in the detachment areas of six of the most important flow-like events that occurred in the last 70 years in different Italian regions having very diverse geological and geomorphological settings. The study included a consistency check made on other six minor flow-like landslides.

2. MATERIALS AND METHODS

2.1 Selection of case studies

We selected six major historical flow-like landslides on the base of the followings data: Information System of Italian Hydrogeological Dysasters (http://sici.irpi.cnr.it/storici_italia.htm), the official Italian landslides archive (IFFI project, 2007) and hystorical papers on Italian Landslides (Palmieri, 2011). We also seek for both landslide having an important soil component and a well balanced geographical distribution of Italian flow-like landslides.

Then, we limited our analysis to the following six flow-like slides case studies locations that occurred in the last 70 years (Table 1): Versilia (Toscana), Platì (Calabria), Albaredo (Lombardia), Ceriana (Liguria), Sarno-Quindici (Campania) and Vietri (Campania).

All of the chosen flow-like mass movements (Hungr at al., 2001) had a catastrophic behavior and were fatal to people, by causing several injuries, and destructive for infrastructures and natural ecosystems.

In addition to these catastrophic landslides, we have sampled other soils from six other minor flow-like landslides that have been used as consistency check. These landslides were chosen on the base of pre-existing knowledge from the authors and seeking a balanced geographical distribution at the country scale.

2.2 Site description and soil sampling

The geographic position of the sampling points is shown in Figure 1 .

Slope, aspect and elevation of the sampling sites were obtained from the GIS analysis of the DEM (reference, resolution), whereas land use and bedrock were extracted, respectively, from the Geological map (Carta geologica d'Italia 1:500000) and the Corine Land Cover (CLC) map (2006, 1:100000), both available on PCN (Portale Cartografico Nazionale - Italian Environment Ministry http://www.pcn.miniambiente.it).

We carried out field description and soil sampling according to official FAO guidelines (FAO, 2006) in each one of the twelve selected slopes and, for each one of them, at least one soil profile (*i.e.* a bidimensional section in which it is possible to observe a soil from the top to the bottom) was described in the field. Each soil profile was localized in the detachment area of the flow-like landslides and considered representative of each specific environment (*pedon*). The choices of detachment areas to be sampled along with each specific sampling site were done considering both easy access and good soil conservation status. We collected bulk soil samples for chemical and physical analyses from every horizon of each soil profile.

2.3 Soil analyses

2.3.1 Standard soil analysis

At first, all bulk samples were air dried and then sieved to 2 mm (to retrieve the fine earth fraction) in order to carry on (perform) chemical analyses according to the USDA method (2004): soil pH was measured on soil-H_2O suspension according the potentiometric method (USDA-NRCS, 2004); organic carbon (OC) content was measured following the Walkley-Black (1934) procedure; the acid ammonium oxalate-extractable forms (Al_o, Fe_o and Si_o) were measured at pH 3 according to Schwertmann (1964) and Blakemore et al. (1987) and their content levels were determined by inductively coupled plasma atomic emission spectrometry (ICP-AES). The acid ammonium oxalate-extractable forms Al_o, Fe_o and Si_o were used to calculate (estimate) the quantity of low order clay minerals, such as allophane and imogolite (rich in Al and Si) that typically characterize (control, regulate, determine, are responsible of) andic soil, by means of the Parfitt's formula (1990). The selective extracted forms also provide the idex of andic property (IAP) $Al_o+1/2Fe_o$ (expressed in %),

a diagnostic criterion required to define andic soil properties (IUSS Working Group WRB, 2014). The cation exchange capacity (CEC) was determined by the method of $BaCl_2$ and triethanolamine at pH 8.2. Because andic soils are rather difficult to disperse due to their high variable charges (Mizota & van Reeuwijk, 1989), we used field textures to estimate the particle-size classes (Iamarino and Terribile, 2008).

2.3.2 Soil Sampling and hydrological analysis

From soil profiles of Platì, Albaredo, Versilia, Ceriana, Sarno, Quindici and Vietri, undisturbed soil samples were collected from selected cohesive horizons in order to determine hydraulic properties. Measurements were carried out by applying both the evaporation method (Arya, 2002) and the tension table method (Dane et al., 2002)[1].

Water retention data were parameterised according to the van Genuchten equation (1980) and used as an additional information to evaluate if the hydraulic behaviour of these soils was consistent with typical hydraulic properties of andic soils. In fact, as previously described, soils showing andic features are typically characterized by low bulk density, large porosity and high water retention capacity. In this sense, water retention curves are intended to be an auxiliary tool to assess whether a soil exhibits andic features.

For each retention curve, the highest water content represents the maximum amount of water stored in the soil pore system (i.e. at saturated conditions) and is directly related to the attitude of a soil to be stable or unstable. In fact, high values of saturated water content are responsible of great weight and high pressure on the underlying materials and are usually associated to periods of prolonged and/or high rainfall rate. Such a condition predisposes the soil to be unstable. Since one of the diagnostic criterion required to define andic soil properties is the Index of Andic Processes (IAP Alo+1/2Feo), and since andic soils are typically characterized by very high water content we evaluated the correlation between the same IAP values characterizing the soils and an Integral Retention Index (IRI). Such an index is an indicator representing the average water retention capacity of the soil between the water content at saturation (assumed at log h=-1 cm) and the water content corresponding to the wilting point (usually fixed to log h = 4.2). It is formally defined as follows (Terribile et al., 2017):

[1] Sampling and laboratory measurements where previously performed by ISAFOM-CNR for a parallel project.

$$IRI = \frac{1}{wp}\int_{-1}^{w_p} \theta \, d\,(log_{10}\, h)$$

where *wp*=4.2 is the logarithm of pressure head at the wilting point. The IRI is an useful index to summarize all the soil water retention curve in one single parameter and allows simple comparisons of the whole water retention capacity. In particular, for our purpose, it is a hydraulic indicator of the andic soil features, to be added to the chemical indicator IAP. Both IRI and saturated water content contain information about the quantity of water stored in the soil, but IRI provides additional and important details about how the water has been stored in the soil. In particular, andic soils are usually characterized by an important system of small pores so that they show high water content also in the final (dryer) part of the water retention curve. In this context, the area under the water retention curve of an andic soil is expected to be significant greater that a non-andic soil.

3. RESULTS AND DISCUSSION

3.1 Soils

The selected six large catastrophic (destructive, devastating) flow-like mass movements occurred between 1951 and 2002; their main features are described in Table 1. They took place at different latitudes in various Italian regions at Versilia, Platì, Albaredo, Ceriana, Sarno-Quindici, Vietri sites.

All the selected flow-like movements were triggered by important rainfall events and hit one or more towns or villages located at the foothill of their slopes where they developed and killed many people (up to 321). The catastrophic behaviour of such landslides was mainly due to (i) the high number of landslides that were triggered at the same time during the same event and that contributed to provide the huge volume of material moving downwards and (ii) the rheological behaviour of the soils involved in the landslides that flowed downslope like a fluid with very high velocity. They occurred under very different geological and geomorphological contexts while the land use was generally forest, ranging from chestnut to fir forest types. With respect to the environmental setting, the bedrock of the six chosen sites showed different nature varying from sedimentary to igneous and metamorphic rocks; the flow-like landslides occurred on moderate to high slope gradient (ranging from 20° to 47°) and at different altitudes (from 275 to 1000 m asl)

and aspects of the slopes. The heterogeneity of the bedrock underlying each soil profile, the land use, the slope and the aspect made our dataset markedly diversified and assorted. Surprisingly, despite the lithological and geomorphological diversities and the different environmental settings and land uses, the analysed soils presented remarkably similar morphological properties (Table 2). Soil profiles were generally deep ranging from medium (90 cm) to very deep (200 cm) and they showed an alternation of A and B horizons. Some profiles were rather complex (*e.g.* Sarno) resulting from the overlapping of different pedogenetical cycles.

In general terms topsoils, having a colour ranging from very dark brown to brown, had a typical weak to strong granular and crumb structures and a sandy loam texture. All topsoils were generally well developed (with an average thickness of 20 cm), demonstrating that investigated sites were not subjected to intense erosion, which would have been expected considering the high to moderate slope gradient, the anthropic effect due to land management (mainly chestnut coppice).

Results of chemical analyses are provided in Table 2. Soils were characterized from similar features: for all the soil profiles, the pH (H_20) varied from extremely to slightly acid (except for Ceriana ranging from neutral to slightly alkaline) and overall pH increased with depth; the OC was in the topsoil always rather high (32 to 178 g kg^{-1}), which is typical of forestry soils, and regularly decreased with depth. For all the soil profiles, the CEC was generally consistently in line with the OC trend. Furthermore, soils showed a variable degree of andic features (evaluated by means of Al_o+1/2Fe_o Index of Andosolization process named IAP). Sarno and Vietri showed a very high value of AIP index (above 4%), Albaredo and Platì showed moderate values (some horizons >1 % AIP) while Ceriana showed values < 0,4% which is the minimum value for andic soils (FAO WRB 2006 – Soil Taxonomy 2006). Allophane and imogolite (%) were present in all the soil profiles with different amounts that generally increased with the depth (in the deepest horizons).

The amount in the soils of allophone and imogolite evaluated according to Parfitt (1990), generally increased with the depth and within the B horizons. In fact, even if the presence of short range order clay minerals is well expressed in all the analyzed soils (except Ceriana), however, an increasing trend of allophane and imogolite with depth was found for many profiles possibly also to be related to the presence of buried soils or more weathered buried soil horizons.

3.2 Soil Hydrology

Hydraulic properties, except for the Ceriana case study, showed from high to very high water content at saturation in the range 47-73% (Table 3, Fig. 2). Ceriana soil was characterized by the lowest water content at saturation (47%) reinforcing the results of chemical analyses showing that, for each horizon of Ceriana soil, IAP was significantly outside of typical IAP values for andic soils. On the other side, Platì, Albaredo, Versilia, Sarno, Quindici and Vietri soils are characterized by high and very high values of water content at saturation (52-73%; Table 3). It is presumable that these high values of saturated water content affected soil stability. In fact, a high water content has to be intended as an important landslide predisposing factor, since it plays a paramount role in weighing down the underlying materials, as previously described.

By looking at the water retention curves, it is evident that the analysed soils show high value of water content at saturation and a rather steep slope. This can help in inferring also information on the hydraulic conductivity curve, because the slope of the water retention curve, representing the rate of the water depletion in response to an increase of the suction, is strongly related to the slope of the unsaturated hydraulic conductivity curve (van Genuchten, 1980). This means that these soils exhibit a high aptitude to conduct water coupled with a high water retention capacity. This is a distinctive hydrological behaviour of soils with andic features. In fact, mineral soils like clay soils showing high water retention capacity (high saturated soil water content and gentle slope of the water retention curve) are not very conductive at least for h>-1000 cm, while mineral soils like sandy soils showing low water retention capacity (low value of saturated soil water content and steep slope of the water retention curve) are rather conductive at least for h>-1000 cm. Therefore, on the contrary of mineral soils, andosols show both high water retention capacity and hydraulic conductivity in the wet and intermediate branch of the functions.

Soil bulk density, showed values consistent with the IAP values. More specifically, Sarno, Quindici and Vietri soils which are characterized by a bulk density lower than 0.9 kg dm^{-3} (which is the bulk density limit for Andosols – FAO WRB 2006) show well expressed andic features, whereas Platì, Albaredo and Versilia having only moderate andic features (IAP 0.4-2%) showed higher bulk density values (Table 3).

For soils included in this study, we calculated IRI values in the interval of integration [-1;4.2] between the logarithm of pressure head (h) at saturation (assumed at h=0.1 cm) and the logarithm of pressure head at the wilting point (assumed at h=15849 cm) (Table 3). We also calculated the correlation between IRI values and the Index of Andic Processes (IAP) of the soils

object of this study and we found a *R* value of 64%. Then, we recalculated, in the interval of integration [-1;4.2], IRI for several European Andosols collected and analysed during the "COST Action 622: Soil resources of Europe volcanic ecosystems" (Basile et al., 2007); then this recalculated IRI was related to IAP. In Figure 3, we show that the distribution of IAP and IRI values of soils included in this study is in line with the distribution of IAP and European Andosols. In particular, as expected and typical of Italian Andosols (orange diamonds in Figure 3), except for the soil of Vietri which showed high IRI and high IAP values, soils of this study are characterized by IAP values belonging to the lowest zone of the graph IAP *vs*. IRI for European Andosols. In fact, within the European Andosols database, Italian Andosols show low IAP values. This feature is mainly due to Italian climatic conditions.

As concerns soil texture, the granulometric analyses revealed that overall the most frequent textural class was sandy loam (26 of the 46 analysed horizons belong to this class) (Figure 4).
Despite the very small dataset consisting of only 10 samples, these results suggest the possible existence of a direct linear relationship, affecting soil stability/instability, between the presence of andic soil features in a soil and the water retention properties of the soil itself. We highlight that, in order to evaluate and ascertain the existence of such relationship, the dataset should be certainly broadened. In fact, our results only represent a clue of the possible existence of the relationship between andic soil properties and water retention properties of a soil. Anyway, such results are important because it was not expected to find a strong correlation between two very different soil properties, having no methodological relationship (and uncertainty associated to casual errors), because the IAP is calculated as an empirical chemical index whereas the IRI results from the hydraulic characterization of the soil.

3.3 Consistency Check With New Soil Observation

In table 4 are given the main environmental features of other six minor flow-like mass movements employed as an independent consistency check about the relationship between andic soils and detachment areas of flow-like mass movements. They are located (from north to south) in Valtellina, Sangone, Penna Mountain, Campitello Matese, Valle Telesina, and Giffone sites and very diverse in terms of locations, elevation, slope and bedrock although they show similarities in terms of their forest land use which anyway varies between beech and chestnut.

In table 5 are given the results of soil analyses of this six minor landslides.

All soils were all characterized by A and Bw sequence. A horizons are dark in colour, reach in OC and having a soil structure granular and crumb. The texture is sandy loam and most pedon are subacid.

Mt. Penna, Campitello Matese, Telesina Valley and Giffone soils were all characterized by high IAP values larger than 2% (cfr. Table) indicating that they satisfy the diagnostic criterion for the andic soil properties (FAO WRB 2006 – Soil Taxonomy 2006) while Sangone an Valtellina showed moderate IAP values (in A and Bw horizons they are always between 0,6 and 1,3 %) always higher than the minimum 0,4% threshold value for Vitric Andosols.

In general terms, these pedon resemble closely to those described for large landslide in table 2 and clearly confirm a close association between andic soils and detachment of flow-like landslides.

3.4 Remarks on Soil Fertility and Soil Stability

Together with the high OC content, typical of forest soils, all the other chemical properties, such as pH H_2O and high CEC, present a picture of very fertile soils. As regards the physical properties, the loamy texture, which allows a good water gravitational drainage, also contribute to improve the physical fertility of these ecosystems. The fertility itself is another peculiar aspect of soils exhibiting andic features and is directly linked to the importance of preserving such soils from land degradation processes.

On the other side, these soils are known to be susceptible to degradation processes because of their physical and chemical properties they can be differently subjected to erosion and landslide phenomena. The analyzed soils were strongly subjected to land degradation because of both physical and chemical reasons that, together with other morphological factors, such as the slope, the aspect, etc., concurred to predispose the slopes to flow-like mass movements.

From a physical and hydraulic point of view, the high depth of the studied soils, probably referable to ancient and recent slope instability phenomena and ranging from 90 to 200 cm, provided a significant potential of water storage, responsible of great weight and high pressure (both considered main landslide predisposing factors) on deepest layers. Moreover, the water retention curves that we evaluated for selected horizons (Figure 2) exhibited high water retention values at both saturation (0.52 to 0.73 cm^3 cm^{-3}) and dry conditions: such a hydraulic behaviour is also characteristic of soils having andic properties, which are typically very light in dry condition, but

extremely heavy at wet and saturated condition. Sandy loamy and loamy textures are responsible of the physical fertility of these soils showing also a very high chemical fertility, as indicated by the high organic carbon content and the acidic values of soil pH (Table 2 and Table 5). In fact, loamy and sandy loamy textures allow the drainage of water. The fertility itself is another peculiar aspect of soils exhibiting andic features and is directly linked to the importance of preserving such soils from land degradation processes.

On the other side, from a functional point of view, the content of short range order clay minerals enabled the soil to quickly liquefy releasing water contained in their typical micro-structure. Such behavior (named smeariness in FAO 2006 and thixotropy in WRB, 2014) typically occurs in most andic soils after the application of an abrupt mechanical force (*i.e.* pressure). This may determine a high potential and a high danger for soil liquefaction under stress conditions (Vingiani and Terribile, 2006).

4. CONCLUSIONS

Because of their peculiar properties, soils displaying andic features are known to be remarkably important as regards both ecosystem fertility and susceptibility to land degradation processes, such as erosion and landslides phenomena. Recent studies have proved that (i) andic soils are much more widespread than previously thought and that they are also diffused in non-volcanic ecosystems under different environmental settings all over the world and (ii) in Campania region the occurrence of flow-like mass movements is directly linked to the presence of Andosols.

In such framework, we attempted to evaluate whether the association between andic soils and flow-like landslide applied elsewhere. Hence, we selected 6 historical catastrophic flow-like mass movements that happened in Italy in different environmental, geological and geomorphological settings in the last 70 years in order to evaluate the physical, chemical and hydrological soil properties and, in particular, to understand if such properties are attributable to andic soil features.

It has been observed that, despite the differences in terms of geological, geomorphological and environmental conditions, overall, the performed analyses revealed the existence of considerable chemical, physical and hydraulic homogeneity and, especially, the presence of andic features characterized most of the studied soils.

In particular, soils collected in the detachment areas of Sarno and Vietri showed a very high andic features (AIP > 4%), Albaredo and Platì showed moderate values (AIP >1%) while Ceriana

showed values < 0,4% which is the minimum value for andic soils (FAO WRB 2006 – Soil Taxonomy 2006). Moreover, other soil features such as soil colors, pH, CEC, OC, allophane and imogolite content are all referable and typical of soil with andic features.

Then, after having found out that the large majority of studies soils - albeit not all - have andic features we made a consistency check using an independent set of six minor flow-like landslides which confirmed the same results of the major landslides.

The current study is of special interest for landslide hazard assessment because these findings shed new light on the similarity of the soils involved by flow-like mass movements, both the catastrophic and the minor ones, suggesting a pedological control on the debris flow hazard. Nevertheless, an extension to other mountain environments, in order to enlarge soil dataset, is required and strongly encouraged.

In conclusion, soils showing andic features require to be protected from land degradation in order to (i) preserve their extraordinary fertility which allows the development of a florid and lush ecosystem of agricultural and ecological importance and (ii) avoid the occurrence of flow-like mass movements, representing a tremendous hazard which exposes people and ecosystems to a very high risk. We also highlight that the understanding of the distribution of andic soils and the existence of a possible direct relationship between the presence of andic soil properties and the occurrence of flow-like movements are useful tools to better understand which areas of the Italian territory could be mostly subjected to flow-like landslides phenomena. In the framework of risk management policies and appropriate forest planning, such information are very useful to (i) improve landslide mitigation strategies, (ii) decrease soil erosion by preserving soil continuity, and (ii) protect mountain soils of key environmental importance.

Moreover, it is fundamental to emphasize that the characterization of soil properties involved in flow-like landslides is of primary importance for setting up flow-like risk mitigation strategies and soil conservation management policy but also to preserve the soil themselves because of their agricultural potential and ecological importance. In particular, the information about the soil depth and the soil layering that we collected in these case studies would be useful towards practical applications and in order to implement soil information in dynamic landslide models. We highlight that the implementation of dynamic models is an essential requirement for the understanding, within entire regions where andic soil features (considered as a landslide predisposing factor) are developed, of which could be the most susceptible areas where a flow-like landslide could happen.

REFERENCES

Alcantara-Ayala, I., 2002. Geomorphology, natural hazards, vulnerability and prevention of natural disasters in developing countries. *Geomorphology*, *47*(2), pp.107-124.

Arnalds, O., Thorarinsdottir, E.F., Metusalemsson, S., Jonsson, A., Gretarsson, E. & Arnason, A. 2001. Soil Erosion in Iceland. Soil Conservation Service and Agricultural Research Institute, Reykjavik, Iceland.

Arya, L.M., 2002. Wind and hot air methods. In: Dane, J.K., Topp, G.C. (Eds.), Methods of Soil Analysis. Part 4. Physical Methods, vol. 5. SSSA Book Ser., SSSA, Madison, WI, pp. 916–920.

Basile A., Coppola A., De Mascellis R., Mele G., Terribile F. (2007) A comparative analysis of the pore system in volcanic soils by means of water-retention measurements and image analysis. In: Arnalds Ó., Óskarsson H., Bartoli F., Buurman P., Stoops G., García-Rodeja E. (eds) Soils of Volcanic Regions in Europe. Springer, Berlin, Heidelberg

Basile, A., Mele, G., Terribile, F. (2003) - Soil hydraulic behavior of a selected benchmark soil involved in the landslide of Sarno 1998. Geoderma, 117, 331–346.

Batjes, N.H. (1996) Total carbon and nitrogen in the soils of the world. European Journal of Soil Science, 47, 151–163.

Baumler, R., Zech, W., 1994. Characterization of Andisols developed from non volcanic material in Eastern Nepal. Soil Science 158 (3), 211–217.

Baumler, R., Caspari, T., Totsche, K.U., Dorji, T., Norbu, C., Baillie, I.C., 2005. Andic properties in soils developed from nonvolcanic materials in central Bhutan. Journal ofPlant Nutrition and Soil Science — Zeitschrift für Pflanzenernahrung und Bodenkunde 168 (5), 703–713.

Calcaterra D., Guarino P.M. (1997) Dinamica morfologica e fenomeni recenti nell'area collinare napoletana (settore occidentale). Geologia tecnica e Ambientale 371, IX Congresso O.N.G., Roma 17-20 Aprile 1997, 1-5.

Calcaterra D., Parise M., Palma B., Palella L. (2002) Multiple debris-flow in volcaniclastic materials mantling carbonate scope. In: Wieczorek GF., Naeser ND (eds.) Debris Flow Hazard Mitigation, mechanics, Predition and Assessment. A.A. Balkema/Rotterdam/Brookfield, 99-107.

Caner, L., Bourgeon, G., Toutain, F., Herbillon, A.J., 2000. Characteristics of non-allophanic Andisols derived from low-activity clay regoliths in the Nilgiri Hills (Southern India). European Journal of Soil Science 51 (4), 553–563.

Cruden D.M., Varnes D.J. (1996) - Landslide types and Processes. In: Turner A.K., Shuster R.L. (eds.), Landslides: Investigation and Mitigation. TransportationResearch Board Special Report 247, National Research Council, 36-75.

Dane, J.H., Hopmans, J.W., 2002. Water retention and storage. In: Dane, J.K., Topp, G.C. (Eds.), Methods of Soil Analysis. Part 4. Physical Methods, vol. 5. SSSA Book Ser., SSSA, Madison, WI, pp. 671–720.

Delvaux, B., Strebl, F., Maes, E., Herbillon, A.J., Brahy, V., Gerzabek, M., 2004. An Andosol–Cambisol toposequence on granite in the Austrian Bohemian Massif. Catena 56 (1–3), 31–43.

De Vita P., Agrello D. & Ambrosino F. (2006) - Landslide susceptibility assessment in ash-fall pyroclastic deposits surrounding mount Somma-Vesuvius. Application of Geophysical Surveys for Soil Thickness Mapping. Journal of Applied Geophysics, 59, 126-139. Elsevier, Amsterdam, Netherlands.

FAO (Food and Agriculture Organization) (2006) - Guidelines for Soil Profile Description (Revised), 4th ed. (Rome).

Fontes, J.C., Pereira, L.S. & Smith, R.E. 2004. Runoff and erosion in volcanic soils of Azores: simulation with OPUS. Catena, 56, 199–212.

Hungr O., S.G. Evans, M.J. Bovis and J.N. Hutchinson (2001) - A review of the classification of landslides of flow type. Environmental and Engineering Geoscience, 7, pp. 221-238.

Iamarino M. & Terribile F. (2008) The importance of andic soils in mountain ecosystems: a pedological investigation in Italy. . European Journal of Soil Science 59 (6), 1284–1292.

IFFI Project (2007) http://193.206.192.136/cartanetiffi/# (last access 22/12/2015)

IUSS Working Group WRB: World Reference Base for Soil Resources (2014) - International soil classification system for naming soils and creating legends for soil map, World Soil Resources Reports No. 106., FAO, Rome, 2014.

Iverson, R. M. (1997): The physics of debris flows. Rev. Geophys. 35(3), 245–296.

Kimble, J.M., Ping, C.L., Sumner, M.E., Wilding, L.P., 2000. Andisols. In: Sumner, M.E. (Ed.), Handbook of Soil Science. CRC PRESS LLC, Boca Raton, FL, pp. E209–E224.

Klute A. (1986) Water retention: Laboratory methods. In: Klute (ed.) Methods of soil analysis, Part I, 2nd edn, Agron Monogr 9, ASA and SSSA, Madison, 635-662.

Leamy, M.L. 1984. Andisols of the world. p. 369-387. In Comm. Congr. Int. Suelos Volcan. Secretariado de Publicaciones Serie Informes 13, Universidad de la Laguna, La Laguna, Spain.

McDaniel, P.A., Wilson, M.A., Burt, R., Lammers, D., Thorson, T.D., Mcgrath, C.L. et al. 2005. Andic soils of the inland Pacific Northwest, USA: properties and ecological significance. Soil Science, 170, 300–311.

Mileti F.A., Langella G., Prins M.A., Vingiani S., Terribile F. (2013) - The hidden nature of parent material in soils of Italian mountain ecosystems. Geoderma, 207-208, 291-309.

Mizota, C. & van Reeuwijk, L.P. 1989. Clay Mineralogy and Chemistry of Soils Formed in Volcanic Material in Diverse Climatic Regions. International Soil Reference and Information Centre, Soil Monograph 2, Wageningen, the Netherlands.

Musso, A., Olivares, L. (2004): Flowslides in pyroclastic soils – transition from ‘‘static liquefaction’’ to ‘‘fluidization’’. In: Picarelli, L. (ed.), Proc. Int. Workshop on Occurrence and Mechanisms of Flows in Natural Slopes and Earthfills, Sorrento, 117–127.

Nanzyo M. (2002) - Unique properties of volcanic ash soils. Global environmental research, 6 (2), 99-112.

Palmieri W. 2011. Per una storia del dissesto e delle catastrofi idrogeologiche in Italia dall’Unità ad oggi. CNR Quaderno ISSM n. 164.

Parfitt R.L. (1990) - Allophane in New Zealand – a review. Aust. J. Soil Res. 28, 343-360.

Picarelli L, Olivares L, Comegna L, Damiano E (2008) Mechanical aspects of flow-like movements in granular and fine grained soils. Rock Mech Rock Eng 41(1):179–197

Revellino P, Hungr O, Guadagno FM, Evans SG (2004) Velocity and runout simulation of destructive debris flows and debris avalanches in pyroclastic deposits, Campania region, Italy. Environ Geol 45(3):295–311

Schwertmann, U. (1964) –Differenzierung der Eisenoxide des Bodensdurch Extraction mit Ammoniumoxalat-Losung. Zeitschrift Pflanzenernhar. Dungung Bodenkunde, 105, 194-202.

Scognamiglio, S., Calcaterra, D., Iamarino, M., Langella, G., Orefice, N., Vingiani, S., & Terribile, F. (2016a). Andic soil features and debris flows in Italy. New perspective towards prediction. In *EGU General Assembly Conference Abstracts* (Vol. 18, p. 10543).

Scognamiglio, S., Terribile, F., Iamarino, M., Orefice, N., & Vingiani, S. (2016b). Soil properties and debris flows in Italy: potential relationships. *RENDICONTI ONLINE SOCIETA GEOLOGICA ITALIANA*, *41*, 199-202.

Shoji, S., M. Nanzyo, and R.A. Dahigren. 1993. Volcanic ash soils: Genesis, properties and utilization. Elsevier, Amsterdam, Netherlands.

Terribile F., Basile, A., De Mascellis R., Di Gennaro A., Mele G., Vingiani S. (2000) – I suoli delle aree di crisi di Quindici e Sarno: proprietà e comportamenti in relazione ai fenomeni franosi. Quaderni di Geologia Applicata, 7 (1), 59-79.

Terribile, F., Basile, A., De Mascellis, R., Iamarino, M., Magliulo, P., Pepe, S., Vingiani S. (2007) – Landslide processes and Andosols: the case study of the Campania region, Italy. In: O. Arnalds, F.Bartoli, P.Buurman, H. O´ Skarsson, G. Stoops, & E. Garcıa-Rodeja (eds.), Soils of Volcanic Regions in Europe (eds O. Arnalds, F Bartoli, P Buurman, H O´ skarsson, G Stoops, & E Garcı´a-Rodeja), pp. 545–563. Springer Verlag, Berlin and Heidelberg, 545–563.

Terribile, F., Iamarino, M., Langella, G., Manna, P., Mileti, F. A., Vingiani, S., and Basile, A. 2017. The hidden ecological resource of andic soils in mountain ecosystems: evidences from Italy, Solid Earth Discuss., https://doi.org/10.5194/se-2017-57.

USDA (2006) Keys to Soil Taxonomy, 10th edn. United States Department of Agriculture NRCS, Washington, DC. USDA-NRCS

USDA-NRCS (2004). Soil Survey laboratory methods manual. Soil Survey Investigation Report. 42**,** Version 4, pp 700

Vallario A. (2001) Il dissesto idrogeologico. CUEN, 295.

Vingiani, S., Mele, G., De Mascellis, R., Terribile, F., Basile, A., 2015. Volcanic soils and landslides: A case study of the island of Ischia (southern Italy) and its relationship with other Campania events. Solid Earth, 6 (2), pp. 783-797. DOI: 10.5194/se-6-783-2015.

Vingiani, S. and Terribile, F., 2006. Properties, geography, classification and management of volcanic ash soils: an overview. Acta Volcanologica, 18(1/2), p.113.

van Genuchten, M.Th., 1980. A closed-form equation for predicting the hydraulic conductivity of unsaturated soils. Soil Sci. Soc. Am. J. 44, 892–898.

Walkley A., Black I.A. (1934) - An examination of the Degtjareff method for determining organic carbon in soils: effect of variations in digestion conditions and of inorganic soil constituents. Soil Sci., 63, 251–263.

WRB (2006) World Reference Base for Soil Resources, 2nd edn. World Soil Resources Reports 103, FAO Rome.

Main data of the entire landslides							Main environmental data of the sampling sites					
Soil profile	**Region**	**Date of the event**	**Slope range of det. areas**	**Number of landslides**	**Rainfall peak**	**Number of Victims**	**Coordinates WGS84**	**Elevation (m)**	**Slope**	**Aspect**	**Land use**	**Bedrock**
ALBAREDO	Lombardia	16/11/2002	41°-50°	50	230 mm/60 h	2	545715 m E 5105989 m N UTM32N	1000	27°	SW	Grassland with chestnut	Till deposits and granitoid gneisses
CERIANA	Liguria	23/11/2000	N/A	1204	180 mm/24 h	3	403100 m E 4860512 m N UTM33N	875	27°	SE	Chestnut forest	Marly sandstones unit (turbiditic)
VERSILIA	Toscana	19/06/1996	31°-45°	647	400 mm/6 h	14	605317 m E 4873717 m N UTM32N	365	20°	SE	Chestnut forest	Arenaceous rocks and phyllitic schist
SARNO	Campania	05/05/1998	33°-55°	161	173 mm/48 h	159	469088 m E 4521127 m N UTM33N	800	47°	SW	Chestnut forest	Limestone
VIETRI	Campania	26/10/1954	40°-50°	321	504 mm/24 h	321	476194 m E 4503127 m N UTM33N	275	40°	N	Chestnut forest	Limestone and dolomites
PLATI'	Calabria	16/10/1951	40°-50°	18	1495 mm/72 h	17	591469 m E 4230816 m N UTM33N	900	28°	SE	Mixed forest (Chestnut - Oak)	Micaschists and paragneisses, phyllites and marbles

***Table 1**: Main features of the six catastrophic flow-like landslides and environmental settings of sampling sites. Abbrev: NA: not available; det.: detachment*

Soil profile	Horizon	Depth (cm)	Colour (moist)	Structure	Texture (USDA)	pH (H_2O)	OC (g kg^{-1})	CEC (cmol kg^{-1})	Al_o (%)	Fe_o(%)	Si_o (%)	Al_o+0,5Fe_o (%)	Allophane and imogolite (%)
ALBAREDO	A	0-40	10YR 3/2	m m SB	**n.a.**	5,1	32,0	4,0	0,8	1,2	0,2	1,4	1,1
	Bw	40-110	10YR 4/4	m m SB	sandy loam	5,3	11,0	1,6	1,3	1,0	0,5	1,8	3,3
CERIANA	A	0-10	10 YR 3/2	n.a.	sandy loam	6,6	52,6	32,4	0,11	0,14	0,03	0,18	0,2
	A/B	10-20	10 YR 4/3	n.a.	clay loam	7,4	9,6	16,4	0,13	0,20	0,03	0,23	0,2
	Bw1	20-50	10 YR 4/4	n.a.	clay loam	7,6	5,7	18,0	0,14	0,16	0,02	0,22	0,2
	Bw2	50-80	10 YR 5/4	n.a.	clay loam	7,3	4,9	15,3	0,14	0,16	0,03	0,22	0,2
	Bw3	80-110	10 YR 3/4	n.a.	clay	7,4	6,8	19,2	0,15	0,19	0,03	0,24	0,2
VERSILIA	OA	0-2	10 YR 2/1	s c GR	sand	4,1	178,8	14,6	0,1	0,2	0,1	0,2	0,4
	Bw1	2-65	10 YR 4/4	m c SB	sandy loam	4,8	12,9	2,8	0,3	0,5	0,1	0,5	0,5
	Bw2	65-150	7,5 YR 4/6	m m SB	sandy loam	4,6	9,6	2,8	0,6	0,9	0,2	1,0	1,1
SARNO	A	0 - 20	10YR 3/1	w m GR	sandy loam	6,8	98,5	34,6	4,4	1,1	2,9	5	20,7
	Bw	20 - 38	10YR 4/3	w m SB	sandy loam	7,3	10,7	21,4	2,0	1,0	1,3	2,5	9,0
	BC	38 - 71	2.5YR 4/2	w c SB	loamy sand	7,5	4,2	12,5	5,4	0,7	2,8	5,7	20,0
	C	71 - 100	5Y 7/3	n.d.	n.d.	n.d.	n.d.	n.d.	n.d.	n.d.	n.d.	n.d.	n.d.
	2A/Bwb	100 - 140	10YR 3/4	w c SB	sandy loam	7,5	10,5	29,6	1,6	0,9	1,2	2,1	8,4
	2Bw/Cb	140 - 150	2.5Y 4/4	w m SB	n.d.	n.d.	n.d.	n.d.	n.d.	n.d.	n.d.	n.d.	n.d.
	2Cb	150 - 200	2.5Y 5/4	w m SB	n.d.	n.d.	n.d.	n.d.	n.d.	n.d.	n.d.	n.d.	n.d.
VIETRI	A	0 - 9	10YR 2/2	s c GR	sandy loam	7,3	58,0	n.d.	3,8	1,2	2,5	4,5	17,6
	B1	9 - 28	10YR 3/3	s m SB	sandy loam	7,4	24,3	26,5	4,3	1,2	3,2	5,0	22,6
	B2	28 - 48	10YR 3/3	m m SB	silty loam	7,6	15,6	27,6	4,9	1,1	4,0	5,5	28,4
	B3	48 - 70	10YR 3/4	m m SB	silty loam	7,8	9,6	32,3	2,9	1,1	2,0	3,5	14,0
PLATI'	A	0-45	10YR 2/2	m c GR	sandy loam	5,1	69,6	19,2	1,0	0,8	0,2	1,3	1,7
	Bw1	45-90	10YR 4/6	m m SB	sandy loam	5,1	25,0	24,9	1,2	0,7	0,9	1,5	6,7
	Bw2	90-120	10YR 3/6	n.a.	sandy loam	5,2	18,9	19,9	0,9	0,8	0,5	1,3	3,8
	B/C	120+	10YR 3/6	n.a.	sandy loam	6,0	19,8	9,7	0,6	0,5	0,4	0,8	3,0

***Table 2**: Main morphological, chemical and physical properties of the investigated soils. Abbrev. Structure (according to FAO, 2006): Grades: w= weak; m= moderate; s=strong. Size classes: c=coarse; vc=very coarse; m=medium; f=fine. Types: CR= crumbly; AB= angular bolcky; PR= prismatic; SB= subangular blocky; MA= massive; SG= single grain; GR= granular; OC = organic carbon; CEC = cation exchange capacity; Alo, Feo, and Sio= acid ammonium oxalate-extractable forms; Allophane and imogolite (%) were calculated using the Parfitt's formula (1990); n.d.= not determined.*

Profile	IAP %	Bulk density [g*cm^3]	Saturated water content [m^3*m^{-3}]	IRI [m^3*m^{-3}]
Platì A	1.30	1	0.61	0.43
Platì Bw	1.50	1.15	0.52	0.38
Albaredo Bw	1.82	1.11	0.64	0.43
Versilia Bw1	0.50	1.04	0.55	0.37
Ceriana Bw1	0.22	1.27	0.47	0.31
Sarno 2Ab/Bwb	2.2	0.66	0.73	0.56
Sarno 2Bwb/Cb	-	0.72	0.65	0.47
Vietri B1	5	0.66	0.72	0.49
Vietri B2	5.5	0.71	0.68	0.47
Quindici A	2.2	0.9	0.73	0.46
Quindici Bw1	3.1	0.66	0.72	0.50

Table 3: *Values of Index of Andosolization Processes (IAP), bulk density, saturated water content and IRI of the analysed soils.*

Location	Region	Coordinates WGS84	Elevation (m)	Slope	Aspect	Land use	Bedrock
VALTELLINA	Lombardia	601415 m E 5148018 m N UTM32N	1500	23°	N	Fir forest	Till deposits and migmatites
SANGONE	Piemonte	366900 m E 4986237 m N UTM32N	950	25°	E	Mixed forest (beach and oak)	Metamorphic rocks (gneiss)
Mt. PENNA	Liguria	539417 m E 4927750 m N UTM32N	1370	23°	NW	Beech forest	Clays and limestones sometimes ophiolitic unit (turbiditic)
CAMPITELLO MATESE	Molise	449881 m E 4590906 m N UTM33N	1367	42°	NE	Broadleaves and beach forest	Limestone
TELESINA VALLEY	Campania	465426 m E 4559684 m N UTM33N	775	27°	N	Mixed forest (Chestnut - Oak)	Limestone
GIFFONE	Calabria	600666 m E 4255031 m N UTM33N	665	27°	NW	Chestnut forest	Granites and granodiorites

Table 4: *Environmental setting of the six minor flow-like landslides used as an independent consistency check*.

Location	Horizon	Depth (cm)	Colour (moist)	Structure	Texture (USDA)	pH (H_2O)	OC (g kg^{-1})	CEC (cmol kg^{-1})	Al_o (%)	Fe_o (%)	Si_o (%)	$Al_o+0,5Fe_o$ (%)	Allophane and imogolite (%)
VALTELLINA	OAE	0-20	7,5YR 4/2	s c GR	sand	4,0	86,0	12,7	0,3	1,3	0,1	1,0	0,6
	Bw	20-50	10YR 4/4	w m SB	sandy loam	5,5	29,8	6,0	0,5	1,5	0,1	1,3	0,5
	BC	50-90	5Y 4/3	SG	n.a.	5,1	n.a.	2,2	0,1	0,2	0,1	0,2	0,5
SANGONE	A	0-5	10YR 3/2	m m GR	sandy loam	4,7	31,8	14,1	n.d.	n.d.	n.d.	n.d.	n.d.
	Bw1	5-45	10YR 3/3	m m SB	sandy loam	4,8	14,5	16,3	0,5	0,7	0,02	0,8	0,1
	Bw2	45-75	10YR 4/3	m m SB	sandy loam	4,7	8,6	12,4	0,3	0,6	0,01	0,6	0,1
	Ab	75-112	10YR 3/2	m m SB	silt loam	4,8	8,1	9,2	n.d.	n.d.	n.d.	n.d.	n.d.
M.TE PENNA	A1	0-5	10YR 2/2	s c CR	sandy loam	5,4	126,3	11,4	1,2	3,1	0,1	2,8	0,8
	A2	5-20	10YR 3/3	s c CR	loam	5,3	109,8	7,1	1,4	2,7	0,1	2,7	0,8
	B/A	20-35	10YR 3/4	m vc GR	loam	5,5	76,8	4,5	1,9	2,3	0,2	3,1	1,3
	Bw1	35-70	10YR 4/4	m c SB	loam	5,5	44,6	3,5	1,9	2,6	0,3	3,2	2,0
	Bw2	70-110	10YR 3/6	m m SB	sandy loam	5,6	47,5	2,1	1,7	1,8	0,3	2,6	2,2
CAMPITELLO MATESE	Ah	0-8	10 YR 3/3	m f GR	n.d.	5,7	53,9	54,2	2,2	0,2	0,6	2,3	4,5
	A	8-20	10YR 3/5	m f GR	n.d.	5,7	45,5	55,2	2,2	0,3	0,6	2,4	4,4
	B	20-35	7,5YR 3/2	m f GR	n.d.	5,6	32,0	46,7	1,9	0,1	0,6	2,0	4,4
	Bb	35-50	10YR 3/4	m f GR	n.d.	5,7	21,2	41,7	1,8	0,1	0,6	1,8	4,2
	BC	50-68	10YR 3/6	m f GR	n.d.	5,5	25,9	43,4	1,8	0,2	0,6	1,9	4,4
	2 Bb	68-80	10YR 4/4	m f GR	n.d.	5,7	22,2	45,7	1,9	0,1	0,6	1,9	4,1
	C	80-120	n.d.	m f GR	n.d.	6,8	16,8	40,6	1,8	0,2	0,6	1,9	4,2
TELESINA VALLEY	A1	0-10	10 YR 3/2	m m GR	sandy loam	5,9	36,2	75,3	2,3	0,6	n.a.	2,6	n.a.
	A2	10-25	10 YR 4/3	m f SB	loam	5,9	35,2	53,2	4,6	1,2	1,5	5,2	10,7
	AB	25-35	10 YR 4/3	m f SB	loam	6,1	26,4	44,3	3,4	0,8	n.a.	3,8	n.a.
	Bw1	35-60	10 YR 3/4	m f SB	loam	6,2	20,7	40,6	3,3	0,8	n.a.	3,7	n.a.
	Bw2	60-90	10 YR 3/4	m c SB	loam	6,3	19,3	38,7	4,1	0,9	1,8	4,5	12,8
	Bw3	90-120	10 YR 3/4	m c SB	clay loam	6,3	13,7	45,5	3,2	0,6	n.a.	3,5	n.a.
GIFFONE	A1	0-15	10YR 2/2	s m GR	sandy loam	5,1	51,4	36,0	1,2	0,6	0,3	1,5	2,0
	A2	15-30	7.5YR 3/3	m m SB	sandy loam	5,0	49,4	38,5	1,8	0,9	0,5	2,3	3,4
	Bw1	30-50	7.5YR 3/3	m m SB	loam	5,3	30,9	26,3	1,9	1,0	0,6	2,4	4,6
	Bw2	50-80	7.5YR 3/3	m m SB	loam	5,6	25,7	26,0	1,2	0,8	0,4	1,6	2,5
	2Ab	80-110	10YR 3/2	m m SB	sandy loam	5,5	30,1	29,2	1,7	1,0	0,6	2,2	4,2

3Bw1	110-150	7.5YR 3/4	m c SB	sandy loam	5,6	17,0	18,0	1,3	1,0	0,4	1,8	3,1
3Bw2	150-200	10YR 4/4	m c SB	sandy loam	6,0	1,8	17,4	0,4	0,7	0,1	0,7	0,6

Table 5: *Main morphological, chemical and physical properties of the investigated soils. Abbrev. Structure (according to FAO, 2006): Grades: w= weak; m= moderate; s=strong. Size classes: c=coarse; vc=very coarse; m=medium; f=fine. Types: CR= crumbly; AB= angular bolcky; PR= prismatic; SB= subangular blocky; MA= massive; SG= single grain; GR= granular; OC = organic carbon; CEC = cation exchange capacity; Alo, Feo, and Sio= acid ammonium oxalate-extractable forms; Allophane and imogolite (%) were calculated using the Parfitt's formula (1990); n.d.= not determined.*

Figure 1: *Distribution of the study areas in Italy. Yellow placemarks represent sites where catastrophic flow-like landslides occurred, whereas green ones are for sites where minor flow-like landslides occurred.*

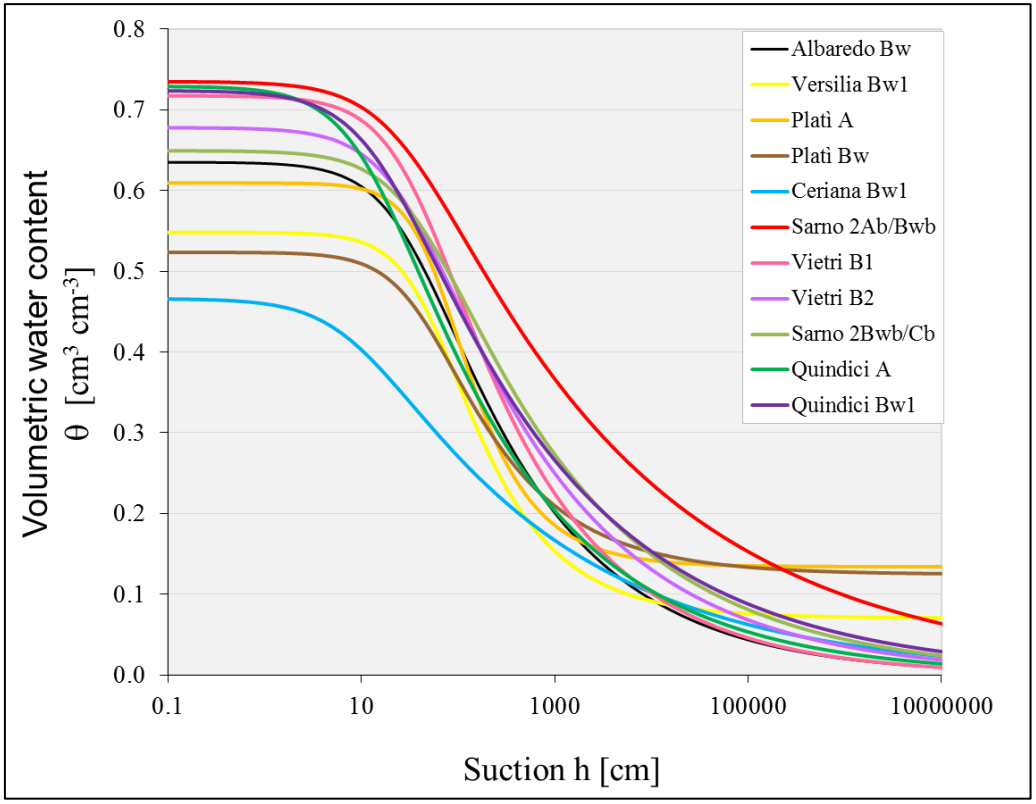

***Figure 2**: Soil water retention curves for the analysed soils.*

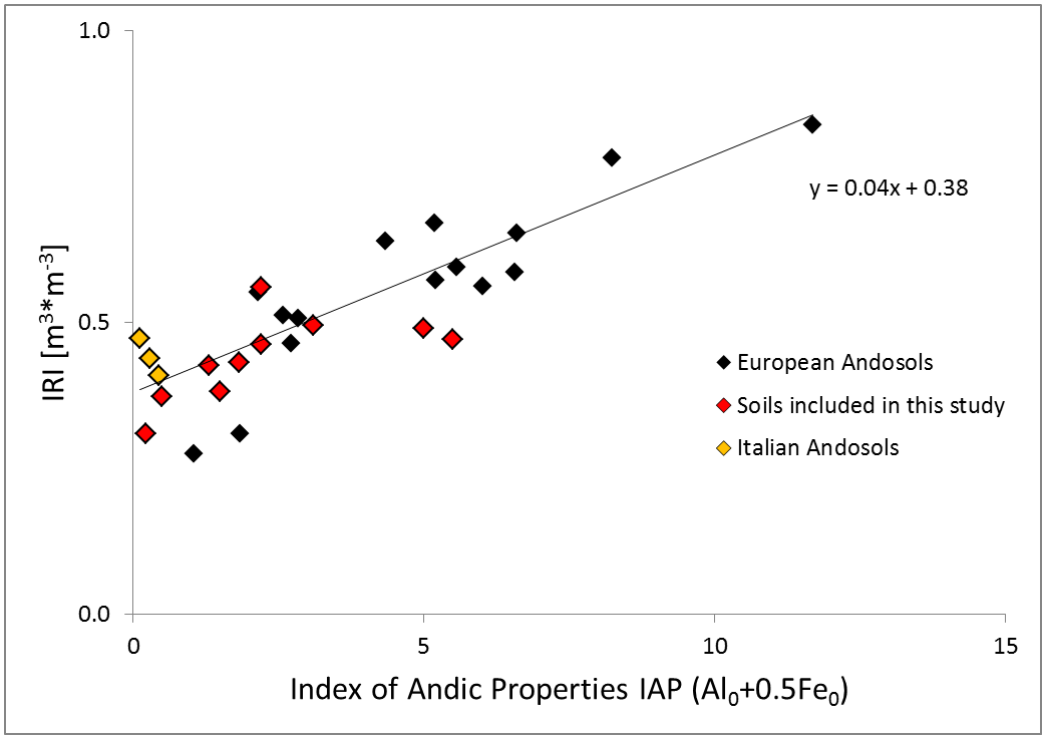

***Figure 3**: Correlation between Integral Retention Index (IRI) and the index of andosolization processes expressed by Al_o+0.5Fe_o. Red symbols represent the soils included in this study, black symbols are for European Andosols, and orange symbols are for Italian Andosols.*

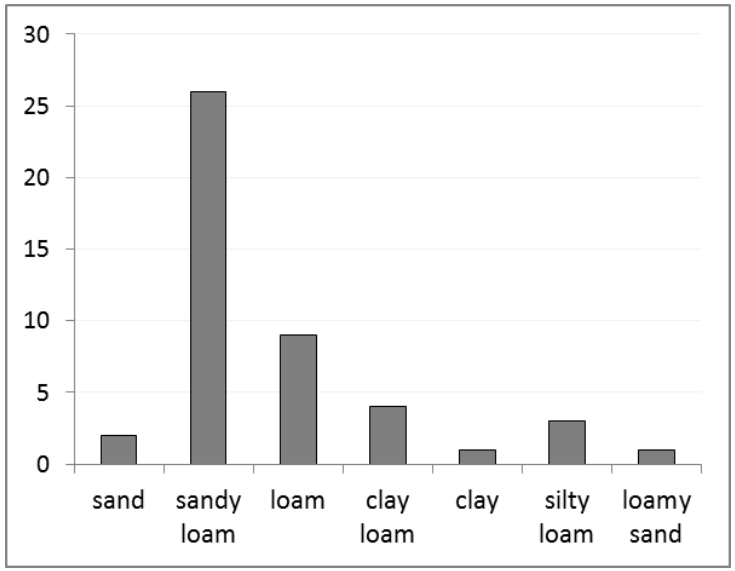

Figure 4: *Frequency of soil textural classes. Total number of the analysed horizons is 42. Specific information about the textural class of each horizon of the twelve different soil profiles object* of this study are reported in Table 2 and in Table 5.

GENERAL CONCLUSIONS

The research work described in the current thesis was an effort to join the different scientific domains of soil science, applied geology and landslide modelling over very important landslide phenomena, namely flow-like landslides (Hungr et al., 2001), which are one of the most dangerous natural hazard.

We introduced the importance of a pedological approach finalized to evaluate key soil properties, intended as predisposing factors of flow-like mass movements. In particular, we found the presence of andic soils where important or minor Italian flow-like landslides occurred. Due to the unique set of properties, andic soils are considered to be highly exposed to landslide phenomena and other land degradation processes. Such findings shed new light on the similarity of the materials involved by flow-like landslides (in Italy), suggesting a pedological control on the flow-like hazard. In this context, we highlight that a multidisciplinary approach would be required in order to deepen the knowledge of landslide predisposing and triggering factors. In fact, soil properties have to be considered a crucial predisposing factor (together with the other commonly recognized hydraulic and geotechnical properties) because they could dramatically increase the susceptibility of a soil to be involved in flow-like landslides.

Among dynamic landslide models, we chose a LHT model (namely, STEP-TRAMM) which gave satisfying performances when implemented on simplified reality (*i.e.* homogeneous soils), indicating the location of the first rupture within the soil and the position and the area of each simulated landslide. Despite the limited resolution of the numerical grid that we set, the model was able to properly detect most susceptible landslide areas for the Napf, Pogliaschina and Camaldoli hill catchments. Such results were strongly encouraging but a bigger effort would be required by considering that, in many Italian environments, landslides usually occur where layered soils occur. In fact, our experience demonstrated that all over Italy there are different environmental and geological contexts where catastrophic or minor flow-like landslides involve layered soils. For such cases, the layering, which is typical of andic soils, is a not negligible landslide predisposing factor. In fact, the contact between different soil horizons, showing different properties (*e.g.* soil texture, saturated water retention, *etc.*), represents a physical and hydraulic discontinuity. In this sense, the layering creates weak surfaces within the entire soil profile, where an increase of positive pore pressure can develop and trigger flow-like landslides. Furthermore, the study conducted in Telesina Valley showed that soil depth can importantly vary not only with

the depth, but also in the space as a function of the different geomorphological contexts that can be found over the same hillslope. A possible further effort made to allow the implementation of the model also on layered soils would provide the possibility to predict flow-like mass movements in a much broader range of possibilities and in different Italian domains exposed to these dangerous hazards.

REFERENCES

Alcantara-Ayala, I., 2002. Geomorphology, natural hazards, vulnerability and prevention of natural disasters in developing countries. *Geomorphology*, *47* (2), pp.107-124.

Arnalds, O., Thorarinsdottir, E.F., Metusalemsson, S., Jonsson, A., Gretarsson, E. & Arnason, A. 2001. Soil Erosion in Iceland. Soil Conservation Service and Agricultural Research Institute, Reykjavik, Iceland.

Basile, A., Mele, G., Terribile, F. 2003. Soil hydraulic behaviour of a selected benchmark soil involved in the landslide of Sarno 1998. Geoderma, 117, 331–346.

Baum R.L. and J.W. Godt (2010) - Early warning of rainfall-induced shallow landslides and debris flows in the USA. Landslides, 7, pp. 259-272.

Caine N., (1980) - The rainfall intensity-duration control of shallow landslides and debris flows. Geografiska Annaler 62A, pp. 23-27.

Calcaterra D., M. Parise, B. Palma and L. Pelella (1999) - The May 5th 1998, landsliding event in Campania (southern Italy): inventory of slope movements in the Quindici area. In Proc. Intern. Symp. on "Slope Stability Engineering", IS – Shikoku 1999, Matsuyama, Japan, pp. 1361-1366.

Campbell R.H. (1975) - Soil slips, debris flows, and rainstorms in the Santa Monica Mountains and vicinity, southern California. In: US Geological Survey Professional Paper 851. Washington DC: U.S. Government Printing Office, 51 pp.

Cascini L., S. Cuomo and D. Guida (2008) - Typical source areas of May 1998 flow-like mass movements in the Campania region, Southern Italy. Engineering geology, 96, pp. 107-125.

Cascini L. S Cuomo, M. Pastor and G. Sorbino (2010) - Modeling of rainfall-induced shallow landslides of the Flow type. Journal of Geotechnical and Geoenvironmental Engineering, pp.85-98.

Del Prete M., F.M. Guadagno and A.B. Hawkins (1998) - Preliminary report on the landslides of 5 May 1998, Campania, southern Italy. Bull Eng Geol Environ, 57, pp. 41-50.

De Vita P., E. Napolitano, J.W. Godt and R. Baum (2013) - Deterministic estimation of hydrological thresholds for shallow landslide initiation and slope stability models: case study from the Somma-Vesuvius area of southern Italy. Landslides, 10, pp. 713-728.

Di Crescenzo G. and A. Santo (2005) - Debris Slides-Rapid Earth Flow In The Carbonate Massifs Of The Campania Region (Southern Italy): Morphological And Morphometric Data For Evaluating Triggering Susceptibility. Geomorphology, 66, pp. 255-276.

Fontes, J.C., Pereira, L.S. & Smith, R.E. 2004. Runoff and erosion in volcanic soils of Azores: simulation with OPUS. Catena, 56, 199–212.

Guadagno F.M, R. Forte, P. Revellino, F. Fiorillo and M. Focareta (2005) - Some aspects of the initiation of debris avalanches in the Campania Region: The role of morphological slope discontinuities and the development of failure. Geomorphology, 66, pp. 237-254.

Guzzetti F., S. Peruccacci, M. Rossi and C.P. Stark (2008) -The rainfall intensity–duration control of shallow landslides and debris flows: an update. Landslides 5, 1, pp. 3-17.

Hungr O., S.G. Evans, M.J. Bovis and J.N. Hutchinson (2001) - A review of the classification of landslides of flow type. Environmental and Engineering Geoscience, 7, pp. 221-238.

IUSS Working Group WRB, 2014. World Reference Base for Soil Resources 2014. International soil classification system for naming soil and creating legends for soil maps. Food and Agriculture Organization of the United Nations. Rome: 182 ss.

Leamy, M.L. 1984. Andisols of the world. p. 369-387. In Comm. Congr. Int. Suelos Volcan. Secretariado de Publicaciones Serie Informes 13, Universidad de la Laguna, La Laguna, Spain.

Lehmann, P., and D. Or (2012), Hydromechanical triggering of landslides: From progressive local failures to mass release, Water Resources Research, 48(3).

McDaniel, P.A., Wilson, M.A., Burt, R., Lammers, D., Thorson, T.D., Mcgrath, C.L. et al. 2005. Andic soils of the inland Pacific Northwest, USA: properties and ecological significance. Soil Science, 170, 300–311.

Nanzyo M. (2002) - Unique properties of volcanic ash soils. Global environmental research, 6, 2, 99-112.

Nanzyo, M., Shoji, S. and Sudjadi, M., 1993. Properties and classification of Andisols from West Java, Indonesia.

Peruccacci S., M.T. Brunetti, S. Luciani, C. Vennari and F. Guzzetti (2012) - Lithological and seasonal control on rainfall thresholds for the possible initiation of landslides in central Italy. Geomorphology, 139-140, pp. 79-90.

Picarelli L., L. Olivares, L. Comegna and E. Damiano (2008) - Mechanical aspects of flow-like movements in granular and fine-grained soils. Rock Mech. Rock Eng., 41(1), pp. 179-197.

Scognamiglio, S., Calcaterra, D., Iamarino, M., Langella, G., Orefice, N., Vingiani, S., & Terribile, F. (2016a). Andic soil features and debris flows in Italy. New perspective towards prediction. In *EGU General Assembly Conference Abstracts* (Vol. 18, p. 10543).

Scognamiglio, S., Terribile, F., Iamarino, M., Orefice, N., & Vingiani, S. (2016b). Soil properties and debris flows in Italy: potential relationships. *RENDICONTI ONLINE SOCIETA GEOLOGICA ITALIANA*, *41*, 199-202.

Shoji, S., M. Nanzyo, and R.A. Dahigren. 1993. Volcanic ash soils: Genesis, properties and utilization. Elsevier, Amsterdam, Netherlands.

Stothoff, S. (2008), Infiltration tabulator for Yucca mountain: Bases and confirmation. Prepared for U.S. Nuclear Regulatory Commission,

[Available at: http://pbadupws.nrc.gov/docs/ML0823/ML082350701.html].

Terribile, F., Basile, A., de Mascellis, R., di Gennaro, A., Mele, G., Vingiani, S., 2000. I suoli delle aree crisi di

Quindici e Sarno: proprieta` comportamenti in relazione ai fenomeni franosi del 1998. Quad. Geol. Appl. 7-1, 59–77.

Terribile, F., Basile, A., De Mascellis, R., Iamarino, M., Magliulo, P., Pepe, S. et al. 2007. Landslide processes and Andosols: the case study of the Campania region, Italy. In Soils of Volcanic Regions in Europe (eds O. Arnalds, F Bartoli, P Buurman, H O´ skarsson, G Stoops, & E Garcı´a-Rodeja), pp. 545–563. Springer Verlag, Berlin and Heidelberg.

Vingiani, S., Mele, G., De Mascellis, R., Terribile, F., Basile, A., 2015. Volcanic soils and landslides: A case study of the island of Ischia (southern Italy) and its relationship with other Campania events. Solid Earth, 6 (2), pp. 783-797. DOI: 10.5194/se-6-783-2015.

Vingiani, S. and Terribile, F., 2006. Properties, geography, classification and management of volcanic ash soils: an overview. Acta Volcanologica, 18 (1/2), p.113.